

Radical Reductive Formylation of N-heteroarenes with Formic acid under Catalyst- and Solvent-Free conditions

Shaofeng Pang^{+, *a} Qi Wei^{+, b} Junxi Liang^{+, a} Liqun Jiang,^b Xinyun Guan,^c Bolin Xia,^c Rong Shang,^a Yanbin Wang^a and Yujing Zhang^{+,*b}

^a Key Laboratory of Environment-Friendly Composite Materials of the State Ethnic Affairs Commission; Gansu Provincial Biomass Function Composites Engineering Research Center; Chemical Engineering Institute; Northwest Minzu University, Lanzhou, Gansu, 730030, P. R. China

^b Key Laboratory of Eco-functional Polymer Materials of the Ministry of Education; Key Laboratory of Polymer Materials of Gansu Province; College of Chemistry and Chemical Engineering; Northwest Normal University, Lanzhou, Gansu, 730070, P. R. China

^c National Engineering Laboratory for VOCs Pollution Control Technology and Equipment (SCUT), School of Environment and Energy; South China University of Technology, Guangzhou, Guangdong, 510640, P. R. China

⁺ These authors contributed equally to this work

***Corresponding author:**

pangshaofeng2006@163.com (S. Pang); yujing0221@163.com (Y. Zhang)

Supporting Information

I. Materials and reagents.....	S1
II. General experimental procedures.....	S1
III. Characterization and computational simulation results.....	S4
IV. NMR peaks and ESI-HRMS of all products.....	S15
V. NMR and ESI-HRMS spectra of all products.....	S26
VI. References.....	S68

I. Materials and reagents

Quinoline and formic acid were purchased from Sigma-Aldrich and Shanghai Maclean Biochemical Technology Co., Ltd., China, respectively. 5,5-Dimethyl-1-pyrroline-N-oxide (DMPO) was purchased from Dojindo. All solvents and chemicals were obtained commercially and were used as received.

II. General experimental procedures

High-resolution mass spectra (HRMS) were reported from the Thermo Orbitrap Elite or Bruker Daltonics APEXII 47e FT-ICR instrument with an ESI source.

For the EPR spin-trapping experiments, the reaction mixture of quinoline (1 mmol) and formic acid (9 mmol) was placed in a round-bottom flask and sealed with a septum under an argon atmosphere, then heated to 160 °C. After 2 minutes of reaction, the mixture was rapidly cooled to room temperature using an ice bath. Approximately 50 µL of the reaction mixture was taken out and mixed with 10 µL of DMPO. About 50 µL of this mixture was then transferred into a glass microcapillary tube (Hirschmann), and EPR spectra were recorded on a Bruker CW spectrometer ELEXSYS 500-10/12 (X-band, $\nu \sim 9.849873$ GHz) at room temperature. The dataset consisted of 1024 data points (X-axis), with a minimum field value of 3460 G and a sweep width of 100 G. The experiment was conducted in CW (continuous wave) mode. The magnetic field axis used was B0VL, with a resolution of 1. The center field for the scan was 3510 G, and the sweep direction was from low field to high field. The microwave power was set at 10.02 mW with an attenuation of 13 dB, and the gain was set to 30 dB. The EPR spectra provided detailed information on various free radicals present in the reaction mixture: Rad0: (DMPO-CO₂⁻): A free radical with a g-factor of 2.00487, a linewidth of 1.77186 G, and an area of 1.84441, containing two different nuclear spins; Rad4 (DMPO-H): A hydrogenated DMPO product with a g-factor of 2.00366, linewidth of 1.8704 G, and an area of 2.04151; Rad4 (DMPO-OH): The DMPO-OH radical with a g-factor of 2.00532, linewidth of 1.10916 G, and an area of 0.305233. Signal fitting was carried out by using the Spin Fit program (Bruker).

NMR spectra were measured by using a Bruker ARX 400 or ARX 600 spectrometer

at 400 MHz (^1H) and 151 MHz (^{13}C). All spectra were recorded in CDCl_3 and chemical shifts (d) are reported in ppm relative to tetramethylsilane referenced to the residual solvent peaks.

The black-box simulation: Molecular configuration of formic acid and quinoline was firstly optimized using the DMol3 module implanted in the Materials Studio (MS) software.^[1] The generalized gradient approximation (GGA) of B3PW91 functional, GGA-B3PW91, together with double-numeric quality basis set with polarization functions (DNP) was selected as the exchange-correlation function. Next, a cubic black-box of $25.60 \times 25.60 \times 25.60 \text{ \AA}$ containing 180 optimized formic acid and 20 optimized quinoline molecules was built using Amorphous Cell program package, in which the molecular ratio was constructed based on the experimental data. Using Forcite module implanted in MS software, the lowest energy simulation based on the built cubic configuration were performed in Condensed-phase Optimized Molecular Potential for Atomistic Simulation Studies (COMPASS) force field. Then, the annealing simulation was carried out in which the number of cycles was set to 10 and the steps per cycle were 10^5 . The coulombic interaction was calculated by the Group method, while van der Waals interaction was calculated by the atom-based summation method. After the annealing simulation the molecular dynamic (MD) simulation was employed to determine the most stable model. MD simulation of the NPT ensemble at 433K and 100 kPa with a time step of 0.5 fs for 5000 ps was firstly performed to obtain density of 1.075 g/L. Subsequently, the NVT simulation was performed for 10 ns (time step = 1 fs, frame output for every step, T = 433K), and the Nose thermostat was used to control the temperature. According to the total energy the most stable model in the trajectory frames was selected to study thermal decomposition of the formic acid because of the effect of the quinoline. The production simulation based on the most stable model was employed to run using the GULP module implanted in MS software with the ReaxFF 6.0 force field. The same parameters were set as in the NVT simulation. In this paper, the RDF (Radial distribution function) that focuses on the distances between particles within the same trajectory's configurations, aggregating these atomic interactions into

a histogram, was performed. This allows for the analysis of the temporal evolution of intermolecular interactions.

For the comparison and discussion of Gibbs free energies, structural optimizations were carried out using the generalized gradient approximation (GGA) of PW91 functional, GGA-PW91, together with double-numeric quality basis set with polarization functions (DNP). Within this computational framework, the electronic structures of all structures were optimized and the transition states (only one imaginary frequency) and intermediates (without any imaginary frequencies) within the reaction mechanism were obtained. The thermal corrections to the Gibbs free energy at 298 K from the frequency analysis were added to the total electronic energy. In addition, all the digital photos were shot with Canon EOS-60D camera.

III. Characterization and computational simulation results

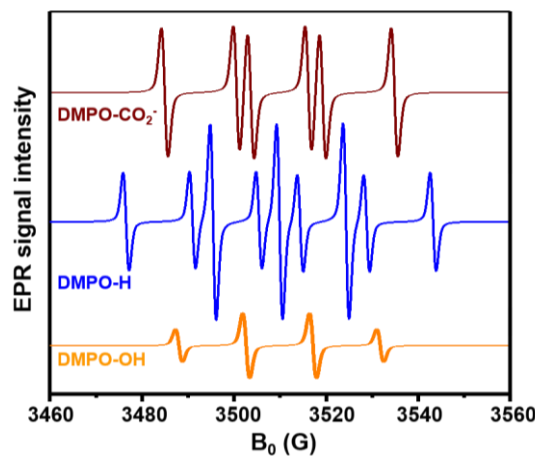


Fig. S1 Simulation of deconvoluted spectra of radical adducts using DMPO.

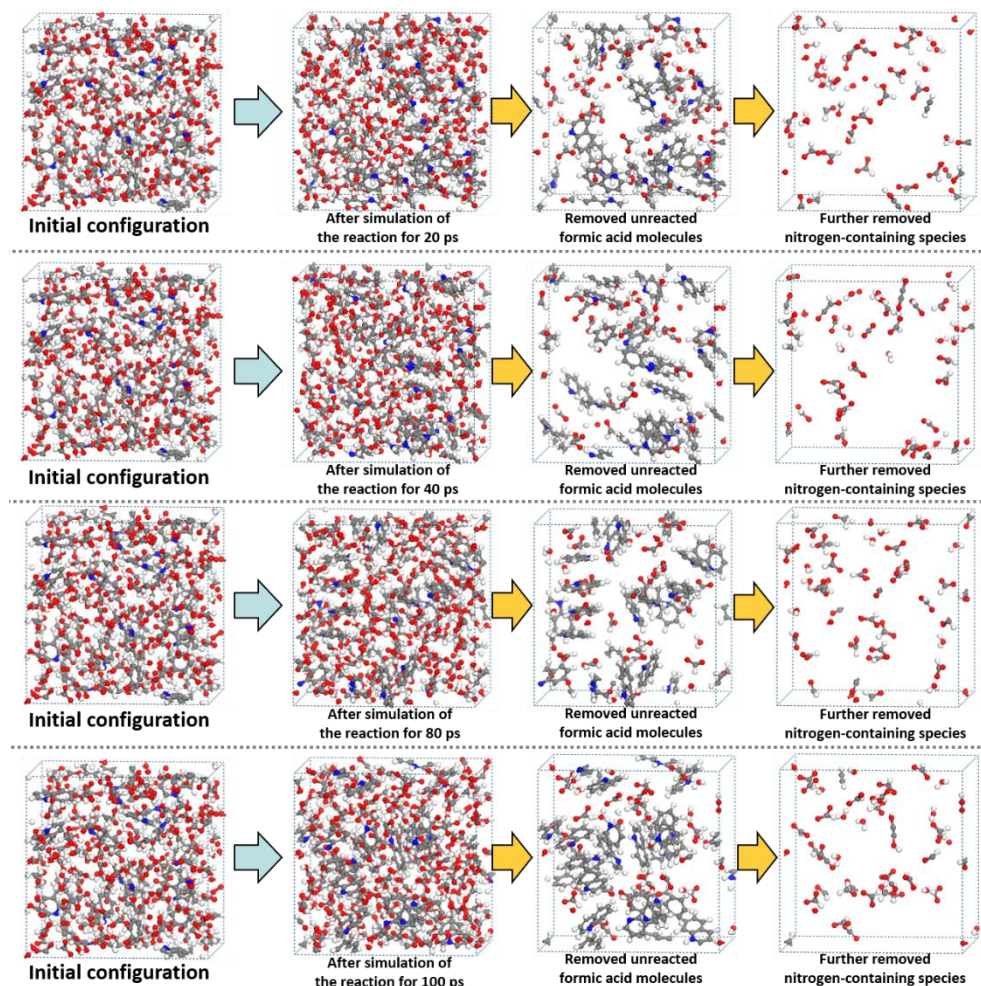


Fig. S2 The configuration of the black-box model after MD simulations performed over different durations.

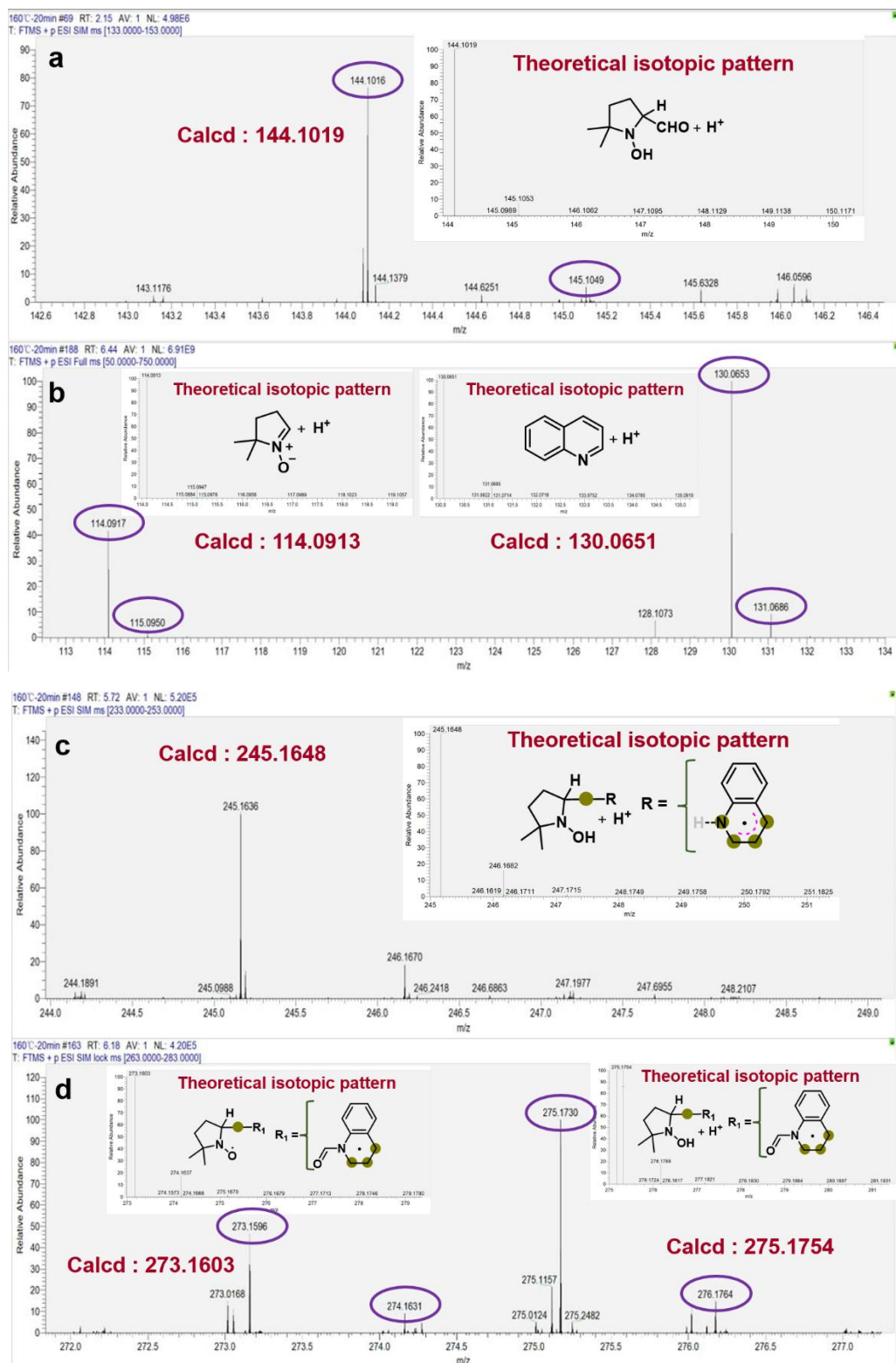


Fig. S3 The ESI-HRMS spectrum for the DMPO-trapped radicals after 20 min of reaction.

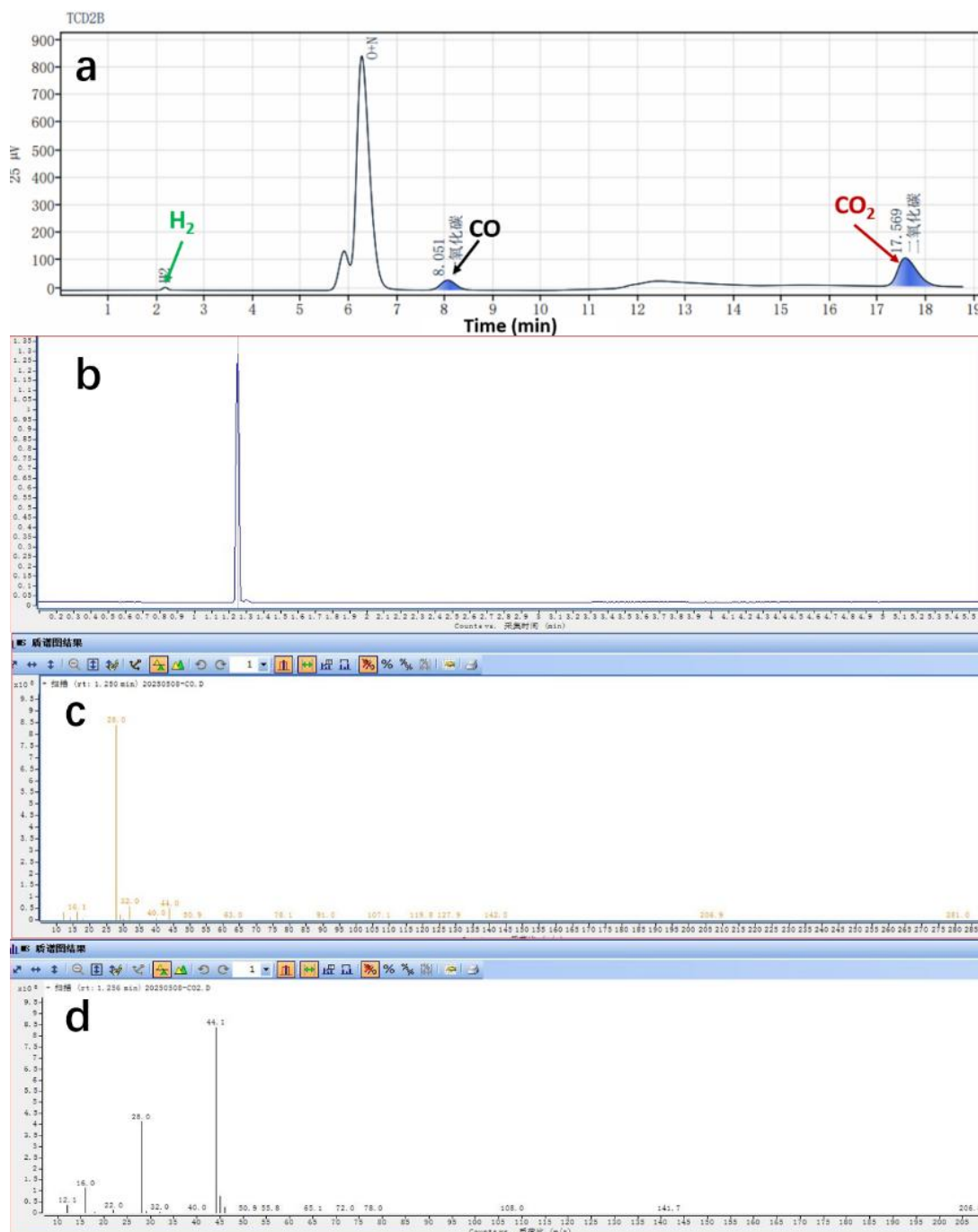


Fig. S4 (a) Detection of gaseous products by GC-TCD. The retention times of CO and CO_2 were 8.051 min and 17.569 min, respectively. In addition, the release of H_2 was also observed; (b) GC chromatograms of CO and CO_2 recorded by GC-MS; (c, d) Corresponding mass spectra of CO and CO_2 , respectively.

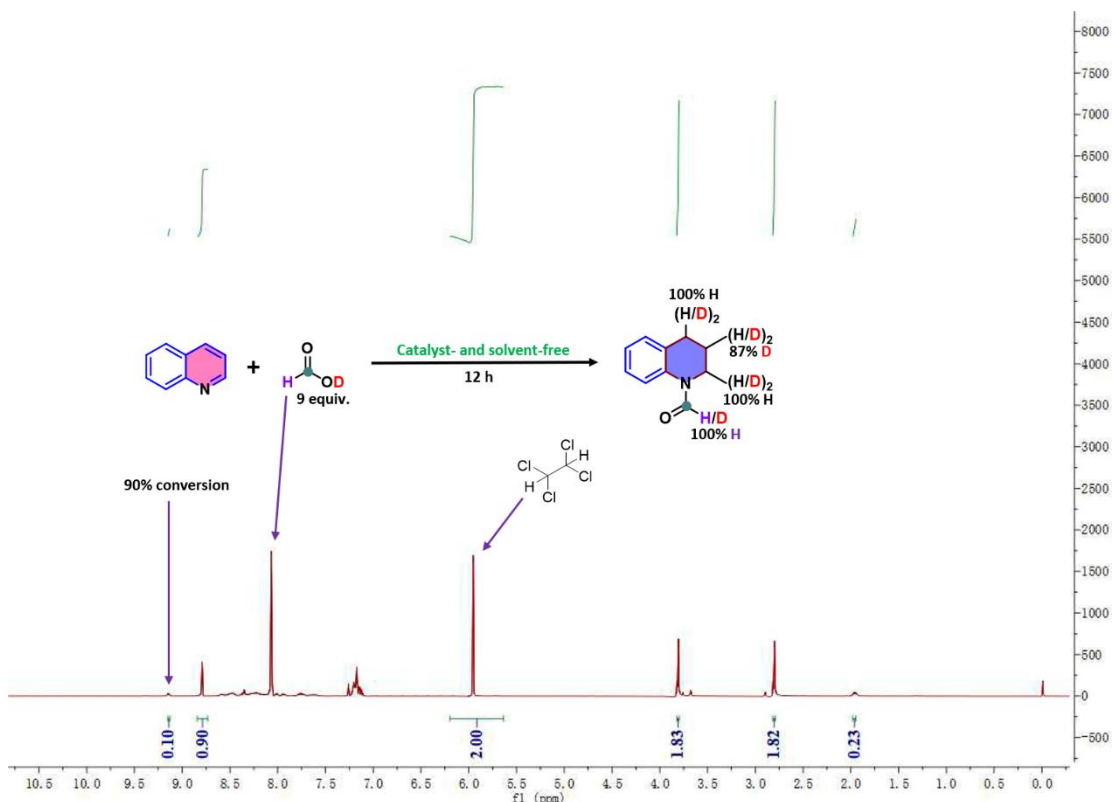


Fig. S5 NMR spectrum of quinoline with HCOOD after 12 h reaction.

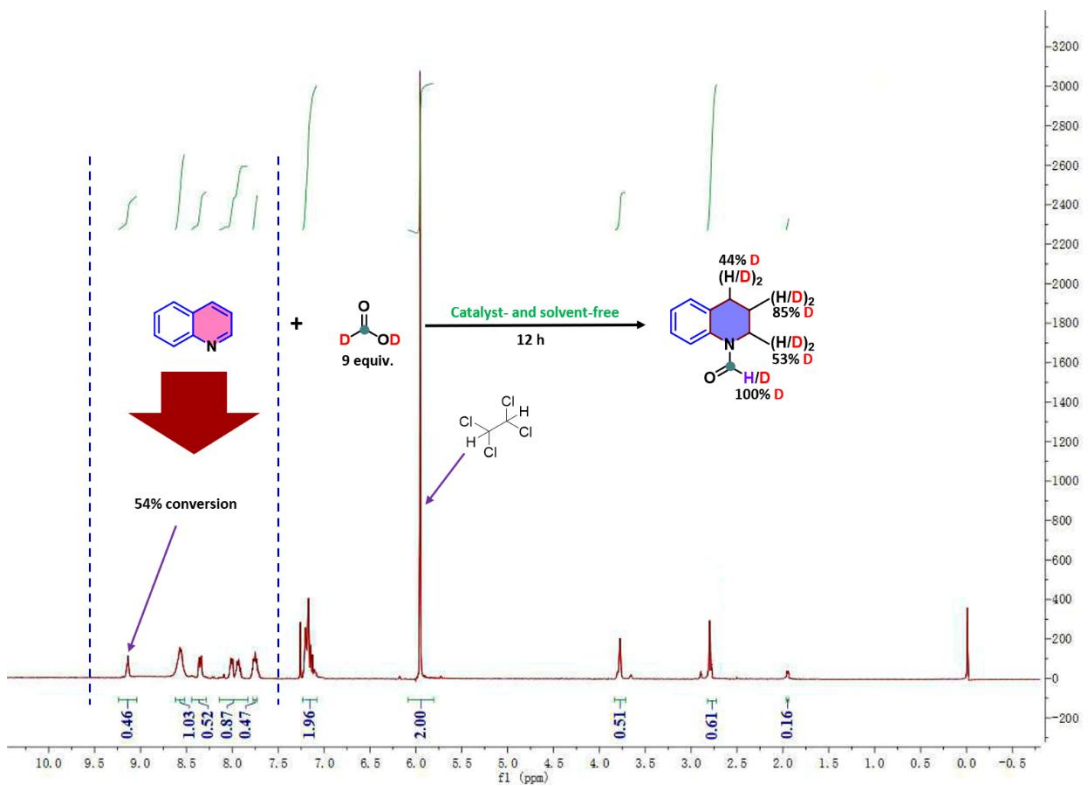


Fig. S6 NMR spectrum of quinoline with DCOOD after 12 h reaction.

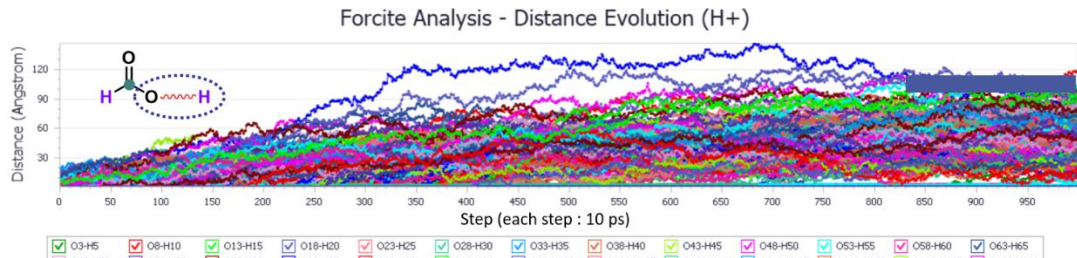


Fig. S7 RDF of O-H bond distance in the formic acid.

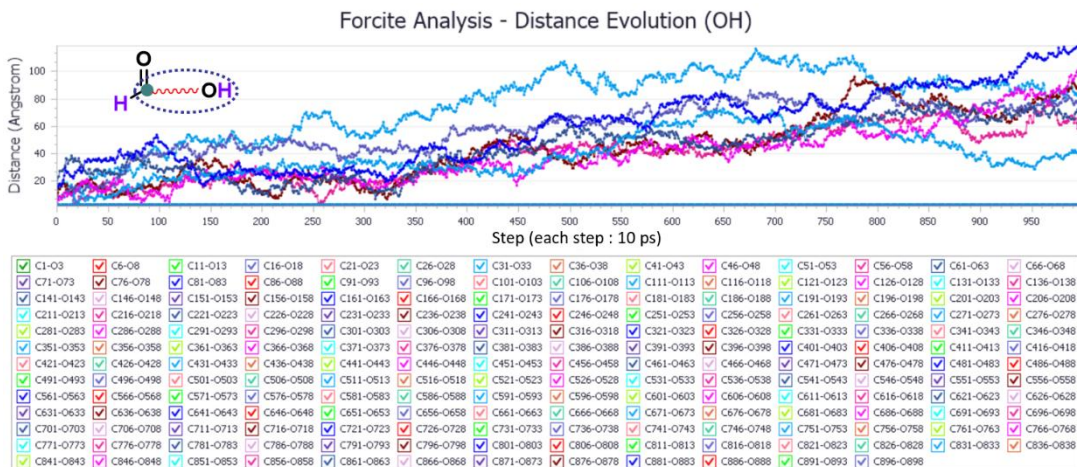


Fig. S8 RDF of C-OH bond distance in the formic acid.

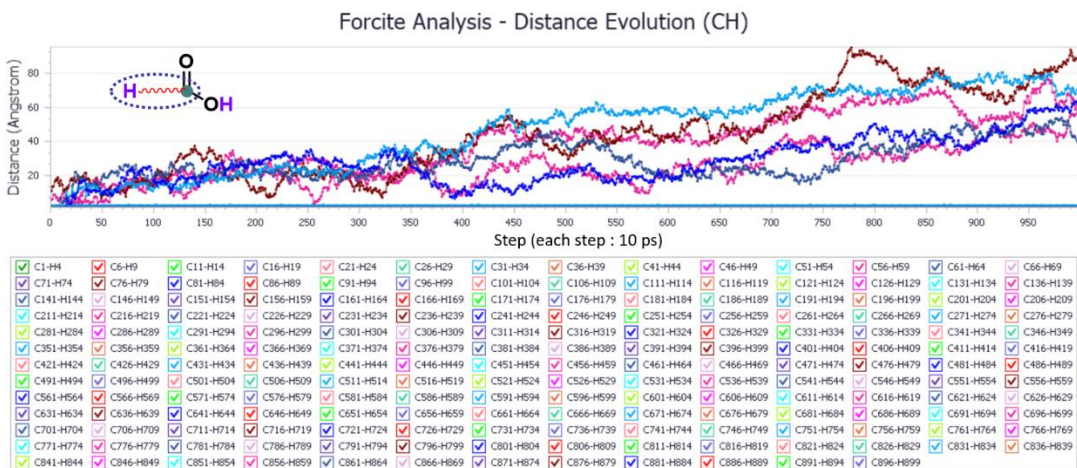
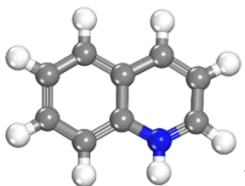
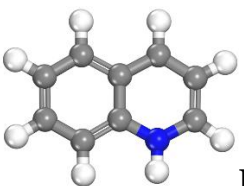
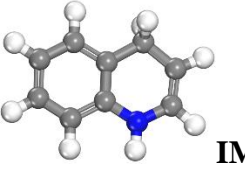
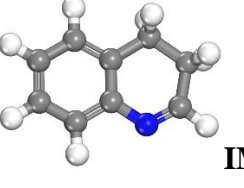
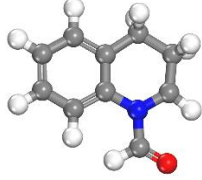
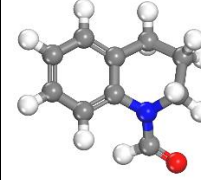
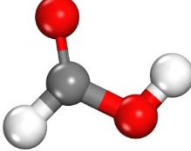
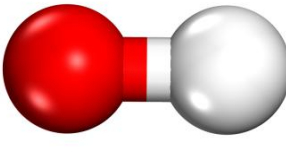
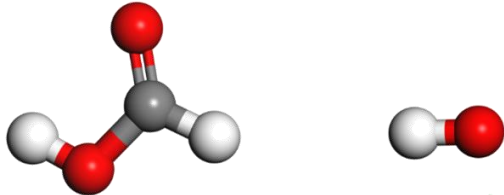
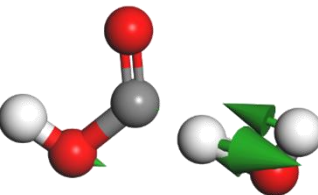
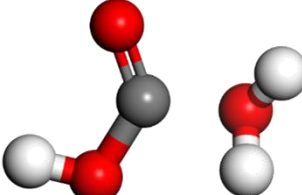
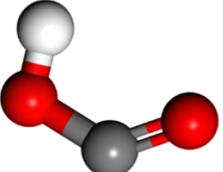


Fig. S9 RDF of C-H bond distance in the formic acid.

Table S1 GGA/PW91 optimized Cartesian Coordinates.

	
IM-1 C, -2.459414, -0.509250, 0.165536 C, -1.778206, -1.737866, 0.317196 C, -0.397650, -1.798480, 0.277693 C, 0.320915, -0.610876, 0.079831 C, -0.344493, 0.644494, -0.078609 C, -1.759501, 0.662020, -0.026449 C, 0.438832, 1.801111, -0.279328 C, 2.440798, 0.491461, -0.161545 N, 1.698607, -0.609297, 0.028655 H, -3.548573, -0.493538, 0.202190 H, -2.349902, -2.653659, 0.465127 H, 0.126069, -2.747928, 0.398809 H, -2.279776, 1.612690, -0.144229 H, -0.062954, 2.761850, -0.403258 H, 3.520544, 0.353194, -0.184135 C, 1.822267, 1.729911, -0.321540 H, 2.436423, 2.614209, -0.476265 H, 2.176013, -1.510045, 0.140321	C, -2.478007, -0.551005, 0.000000 C, -1.809919, -1.774324, 0.000000 C, -0.411130, -1.804451, 0.000000 C, 0.314838, -0.614316, 0.000000 C, -0.346995, 0.649929, 0.000000 C, -1.756229, 0.641174, 0.000000 C, 0.441324, 1.839951, 0.000000 C, 2.471289, 0.534775, 0.000000 N, 1.707815, -0.622398, 0.000000 H, -3.568787, -0.524362, 0.000000 H, -2.370269, -2.710467, 0.000000 H, 0.121233, -2.759224, 0.000000 H, -2.276767, 1.601070, 0.000000 H, -0.058250, 2.808731, 0.000000 H, 3.548806, 0.397497, 0.000000 C, 1.842797, 1.755861, 0.000000 H, 2.454931, 2.658083, 0.000000 H, 2.173320, -1.526525, 0.000000
	
IM-3	IM-4

C, -2.501140, -0.658413, 0.183421 C, -1.824655, -1.867890, 0.339579 C, -0.435029, -1.897634, 0.296496 C, 0.296681, -0.718307, 0.098097 C, -0.372751, 0.512565, -0.058931 C, -1.767298, 0.511542, -0.012843 C, 0.390999, 1.809609, -0.278425 C, 2.439097, 0.393656, -0.145858 N, 1.687312, -0.757153, 0.054471 H, -3.590917, -0.624061, 0.218236 H, -2.378888, -2.794264, 0.498664 H, 0.100466, -2.842670, 0.420225 H, -2.290709, 1.463606, -0.134933 H, 0.114091, 2.538072, 0.510354 H, 3.517234, 0.236676, -0.167251 C, 1.881348, 1.603236, -0.301533 H, 2.529787, 2.466013, -0.453810 H, 2.151270, -1.653525, 0.159141 H, 0.053103, 2.278941, -1.225099	C, -2.491202, -0.848653, 0.205505 C, -1.802230, -2.050324, 0.366135 C, -0.411184, -2.054375, 0.324471 C, 0.303601, -0.867128, 0.124560 C, -0.387629, 0.346582, -0.033560 C, -1.781530, 0.336808, 0.007224 C, 0.363757, 1.644181, -0.249988 C, 2.404065, 0.085662, -0.099997 N, 1.714524, -0.975327, 0.089276 H, -3.582092, -0.828774, 0.244056 H, -2.347969, -2.980872, 0.530375 H, 0.162821, -2.973889, 0.445433 H, -2.323710, 1.279020, -0.113724 H, 0.080188, 2.351188, 0.546994 H, 3.497131, -0.035914, -0.126150 C, 1.900387, 1.490646, -0.293330 H, 2.384615, 2.122545, 0.472677 H, 0.007844, 2.102148, -1.187567 H, 2.308612, 1.856476, -1.252390
 IM-5	 P
C, -2.856053, -0.524050, 0.180265 C, -2.179359, -1.728436, 0.374725 C, -0.790898, -1.765694, 0.346513 C, -0.042376, -0.598626, 0.107205 C, -0.716836, 0.625191, -0.062220 C, -2.116487, 0.632499, -0.025281 C, -0.011845, 1.942058, -0.270186 C, 2.115157, 0.542824, -0.102055 N, 1.387227, -0.618862, 0.040966 H, -3.946257, -0.486324, 0.200744 H, -2.732954, -2.650125, 0.556702 H, -0.305193, -2.721847, 0.523561 H, -2.628613, 1.587910, -0.165944 H, -0.346413, 2.634943, 0.519146 H, 3.187973, 0.379049, -0.141817 C, 1.527065, 1.885699, -0.281467 H, 1.932986, 2.558610, 0.498118 H, -0.370014, 2.383202, -1.214964 H, 1.906026, 2.312565, -1.230986 C, 2.127631, -1.817910, 0.051957	C, -2.895750, -0.506919, 0.482284 C, -2.225384, -1.716153, 0.666431 C, -0.844455, -1.782158, 0.486503 C, -0.145255, -0.641915, 0.079136 C, -0.810734, 0.577988, -0.132603 C, -2.186304, 0.631472, 0.094573 C, -0.022441, 1.729897, -0.699035 C, 1.956038, 0.537090, 0.448604 N, 1.260136, -0.636309, -0.092452 H, -3.972368, -0.446539, 0.649278 H, -2.773107, -2.605337, 0.982817 H, -0.297439, -2.703528, 0.687852 H, -2.713960, 1.575714, -0.059178 H, -0.571353, 2.672114, -0.553193 H, 3.023756, 0.388464, 0.247393 C, 1.425671, 1.851347, -0.153300 H, 1.470536, 2.628229, 0.624193 H, 0.037111, 1.577813, -1.791671 H, 2.084591, 2.182345, -0.969506 C, 1.954730, -1.669746, -0.677817

O, 3.351844, -1.847830, 0.009248 H, 1.507386, -2.724848, 0.085772	O, 3.173111, -1.732481, -0.779788 H, 1.266704, -2.444462, -1.081336 H, 1.806167, 0.533075, 1.540817
 R-formic acid	 R-•OH radical
H, -1.202792, -0.776094, 0.019793 C, -0.424447, 0.007795, 0.013221 O, 0.796592, -0.585562, -0.010497 O, -0.620695, 1.200172, 0.022205 H, 1.451343, 0.153688, -0.044721	O, 0.000000, 0.000000, -0.495339 H, 0.000000, 0.000000, 0.495339
 IM1-H	 TS1-H
C, 0.636516, 0.832940, -0.051770 H, 0.187573, -0.176976, 0.002856 O, 0.025060, 1.862657, -0.215450 O, 1.977968, 0.731389, 0.094735 O, -2.956140, -2.770274, 0.036669 H, -2.195611, -2.136614, 0.064181 H, 2.324634, 1.656878, 0.068780	C, -28.75873829628827, 4.22816172885597, 2.49592949509451 O, -29.69260198271508, 6.12542869213890, 1.63612557923430 O, -26.75407710749379, 3.02484117335759, 1.48582539387580 H, -29.61074276371498, 3.18132171977846, 4.29172576447229 O, -31.09007125075293, 1.99221797866747, 6.31792242661876 H, -32.82402625262707, 2.65312740098342, 6.09465114917873 H, -26.44144579143022, 3.91278674894047, -0.13843292914368
 IM2-H	 P-H •CHO radical

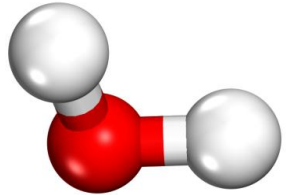
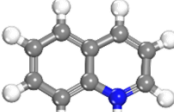
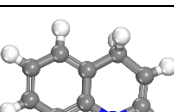
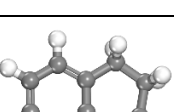
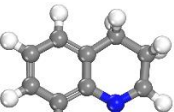
C, -0.473077, 0.245579, -0.803755 O, -0.083869, 1.136288, -1.502131 O, -0.391980, -1.080204, -0.98620 H, 0.020926, -0.433347, 1.718312 O, 0.683872, 0.285205, 1.728924 H, 0.136539, 1.093952, 1.676654 H, 0.107588, -1.247472, -1.831801	C, -0.13821100, 0.40081100, -0.00000100 O, -1.21438300, -0.14285700, 0.00000000 O, 1.09092800, -0.21306900, 0.00000000 H, 1.81690900, 0.44253900, 0.00000400
 P-H H₂O	
O, 0.000000, 0.000000, -0.434589 H, 0.837830, 0.000000, 0.217294 H, -0.837830, 0.000000, 0.217294	

Table S2 GGA/PW91 computed energetic data. HF, Hartree Fock; Zero-point energy, ZPE, in a.u.; Number of imaginary frequencies, NIImag; as well as sum of electronic and thermal enthalpy, H_{tot}, in Hartree, and sum of electronic and thermal free energy, G_{tot}, in Hartree.

	IM-1 HF = -402.39960646 a.u. ZPE = 0.148115 a.u. NIImag = 0	H _{tot} = -402.244179 a.u. G _{tot} = -402.282985 a.u.
	IM-2 HF = -402.40461691 a.u. ZPE = 0.147892 a.u. NIImag = 0	H _{tot} = -402.248779 a.u. G _{tot} = -402.288810 a.u.
	IM-3 HF = 403.02055983 a.u. ZPE = 0.160432 a.u. NIImag = 0	H _{tot} = -402.851830 a.u. G _{tot} = -402.892418 a.u.
	IM-4 HF = -403.01191392 a.u. ZPE = 0.159739 a.u. NIImag = 0	H _{tot} = -402.844643 a.u. G _{tot} = -402.883470 a.u.
	IM-5 HF = -516.87580195 a.u. ZPE = 0.179606 a.u. NIImag = 0	H _{tot} = -516.686883 a.u. G _{tot} = -516.731293 a.u.

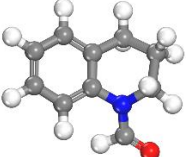
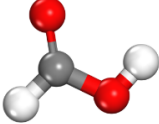
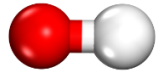
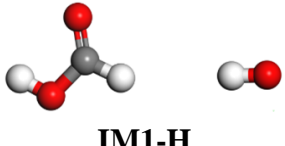
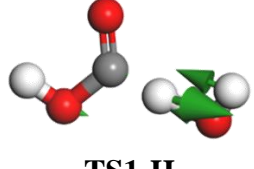
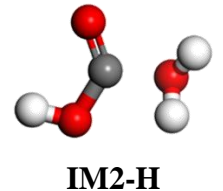
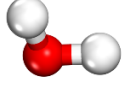
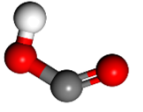
	HF = -517.53536437 a.u. ZPE = 0.194084 a.u. NImag = 0	H _{tot} = -517.331456 a.u. G _{tot} = -517.376143 a.u.
	HF = -189.67722792 a.u. ZPE = 0.032773 a.u. NImag = 0	H _{tot} = -189.640238 a.u. G _{tot} = -189.668600 a.u.
R-formic acid		
	HF = -75.70851866 a.u. ZPE = 0.008074 a.u. NImag = 0	H _{tot} = -75.697140 a.u. G _{tot} = -75.717401 a.u.
R•OH radical		
	HF = -265.41474941 a.u. ZPE = 0.044410 a.u. NImag = 0	H _{tot} = -265.364011 a.u. G _{tot} = -265.398782 a.u.
IM1-H		
	HF = -265.39243852 a.u. ZPE = 0.037979 a.u. NImag = 1	H _{tot} = -265.351336 a.u. G _{tot} = -265.386918 a.u.
TS1-H		
	HF = -265.40478099 a.u. ZPE = 0.041956 a.u. NImag = 0	H _{tot} = -265.357707 a.u. G _{tot} = -265.390967 a.u.
IM2-H		
	HF = -76.38611663 a.u. ZPE = 0.020543 a.u. NImag = 0	H _{tot} = -76.361794 a.u. G _{tot} = -76.383242 a.u.
P-H H₂O		
	HF = -189.01930857 a.u. ZPE = 0.020066 a.u. NImag = 0	H _{tot} = -188.995051 a.u. G _{tot} = -189.023702 a.u.
P-H •CHO radical		

Table S3 Quantitative analysis of gaseous products from the thermal decomposition of pure formic acid under variable temperatures and from the model reaction system.

T (°C)	H ₂ (mmoL) ^a	CO (mmoL) ^a	CO ₂ (mmoL) ^a
--------	------------------------------------	------------------------	-------------------------------------

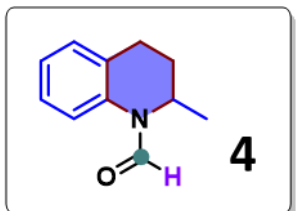
150	0.068	0.884	0.071
160	0.072(0.099) ^b	0.979(1.640) ^b	0.078(2.214) ^b
170	0.075	1.186	0.083
180	0.063	1.419	0.710
190	0.059	1.609	0.064

Conditions: ^a Formic acid only (9 mmol); ^b Quinoline (1 mmol) and formic acid (9 mmol) mixture, Ar, 24 h, catalyst- and solvent-free, T (°C) = Heating module temperature, the yields of various gases were quantitatively determined using calibration factors obtained from reference standard gases, employing a GC system equipped with a TDX-01 packed column and a thermal conductivity detector (TCD, Agilent 7820A).

IV. NMR peaks and ESI-HRMS of all products

NMR peaks and ESI-HRMS of products

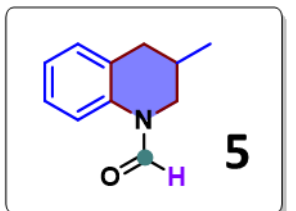
Acquired NMR peaks matched those of the literature.^[2-7]



¹H NMR (400 MHz, Chloroform-*d*) δ 8.66 (s, 1H), 7.21-7.09 (m, 4H), 4.79 (q, *J* = 6.3 Hz, 1H), 2.85-2.78 (m, 1H), 2.72-2.65 (m, 1H), 2.15-2.06 (m, 1H), 1.68 (dq, *J* = 12.2, 5.9 Hz, 1H), 1.19 (d, *J* = 6.6 Hz, 3H).

¹³C NMR (151 MHz, Chloroform-*d*) δ 161.14, 136.30, 129.82, 129.14, 127.21, 124.79, 118.47, 45.23, 29.22, 24.27, 18.16.

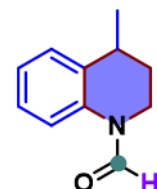
HRMS (ESI): m/z [M+H]⁺ calcd: 176.10699; found: 176.10703.



¹H NMR (400 MHz, Chloroform-*d*) δ 8.79 (s, 1H), 7.20-7.07 (m, 4H), 4.16 (dd, *J* = 12.7, 4.1 Hz, 1H), 3.11-3.01 (m, 1H), 2.88 (dd, *J* = 16.3, 4.9 Hz, 1H), 2.45 (dd, *J* = 16.2, 10.1 Hz, 1H), 2.01 (td, *J* = 10.4, 5.3 Hz, 1H), 1.08 (d, *J* = 6.6 Hz, 3H).

¹³C NMR (151 MHz, Chloroform-*d*) δ 161.06, 136.90, 129.86, 128.28, 127.03, 124.59, 116.66, 46.37, 35.54, 27.94, 18.75.

HRMS (ESI): m/z [M+H]⁺ calcd: 176.10699; found: 176.10701.

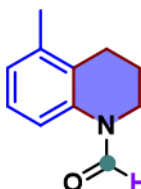


6

¹H NMR (400 MHz, Chloroform-*d*) δ 8.74 (s, 1H), 7.24-7.07 (m, 4H), 3.88-3.70 (m, 2H), 2.90 (q, *J* = 6.6 Hz, 1H), 2.01 (h, *J* = 7.1, 6.2 Hz, 1H), 1.71-1.59 (m, 1H), 1.30 (d, *J* = 6.9 Hz, 3H).

¹³C NMR (151 MHz, Chloroform-*d*) δ 161.03, 136.50, 133.85, 128.01, 127.01, 124.61, 117.08, 38.12, 30.67, 29.94, 20.75.

HRMS (ESI): m/z [M+H]⁺ calcd: 176.10699; found: 176.10701.

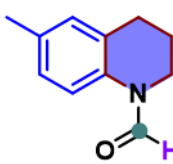


7

¹H NMR (400 MHz, Chloroform-*d*) δ 8.71 (s, 1H), 7.14-6.95 (m, 3H), 3.78 (t, *J* = 5.8 Hz, 2H), 2.69 (t, *J* = 6.8 Hz, 2H), 2.24 (s, 3H), 1.95 (p, *J* = 6.2 Hz, 2H).

¹³C NMR (151 MHz, Chloroform-*d*) δ 161.02, 137.53, 137.32, 127.05, 126.38, 126.22, 115.24, 39.15, 24.19, 22.38, 19.42.

HRMS (ESI): m/z [M+H]⁺ calcd: 176.10699; found: 176.10701.



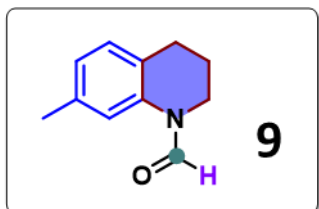
8

¹H NMR (400 MHz, Chloroform-*d*) δ 8.71 (s, 1H), 6.98 (dd, *J* = 15.5, 7.5 Hz, 3H), 3.79-3.72 (m, 2H), 2.74 (t, *J* = 6.4 Hz, 2H), 2.27 (s, 3H), 1.90 (p, *J* = 6.3 Hz, 2H).

¹³C NMR (151 MHz, Chloroform-*d*) δ 160.76, 134.64, 133.96, 130.03, 128.49, 127.52,

116.70, 40.09, 26.91, 22.23, 20.53.

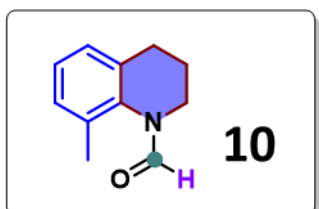
HRMS (ESI): m/z [M+H]⁺ calcd: 176.10699; found: 176.10701.



¹H NMR (400 MHz, Chloroform-*d*) δ 8.75 (s, 1H), 7.06-6.87 (m, 3H), 3.76 (t, *J* = 6.1 Hz, 2H), 2.75 (t, *J* = 6.5 Hz, 2H), 2.32 (s, 3H), 1.91 (p, *J* = 6.3 Hz, 2H).

¹³C NMR (151 MHz, Chloroform-*d*) δ 161.00, 137.03, 136.83, 129.40, 125.73, 125.30, 117.55, 40.22, 26.69, 22.37, 21.20.

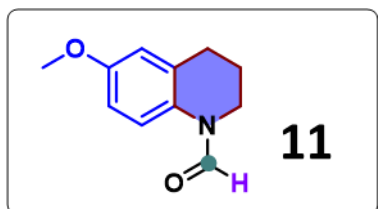
HRMS (ESI): m/z [M+Na]⁺ calcd: 198.08894; found: 198.08902.



¹H NMR (400 MHz, Chloroform-*d*) δ 8.32 (s, 1H), 7.14-6.99 (m, 3H), 3.77 (t, *J* = 6.8 Hz, 2H), 2.67 (t, *J* = 6.5 Hz, 2H), 2.32 (s, 3H), 1.93 (t, *J* = 6.7 Hz, 2H).

¹³C NMR (151 MHz, Chloroform-*d*) δ 163.34, 136.64, 134.44, 129.88, 129.71, 126.08, 125.51, 40.05, 26.98, 23.52, 18.69.

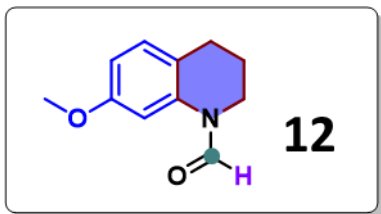
HRMS (ESI): m/z [M+H]⁺ calcd: 176.10699; found: 176.10699.



¹H NMR (400 MHz, Chloroform-*d*) δ 8.65 (s, 1H), 7.03 (d, *J* = 8.6 Hz, 1H), 6.74-6.68 (m, 2H), 3.76 (s, 5H), 2.76 (t, *J* = 6.4 Hz, 2H), 1.92 (q, *J* = 6.2 Hz, 2H).

¹³C NMR (151 MHz, Chloroform-*d*) δ 160.93, 156.74, 130.68, 130.44, 118.32, 114.60, 112.60, 55.51, 40.18, 27.32, 22.44.

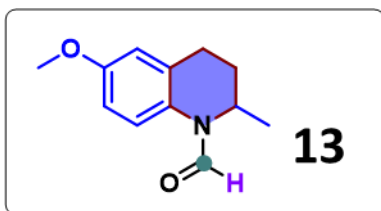
HRMS (ESI): m/z [M+H]⁺ calcd: 192.10191; found: 192.10191.



¹H NMR (400 MHz, Chloroform-*d*) δ 8.75 (s, 1H), 7.04 (d, *J* = 8.2 Hz, 1H), 6.69-6.60 (m, 2H), 3.78-3.74 (m, 5H), 2.71 (t, *J* = 6.5 Hz, 2H), 1.90 (q, *J* = 6.4 Hz, 2H).

¹³C NMR (151 MHz, Chloroform-*d*) δ 161.06, 158.64, 137.92, 130.30, 120.88, 109.82, 103.27, 55.45, 40.32, 26.40, 22.41.

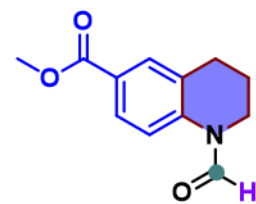
HRMS (ESI): m/z [M+H]⁺ calcd: 192.10191; found: 192.10194.



¹H NMR (400 MHz, Chloroform-*d*) δ 8.55 (s, 1H), 7.01 (d, *J* = 8.5 Hz, 1H), 6.73 (dd, *J* = 11.6, 3.1 Hz, 2H), 4.76 (q, *J* = 6.3 Hz, 1H), 3.77 (s, 3H), 2.79-2.73 (m, 1H), 2.67-2.60 (m, 1H), 2.14-2.07 (m, 1H), 1.63 (dd, *J* = 13.0, 7.3 Hz, 1H), 1.17 (d, *J* = 6.6 Hz, 3H).

¹³C NMR (151 MHz, Chloroform-*d*) δ 161.05, 157.10, 131.72, 129.69, 119.89, 114.35, 112.66, 55.60, 45.37, 29.62, 24.82, 18.27.

HRMS (ESI): m/z [M+H]⁺ calcd: 206.11756; found: 206.11740.

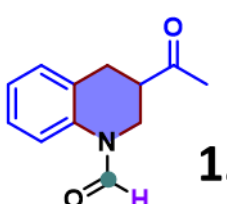


14

¹H NMR (400 MHz, Chloroform-*d*) δ 8.89 (s, 1H), 7.86 (d, *J* = 6.9 Hz, 2H), 7.21 (d, *J* = 9.1 Hz, 1H), 3.90 (s, 3H), 3.84-3.80 (m, 2H), 2.85 (t, *J* = 6.4 Hz, 2H), 1.98 (q, *J* = 6.2 Hz, 2H).

¹³C NMR (151 MHz, Chloroform-*d*) δ 166.64, 161.11, 141.41, 131.38, 128.89, 128.54, 126.07, 116.35, 52.25, 40.76, 27.40, 21.94.

HRMS (ESI): m/z [M+H]⁺ calcd: 220.09682; found: 220.09680.

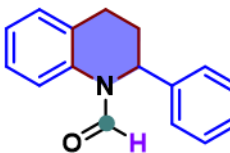


15

¹H NMR (400 MHz, Chloroform-*d*) δ 8.75 (s, 1H), 7.23-7.12 (m, 4H), 4.33 (dd, *J* = 13.1, 3.4 Hz, 1H), 3.64 (dd, *J* = 13.0, 8.3 Hz, 1H), 3.06-2.96 (m, 3H), 2.28 (s, 3H).

¹³C NMR (151 MHz, Chloroform-*d*) δ 207.25, 161.06, 136.72, 130.01, 127.54, 126.75, 125.19, 117.16, 46.12, 40.58, 28.85, 28.68.

HRMS (ESI): m/z [M+H]⁺ calcd: 204.10191; found: 204.10196.

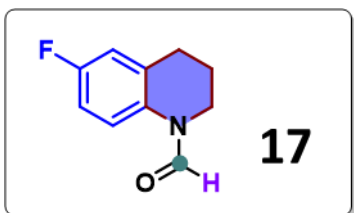


16

¹H NMR (400 MHz, Chloroform-*d*) δ 8.86 (s, 1H), 7.32-7.25 (m, 4H), 7.17 (dd, *J* = 16.9, 7.9 Hz, 5H), 5.76 (t, *J* = 6.3 Hz, 1H), 2.70 (q, *J* = 5.4, 4.7 Hz, 2H), 2.38 (dd, *J* = 13.6, 5.7 Hz, 1H), 2.14 (dq, *J* = 13.4, 6.6 Hz, 1H).

¹³C NMR (151 MHz, Chloroform-*d*) δ 161.75, 141.18, 137.36, 130.36, 129.28, 128.65, 127.65, 127.07, 126.04, 124.95, 118.01, 53.56, 30.29, 24.84.

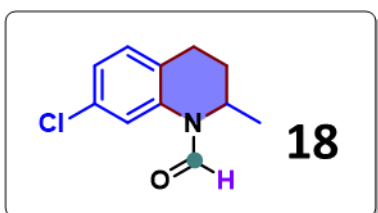
HRMS (ESI): m/z [M+Na]⁺ calcd: 260.10459; found: 260.10461.



¹H NMR (400 MHz, Chloroform-*d*) δ 8.64 (s, 1H), 7.08-6.99 (m, 1H), 6.83 (q, *J* = 12.6, 10.7 Hz, 2H), 3.73 (t, *J* = 6.3 Hz, 2H), 2.75 (t, *J* = 6.6 Hz, 2H), 1.90 (d, *J* = 6.3 Hz, 2H).

¹³C NMR (151 MHz, Chloroform-*d*) δ 161.26, 160.88, 160.46, 158.84, 133.42, 133.40, 131.05, 131.00, 118.51, 118.46, 116.07, 115.92, 113.86, 113.71, 40.05, 27.10, 22.04.

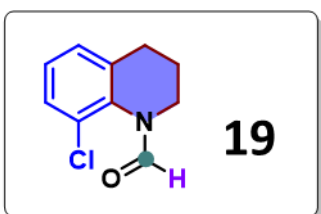
HRMS (ESI): m/z [M+Na]⁺ calcd: 202.06386; found: 202.06389.



¹H NMR (400 MHz, Chloroform-*d*) δ 8.66 (s, 1H), 7.12 (s, 1H), 7.11-7.04 (m, 2H), 4.81 (h, *J* = 6.3 Hz, 1H), 2.86-2.77 (m, 1H), 2.66 (dd, *J* = 16.4, 5.7 Hz, 1H), 2.11-2.03 (m, 1H), 1.70 (dd, *J* = 13.5, 5.8 Hz, 1H), 1.20 (d, *J* = 6.6 Hz, 3H).

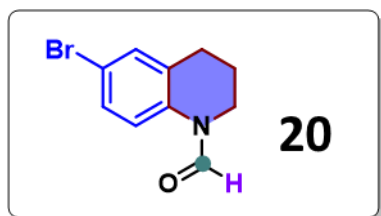
¹³C NMR (151 MHz, Chloroform-*d*) δ 160.89, 137.50, 132.62, 130.38, 128.04, 124.84, 118.52, 45.22, 28.91, 23.87, 18.17.

HRMS (ESI): m/z [M+H]⁺ calcd: 210.06802; found: 210.06799.



¹H NMR (400 MHz, Chloroform-*d*) δ 8.62 (s, 1H), 7.29 (dd, *J* = 6.2, 3.2 Hz, 1H), 7.10-7.06 (m, 2H), 3.78 (d, *J* = 6.7 Hz, 2H), 2.72 (d, *J* = 6.7 Hz, 2H), 1.95 (t, *J* = 5.6 Hz, 2H).
¹³C NMR (151 MHz, Chloroform-*d*) δ 163.63, 136.09, 135.08, 128.92, 127.29, 126.59, 126.36, 40.10, 27.24, 23.48.

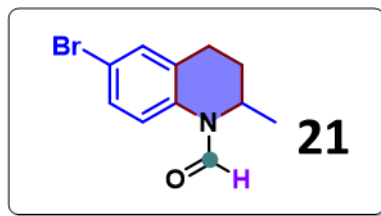
HRMS (ESI): m/z [M+H]⁺ calcd: 196.05237; found: 196.05246.



¹H NMR (400 MHz, Chloroform-*d*) δ 8.75 (s, 1H), 7.30 (d, *J* = 6.9 Hz, 2H), 7.04-7.00 (m, 1H), 3.80-3.76 (m, 2H), 2.79 (t, *J* = 6.5 Hz, 2H), 1.97-1.91 (m, 2H).

¹³C NMR (151 MHz, Chloroform-*d*) δ 160.89, 136.56, 132.54, 131.10, 130.20, 118.60, 117.62, 40.38, 27.13, 22.06.

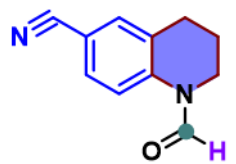
HRMS (ESI): m/z [M+H]⁺ calcd: 240.00185; found: 240.00186.



¹H NMR (400 MHz, Chloroform-*d*) δ 8.63 (s, 1H), 7.31 (d, *J* = 6.5 Hz, 2H), 6.99 (d, *J* = 9.2 Hz, 1H), 4.80 (h, *J* = 6.2 Hz, 1H), 2.84-2.77 (m, 1H), 2.66 (dd, *J* = 16.5, 5.8 Hz, 1H), 2.12-2.05 (m, 1H), 1.73-1.65 (m, 1H), 1.22 (d, *J* = 19.8 Hz, 3H).

¹³C NMR (151 MHz, Chloroform-*d*) δ 160.84, 135.54, 132.10, 131.87, 130.28, 119.98, 117.86, 45.23, 28.87, 24.16, 18.14.

HRMS (ESI): m/z [M+H]⁺ calcd: 254.01750; found: 254.01753.

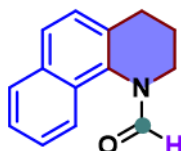


22

¹H NMR ¹H NMR (400 MHz, Chloroform-*d*) δ 8.87 (s, 1H), 7.50-7.44 (m, 2H), 7.25 (d, *J* = 8.3 Hz, 1H), 3.84-3.79 (m, 2H), 2.84 (t, *J* = 6.4 Hz, 2H), 1.96 (q, *J* = 6.3 Hz, 2H).

¹³C NMR (151 MHz, Chloroform-*d*) δ 160.79, 141.47, 133.65, 131.35, 129.70, 118.61, 117.04, 107.90, 40.78, 27.28, 21.60.

HRMS (ESI): m/z [M+H]⁺ calcd: 187.08659; found: 187.08658.

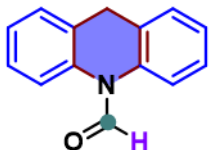


23

¹H NMR (400 MHz, Chloroform-*d*) δ 8.65 (s, 1H), 7.93 (d, *J* = 8.4 Hz, 1H), 7.85 (d, *J* = 6.9 Hz, 1H), 7.67 (d, *J* = 8.4 Hz, 1H), 7.49 (ddd, *J* = 11.2, 8.0, 1.4 Hz, 2H), 7.29 (d, *J* = 8.3 Hz, 1H), 3.95 (s, 2H), 2.94 (d, *J* = 6.7 Hz, 2H), 2.11-2.06 (m, 2H).

¹³C NMR (151 MHz, Chloroform-*d*) δ 164.49, 133.61, 133.26, 129.62, 128.63, 127.59, 127.01, 126.76, 125.89, 125.73, 122.21, 40.58, 27.24, 23.78.

HRMS (ESI): m/z [M+H]⁺ calcd: 212.10699; found: 212.10696.



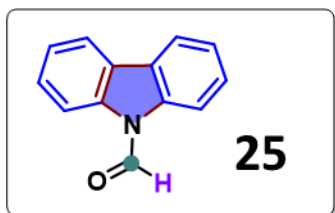
24

¹H NMR (400 MHz, Chloroform-*d*) δ 8.90 (s, 1H), 7.33 (t, *J* = 6.8 Hz, 8H), 3.90 (s, 2H).

¹³C NMR (151 MHz, Chloroform-*d*) δ 160.59, 131.29, 130.73, 128.24, 127.62, 127.48,

127.42, 126.23, 123.50, 119.88, 119.11, 33.04.

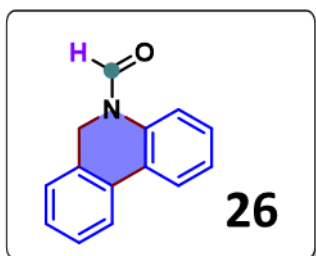
HRMS (ESI): m/z [M+H]⁺ calcd: 210.09134; found: 210.09125.



¹H NMR (400 MHz, Chloroform-*d*) δ 9.69 (s, 1H), 8.58 (s, 1H), 7.98 (d, *J* = 7.2 Hz, 2H), 7.71 (s, 1H), 7.52-7.40 (m, 4H).

¹³C NMR (151 MHz, Chloroform-*d*) δ 157.44, 127.81, 127.07, 126.17, 124.70, 124.33, 120.78, 119.84, 116.83, 109.95.

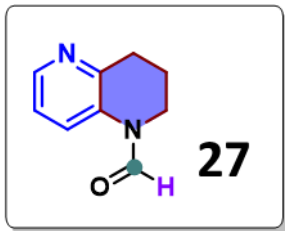
HRMS (ESI): m/z [M+H]⁺ calcd: 196.07569; found: 196.07553.



¹H NMR (400 MHz, Chloroform-*d*) δ 8.58 (s, 1H), 7.89-7.83 (m, 1H), 7.79 (d, *J* = 7.7 Hz, 1H), 7.29 (dd, *J* = 9.5, 8.9, 6.6, 4.4 Hz, 6H), 4.91 (s, 2H).

¹³C NMR (151 MHz, Chloroform-*d*) δ 160.62, 136.25, 132.69, 130.77, 128.80, 128.29, 128.22, 127.85, 126.43, 126.26, 124.39, 123.28, 119.18, 42.15.

HRMS (ESI): m/z [M+H]⁺ calcd: 210.09134; found: 210.09132.

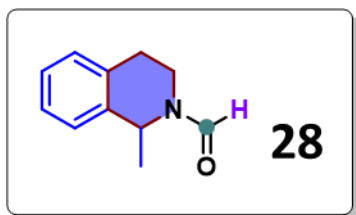


¹H NMR (400 MHz, Chloroform-*d*) δ 8.76 (s, 1H), 8.37 (d, *J* = 11.4 Hz, 1H), 7.48 (d, *J* = 8.2 Hz, 1H), 7.15 (s, 1H), 3.89-3.77 (m, 2H), 3.02 (t, *J* = 6.6 Hz, 2H), 2.04 (dd, *J* =

12.3, 6.3 Hz, 2H).

^{13}C NMR (151 MHz, Chloroform-*d*) δ 160.50, 149.07, 145.23, 129.41, 123.56, 39.98, 30.39, 21.57.

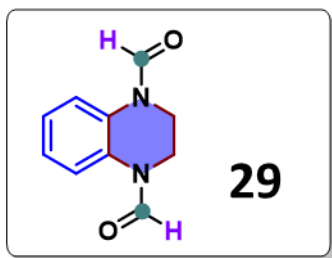
HRMS (ESI): m/z [M+H]⁺ calcd: 163.08659; found: 163.08652.



^1H NMR (400 MHz, Chloroform-*d*) δ 8.13 (s, 1H), 7.17 (dd, *J* = 21.2, 10.5, 8.0, 5.9 Hz, 4H), 5.45 (q, *J* = 6.9 Hz, 1H), 3.69 (dd, *J* = 13.3, 6.0 Hz, 1H), 3.58-3.51 (m, 1H), 2.99-2.77 (m, 2H), 1.55 (d, *J* = 6.9 Hz, 1H), 1.47 (d, *J* = 6.9 Hz, 2H).

^{13}C NMR (151 MHz, Chloroform-*d*) δ 161.14, 137.39, 133.75, 132.85, 129.36, 129.05, 127.18, 127.09, 126.77, 126.70, 126.52, 52.74, 47.09, 39.93, 34.03, 29.96, 28.25, 24.43, 21.73.

HRMS (ESI): m/z [M+H]⁺ calcd: 176.10699; found: 176.10693.



^1H NMR (400 MHz, Chloroform-*d*) δ 8.84 (s, 2H), 7.31 (dd, *J* = 6.1, 3.5 Hz, 2H), 7.20 (dd, *J* = 6.1, 3.5 Hz, 2H), 3.91 (s, 4H).

^{13}C NMR (126 MHz, Chloroform-*d*) δ 159.95, 128.59, 125.78, 117.60, 38.83.

HRMS (ESI): m/z [M+H]⁺ calcd: 191.08150; found: 191.08150.

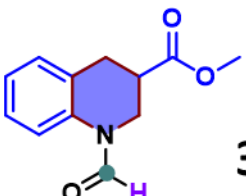


30

¹H NMR (400 MHz, Chloroform-*d*) δ 8.24 (s, 1H), 8.02 (s, 1H), 7.14 (t, *J* = 7.8 Hz, 1H), 6.93 (d, *J* = 8.1 Hz, 1H), 6.76 (d, *J* = 7.5 Hz, 1H), 3.77-3.74 (m, 2H), 2.95 (t, *J* = 7.1 Hz, 2H), 2.14-2.08 (m, 2H).

¹³C NMR (126 MHz, Chloroform-*d*) δ 162.54, 150.18, 131.56, 127.96, 126.43, 121.48, 118.46, 47.14, 26.58, 24.25.

HRMS (ESI): m/z [M+H]⁺ calcd: 178.08626; found: 178.08612.



31

¹H NMR (400 MHz, Chloroform-*d*) δ 8.77 (s, 1H), 7.22-7.12 (m, 4H), 4.38 (dd, *J* = 12.8, 4.6 Hz, 1H), 3.72 (s, 3H), 3.65 (dd, *J* = 13.0, 9.2 Hz, 1H), 3.10-3.07 (m, 2H), 2.93 (ddd, *J* = 16.8, 8.0, 4.4 Hz, 1H).

¹³C NMR (151 MHz, Chloroform-*d*) δ 172.80, 161.06, 136.81, 129.99, 127.65, 126.66, 125.13, 117.17, 52.29, 41.17, 38.77, 29.71.

HRMS (ESI): m/z [M+H]⁺ calcd: 220.09682; found: 220.09673.

V. NMR and ESI-HRMS spectra of all products

Fig. S10 ^1H NMR of 4

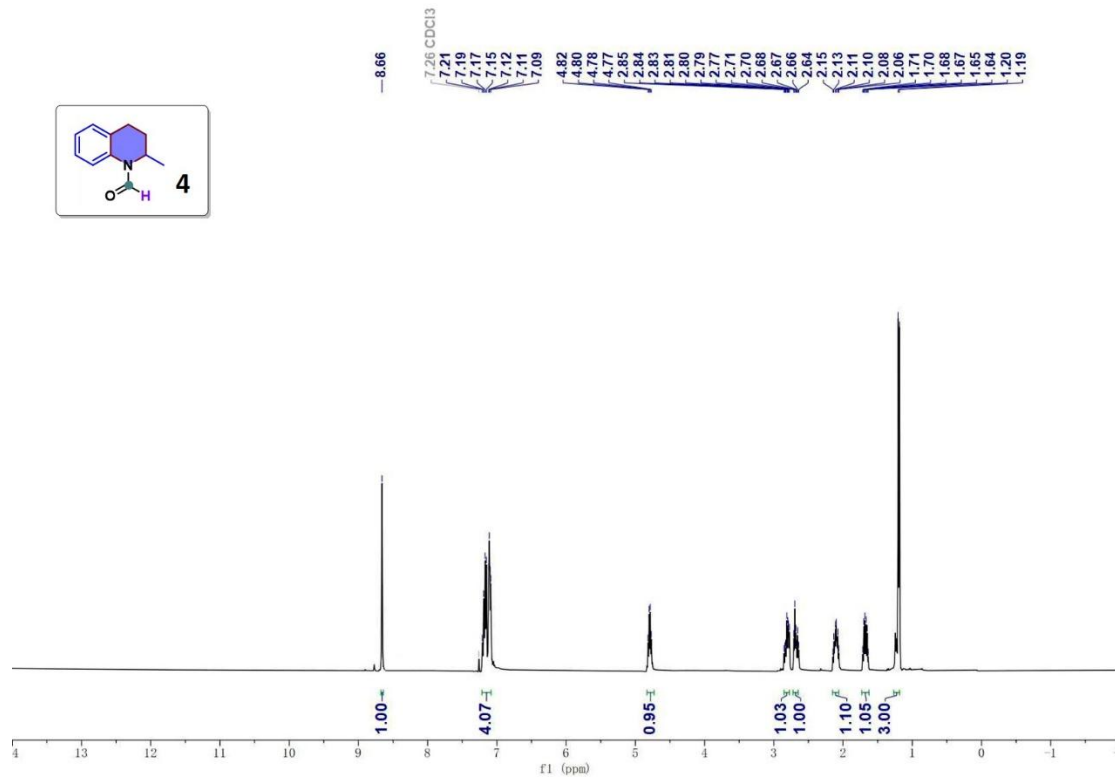


Fig. S11 ^{13}C NMR of 4

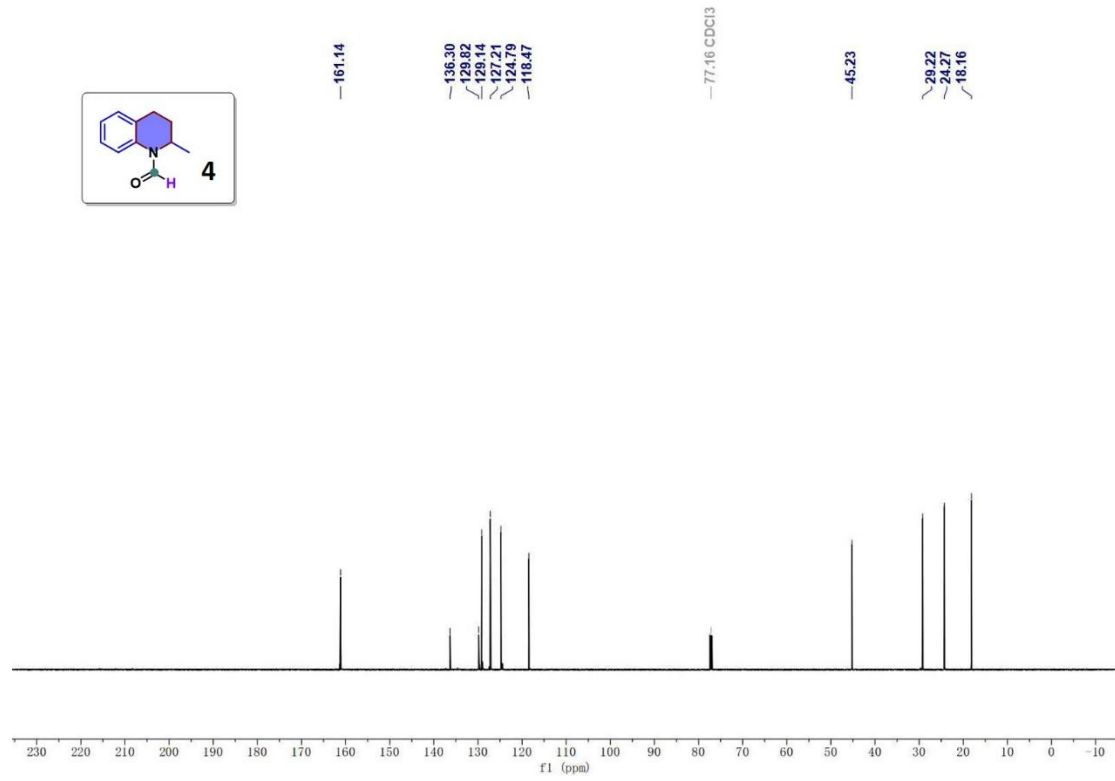


Fig. S12 ^1H NMR of **5**

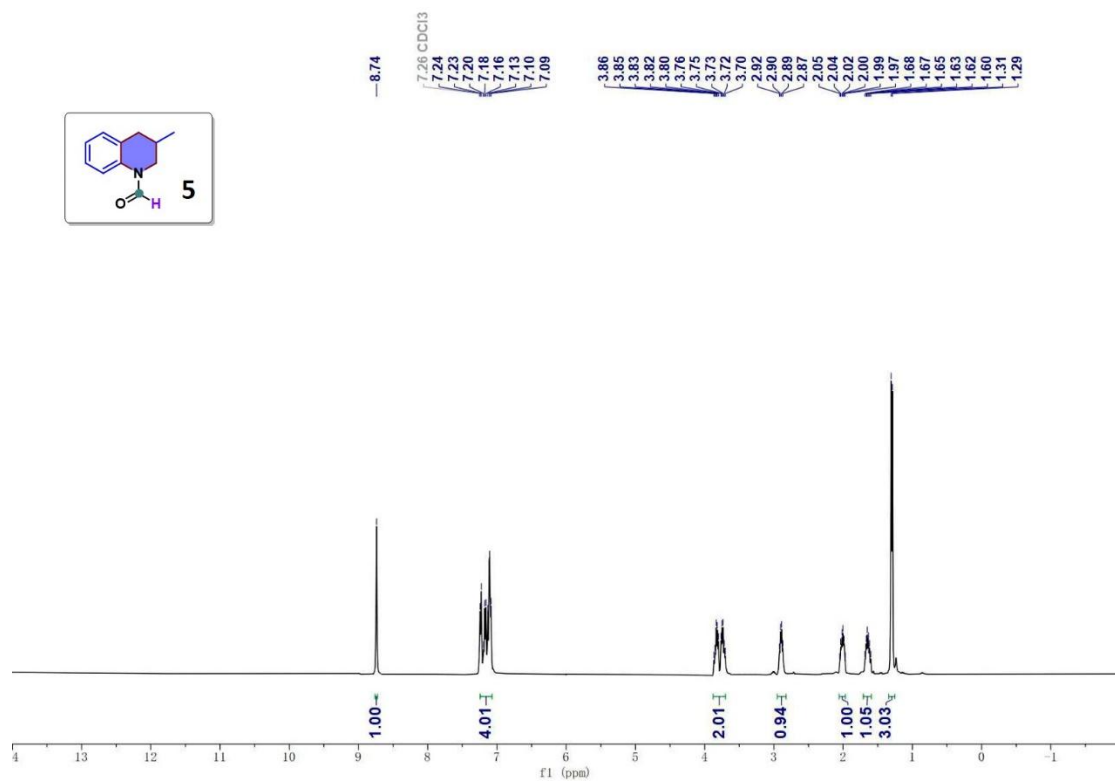


Fig. S13 ^{13}C NMR of **5**

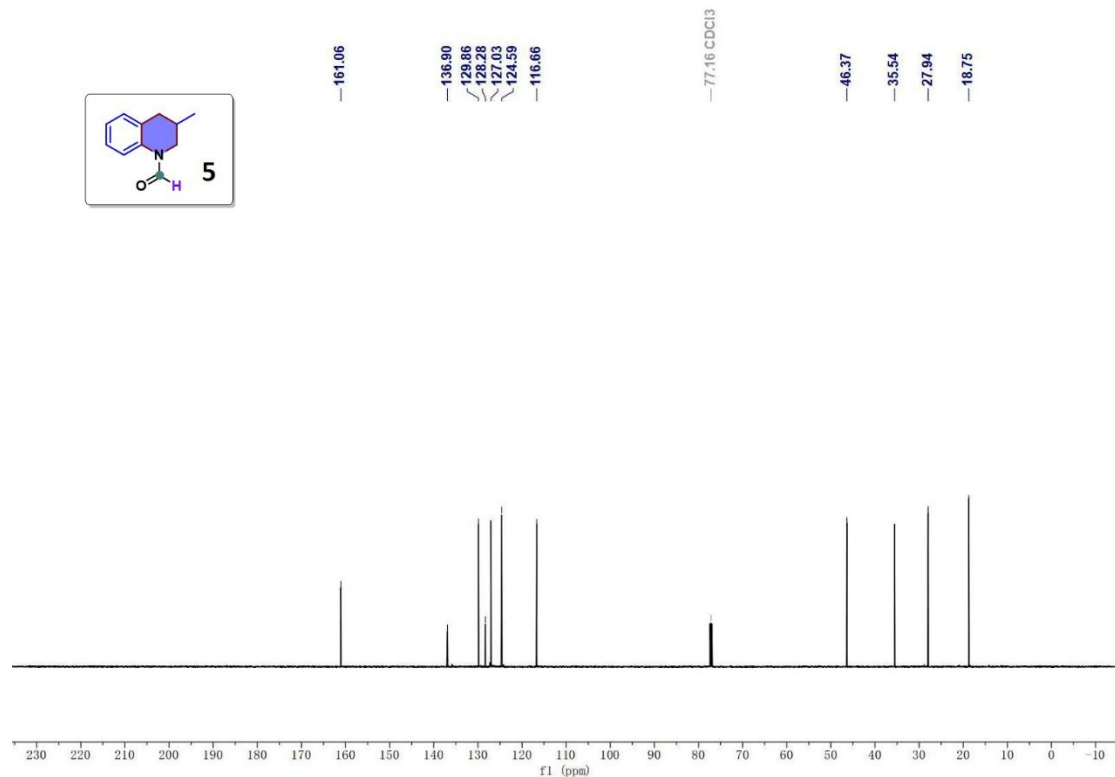


Fig. S14 ^1H NMR of **6**

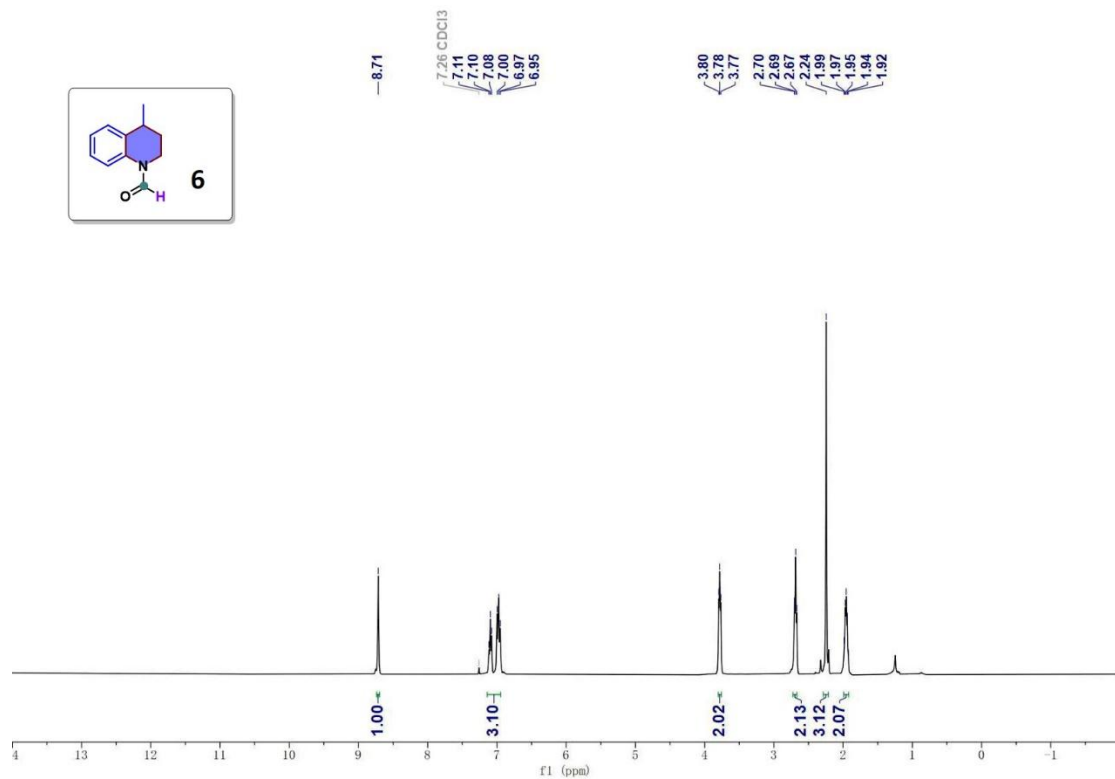


Fig. S15 ^{13}C NMR of **6**

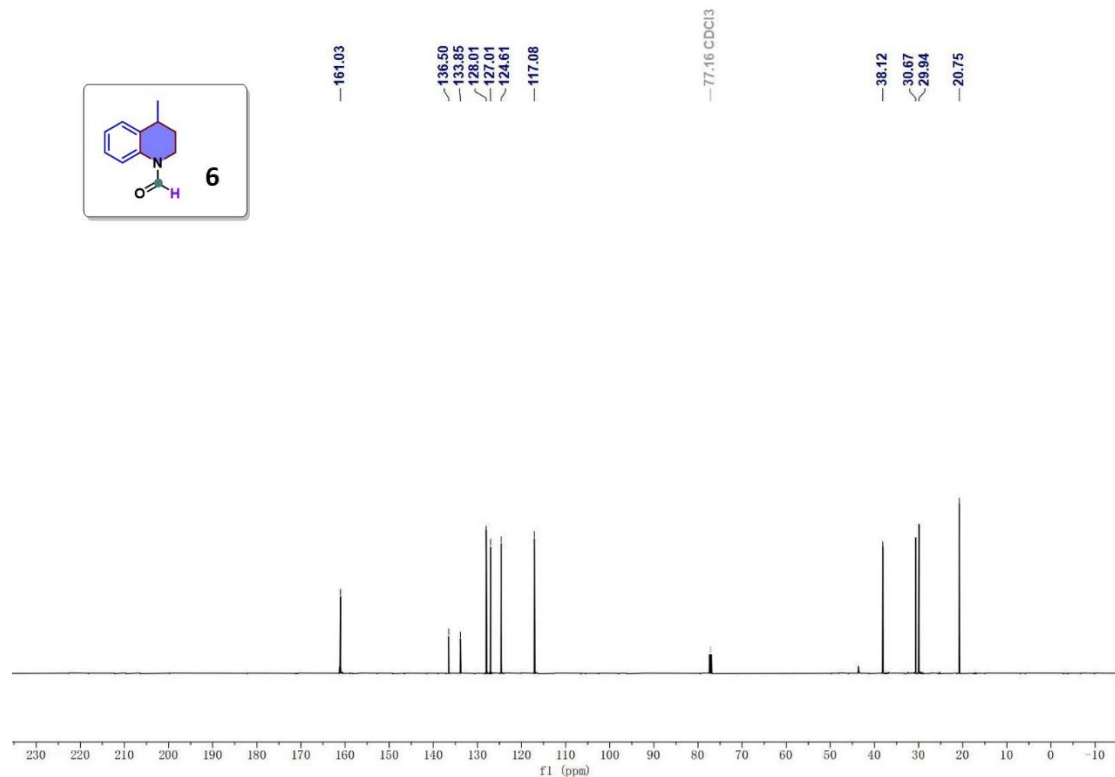


Fig. S16 ^1H NMR of **7**

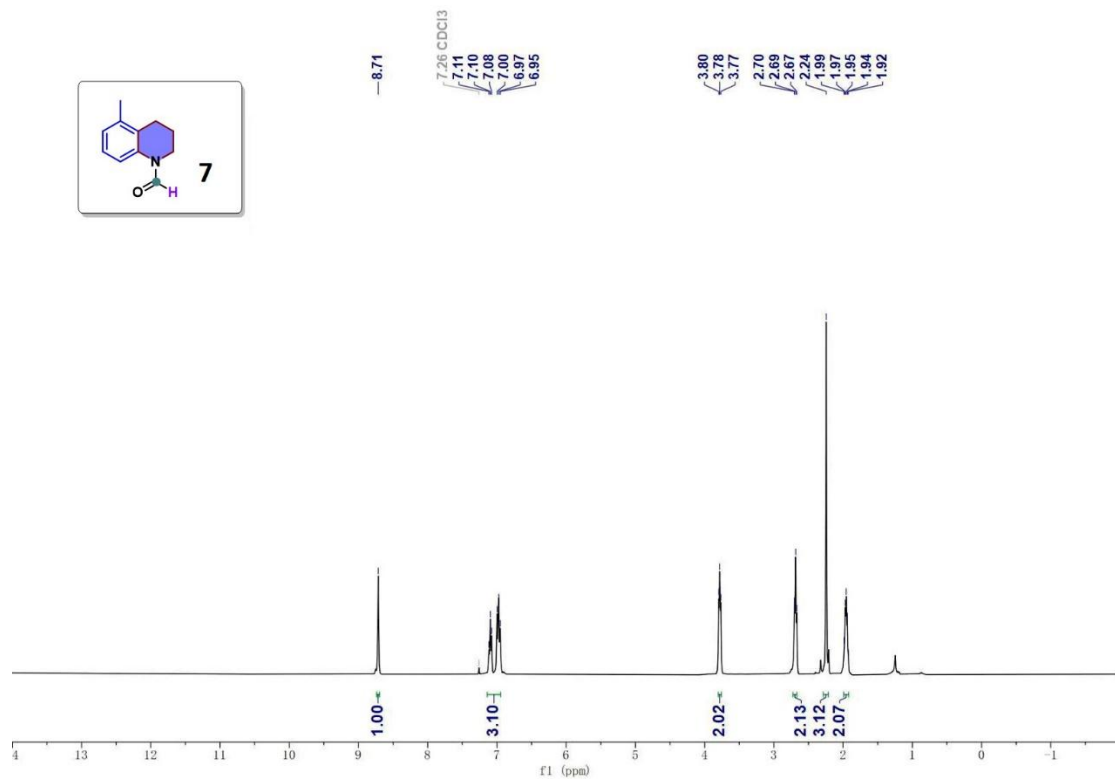


Fig. S17 ^{13}C NMR of **7**

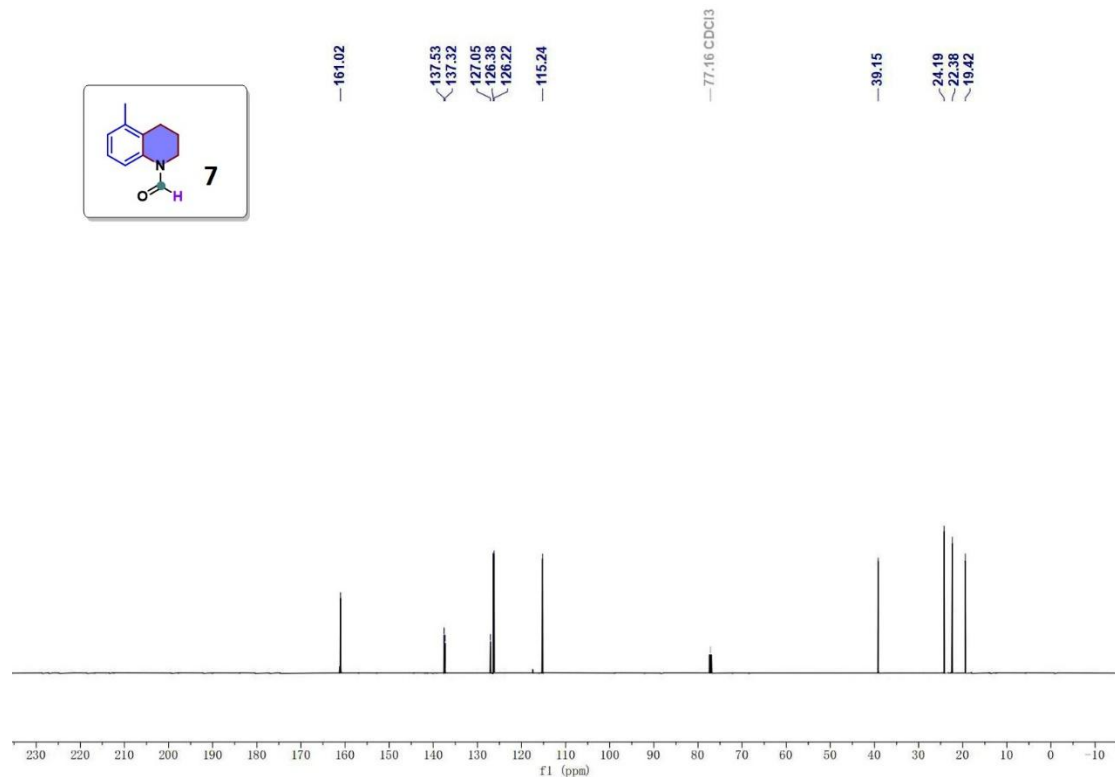


Fig. S18 ^1H NMR of **8**

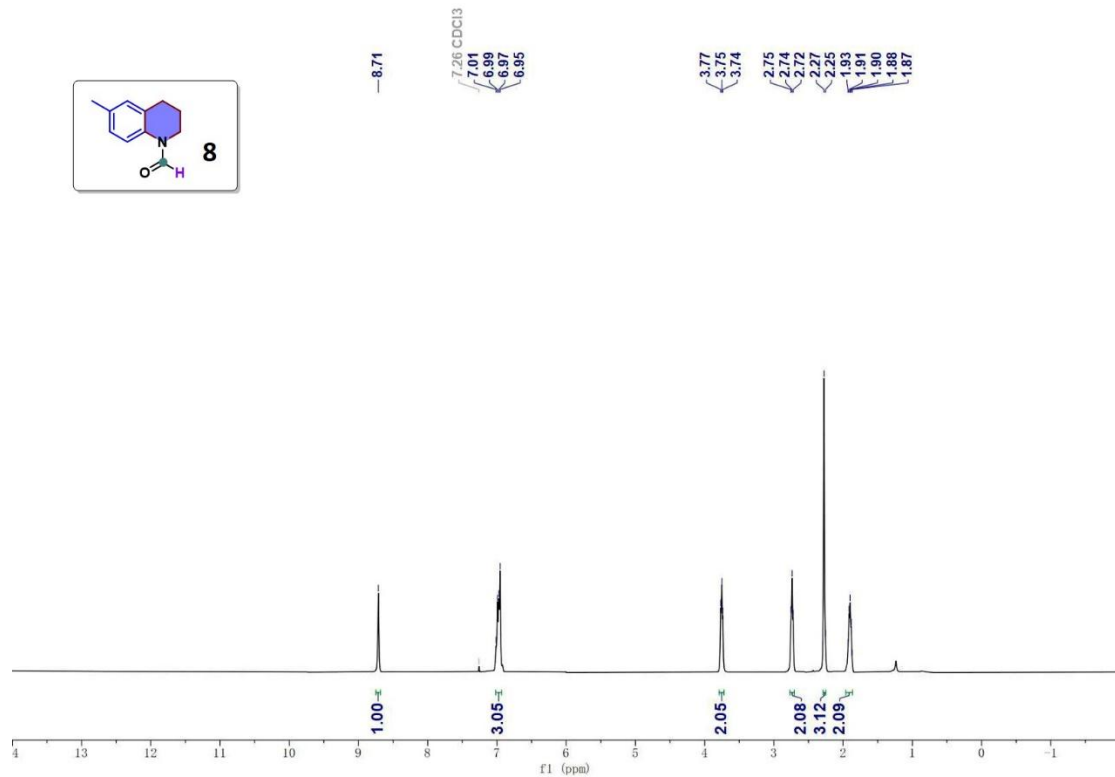


Fig. S19 ^{13}C NMR of **8**

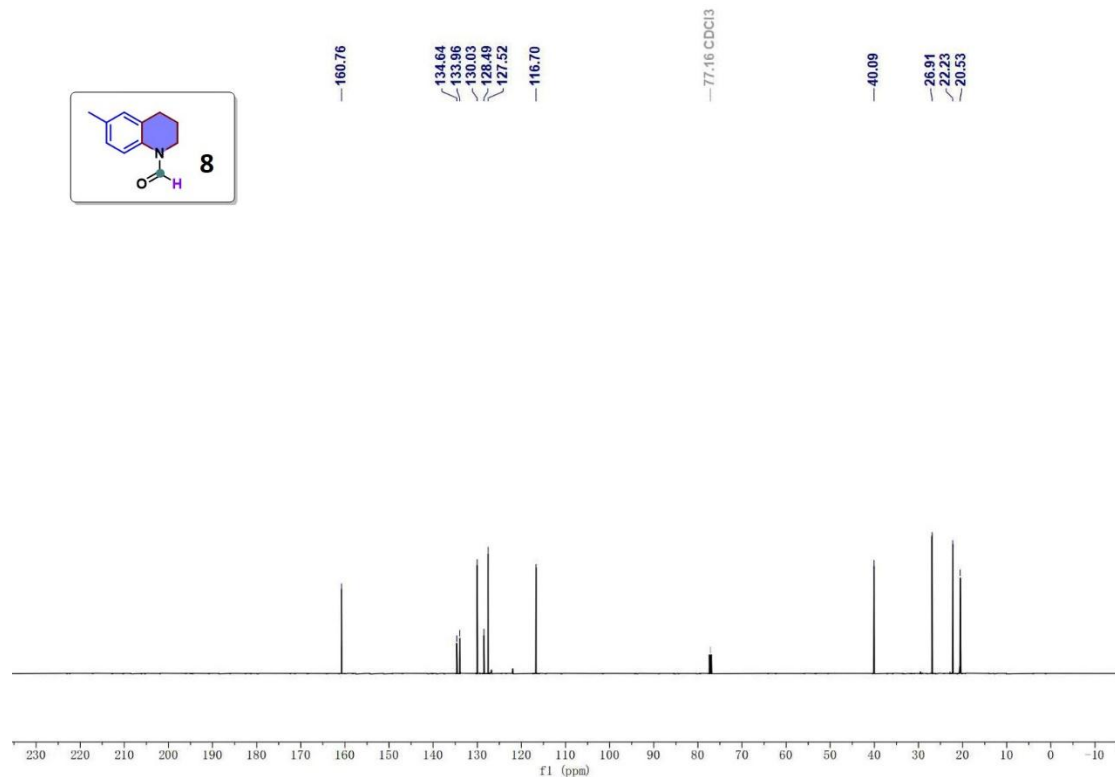


Fig. S20 ^1H NMR of **9**

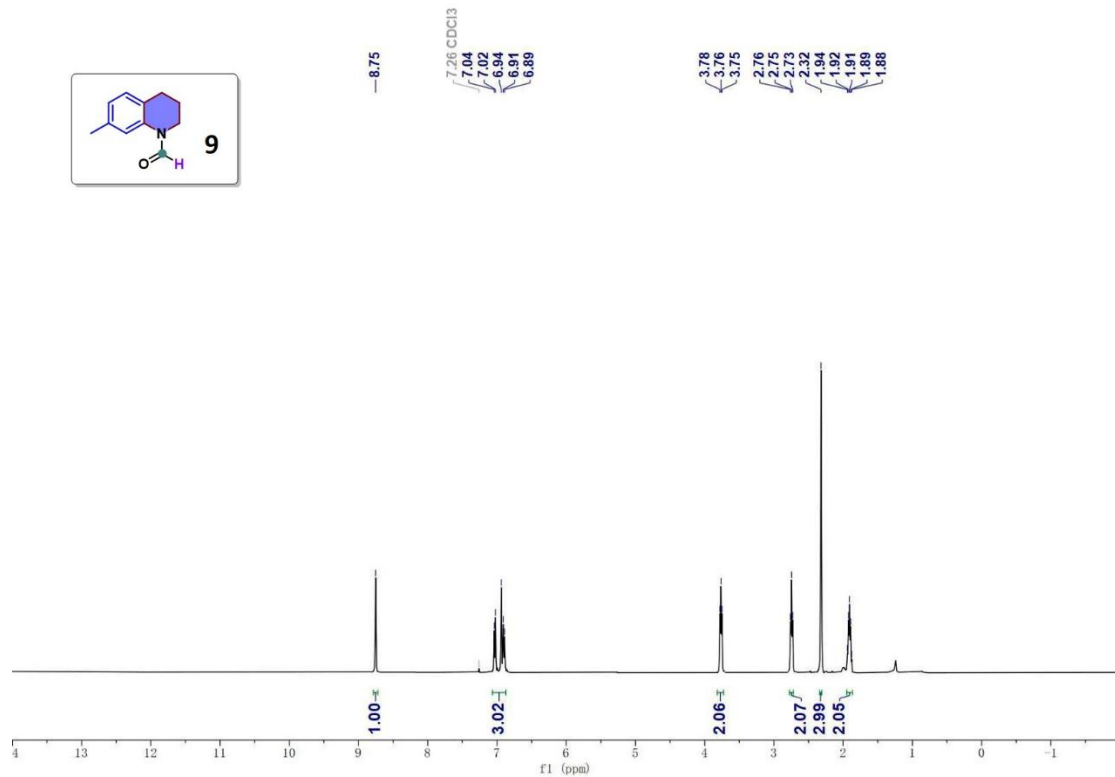


Fig. S21 ^{13}C NMR of **9**

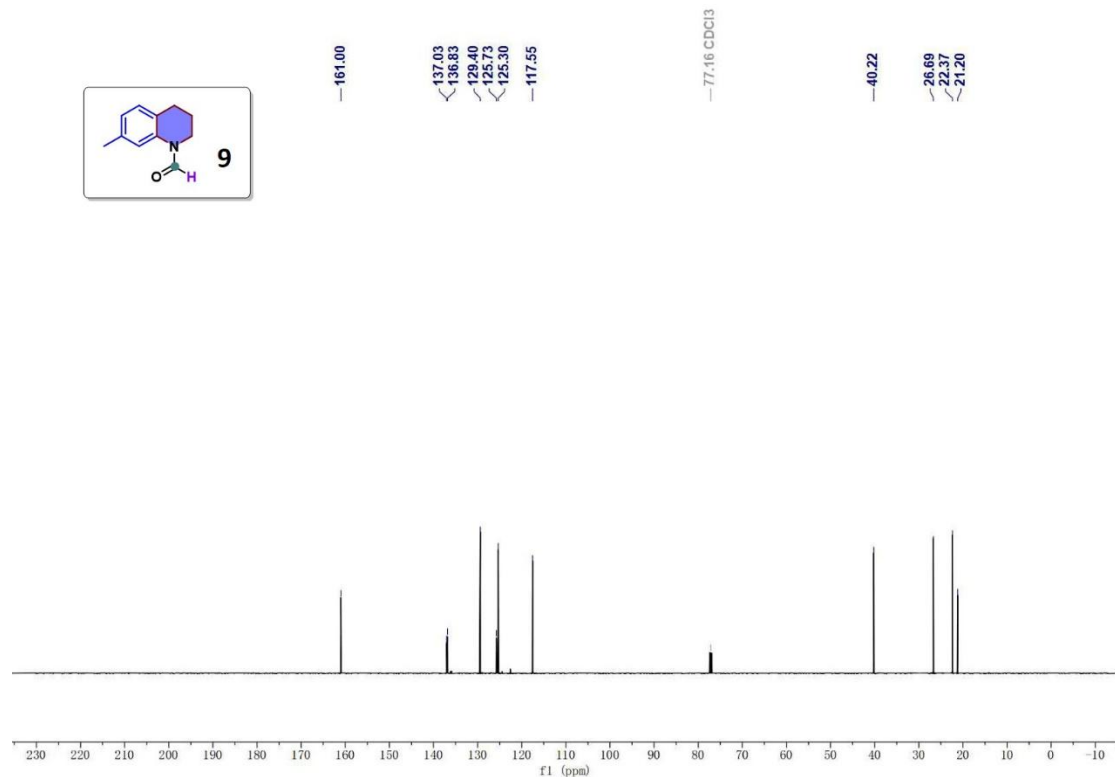


Fig. S22 ^1H NMR of **10**

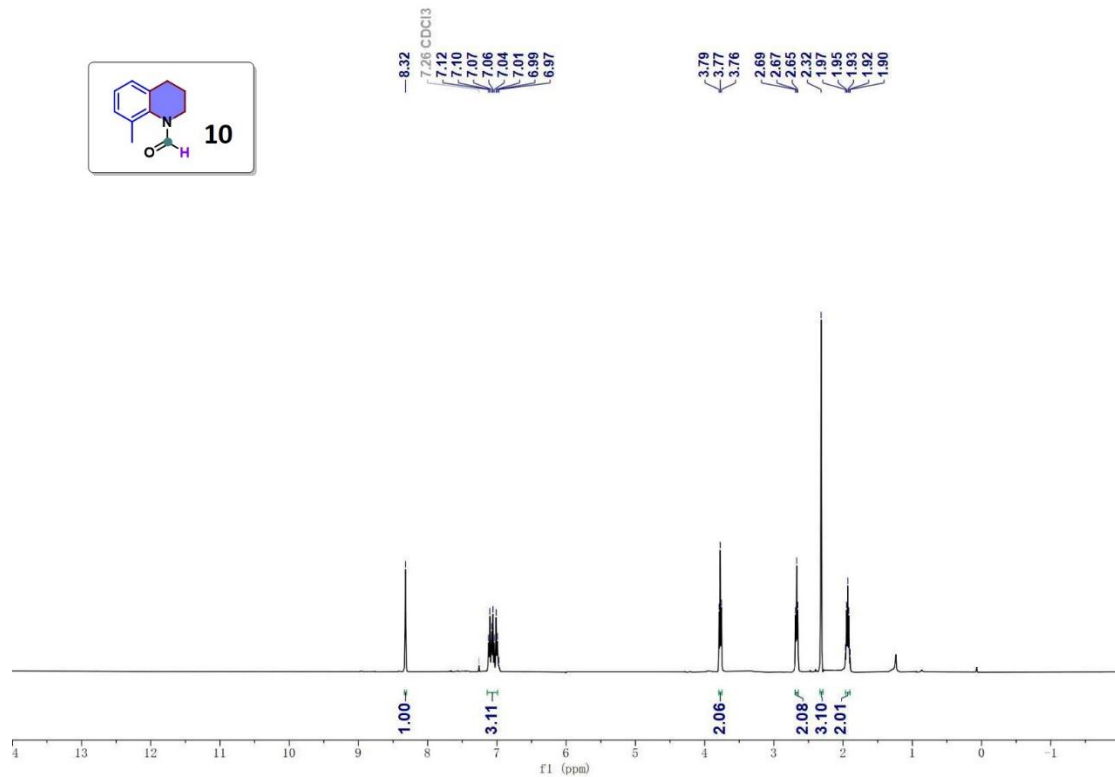


Fig. S23 ^{13}C NMR of **10**

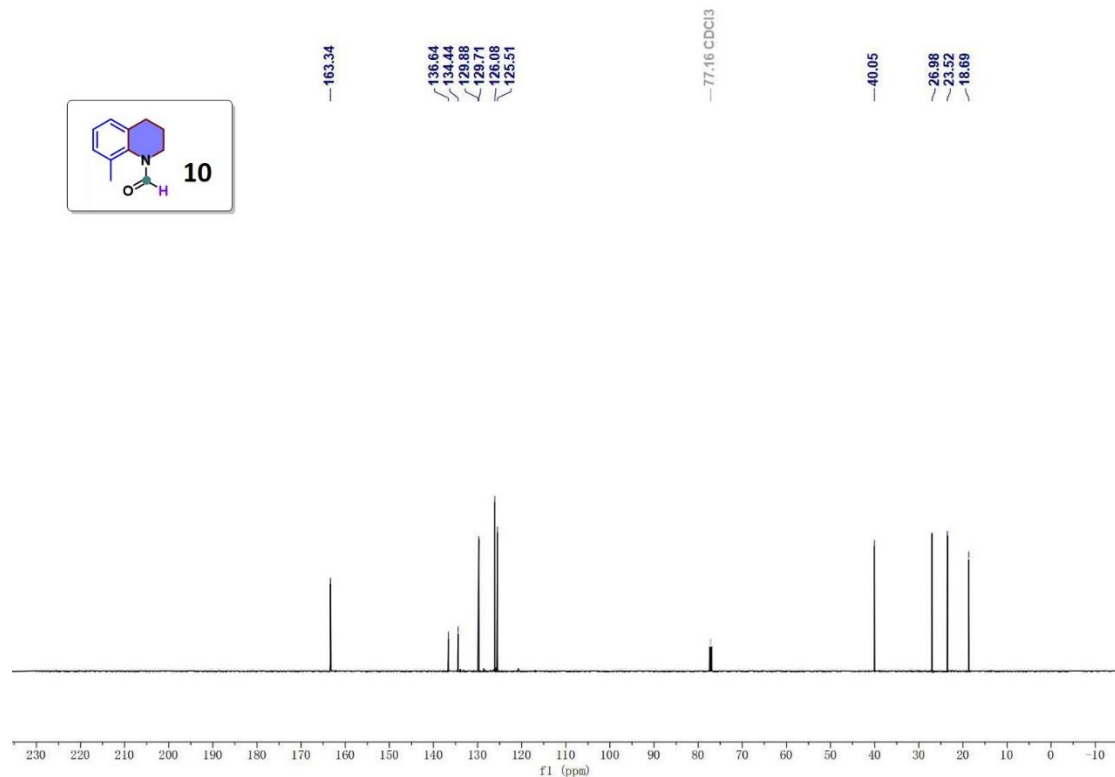


Fig. S24 ^1H NMR of **11**

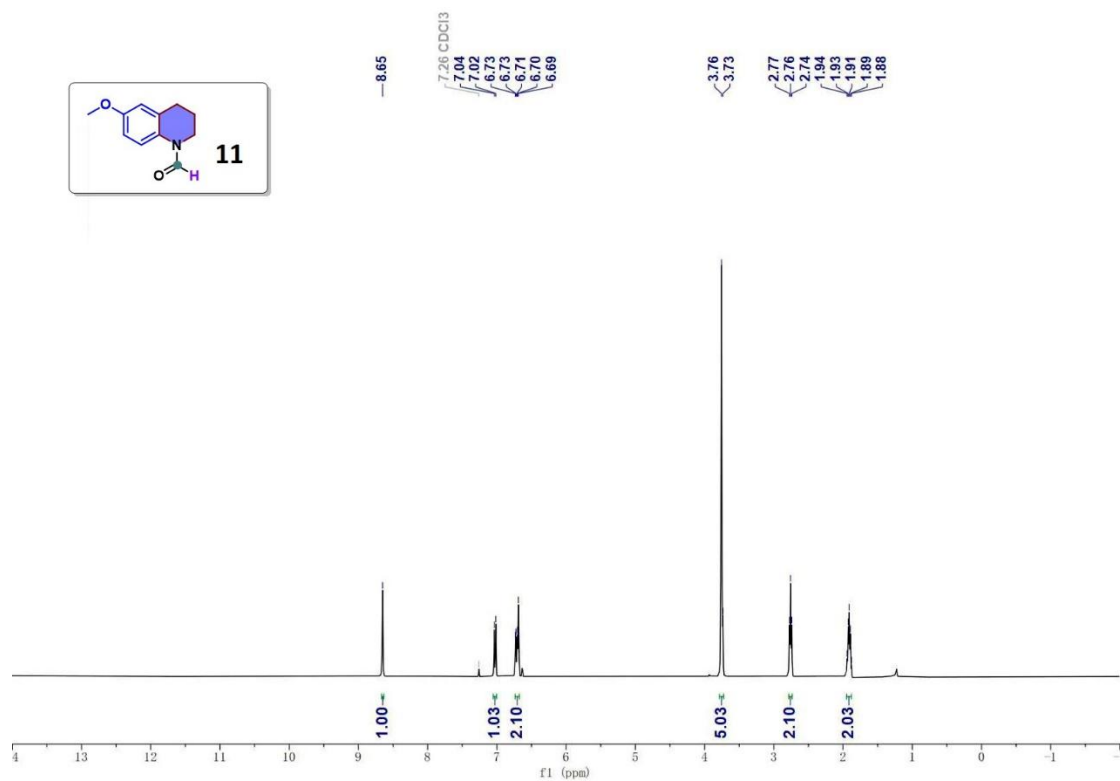


Fig. S25 ^{13}C NMR of **11**

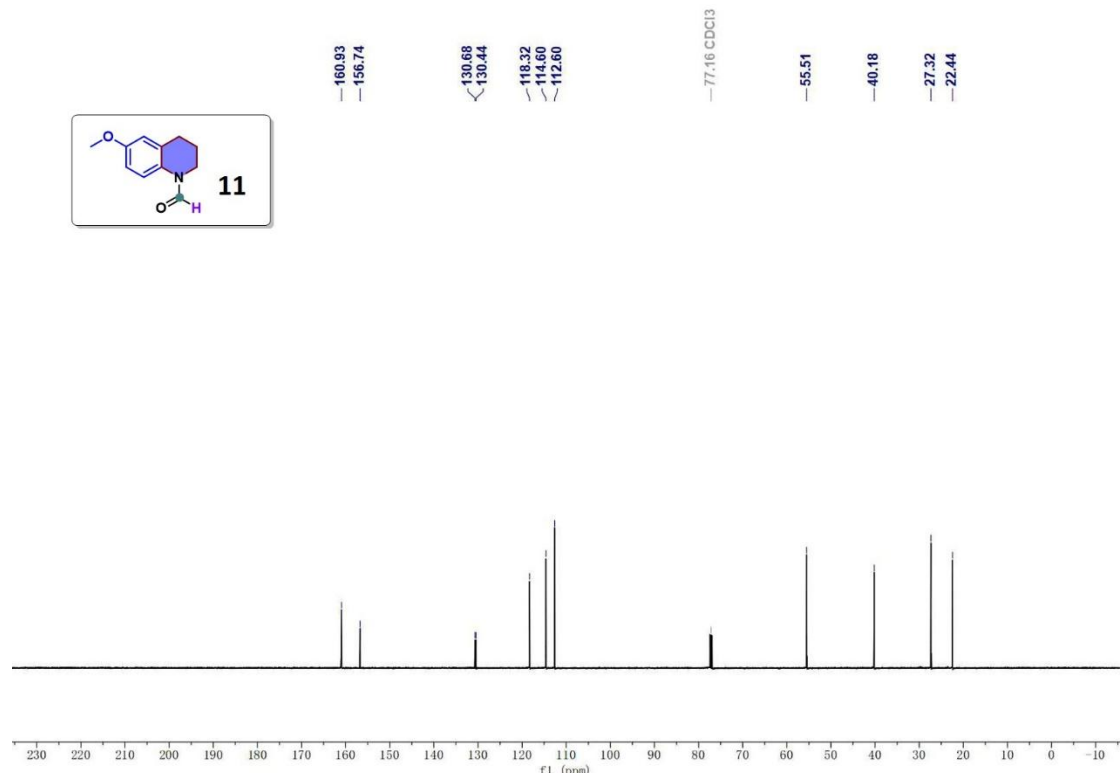


Fig. S26 ^1H NMR of **12**

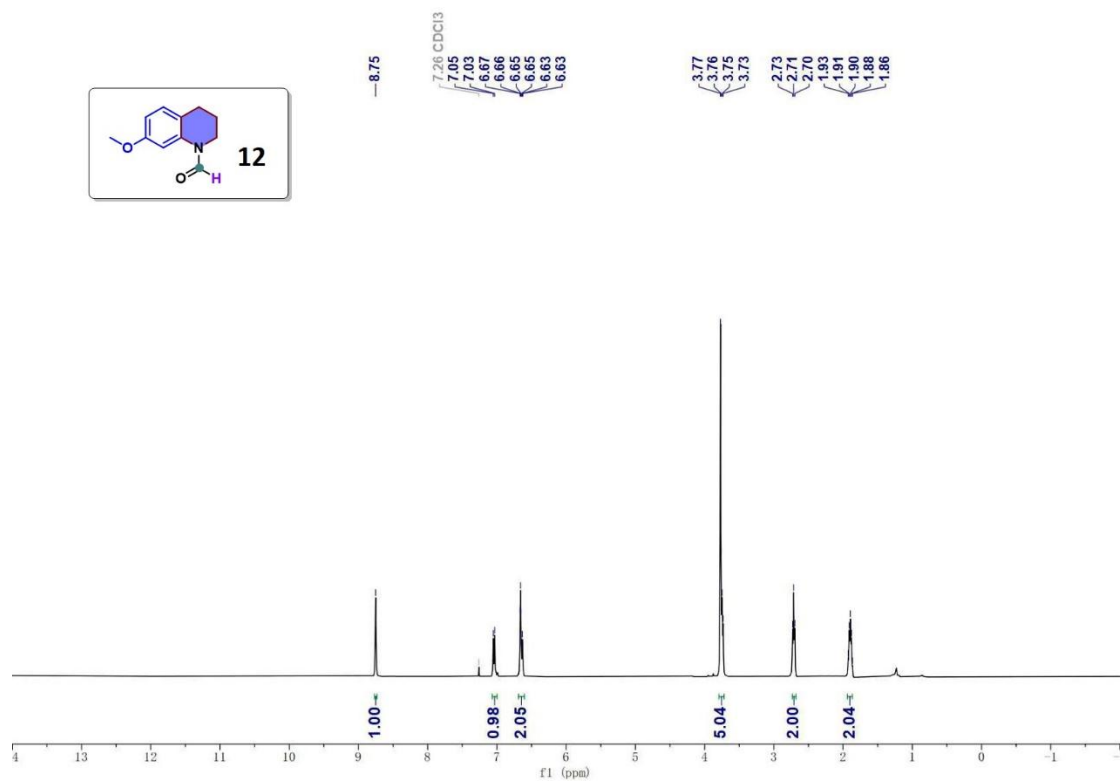


Fig. S27 ^{13}C NMR of **12**

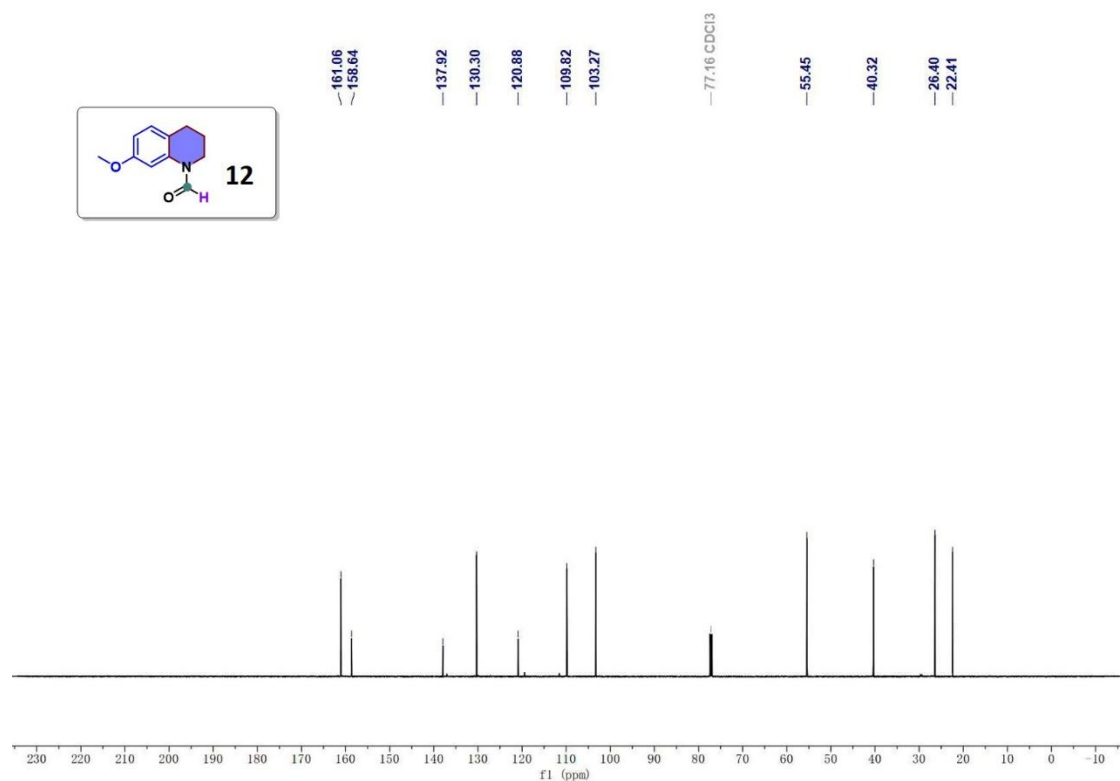


Fig. S28 ^1H NMR of **13**

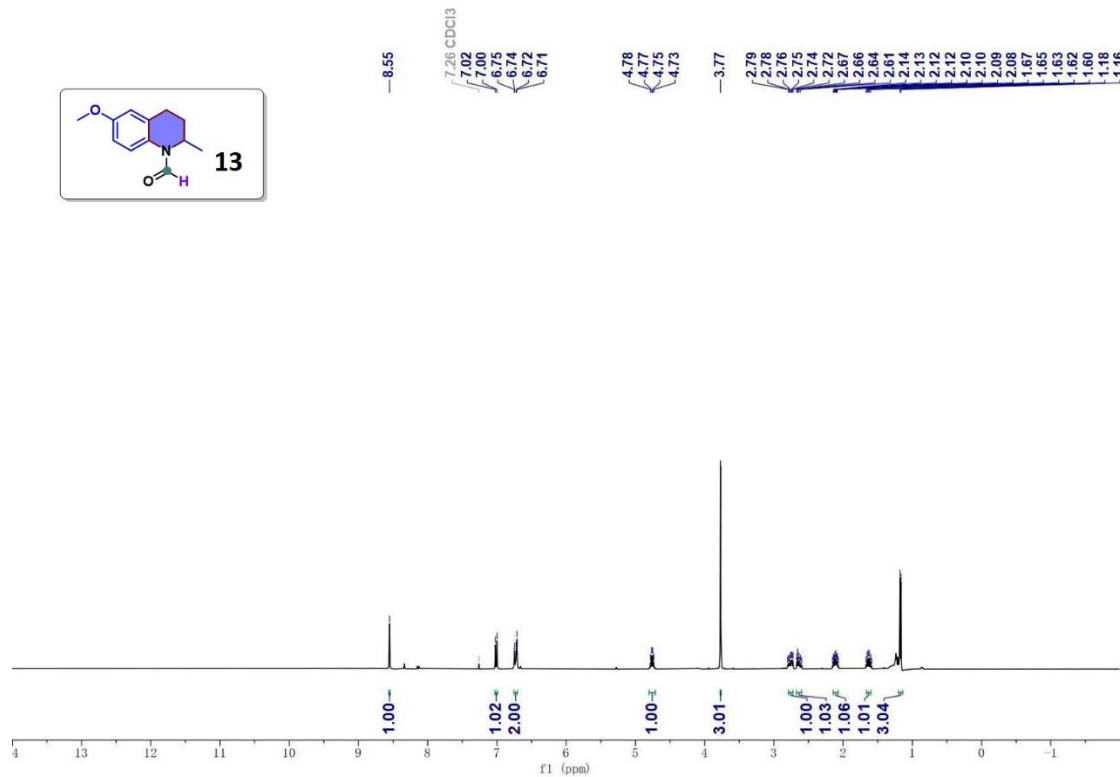


Fig. S29 ^{13}C NMR of **13**

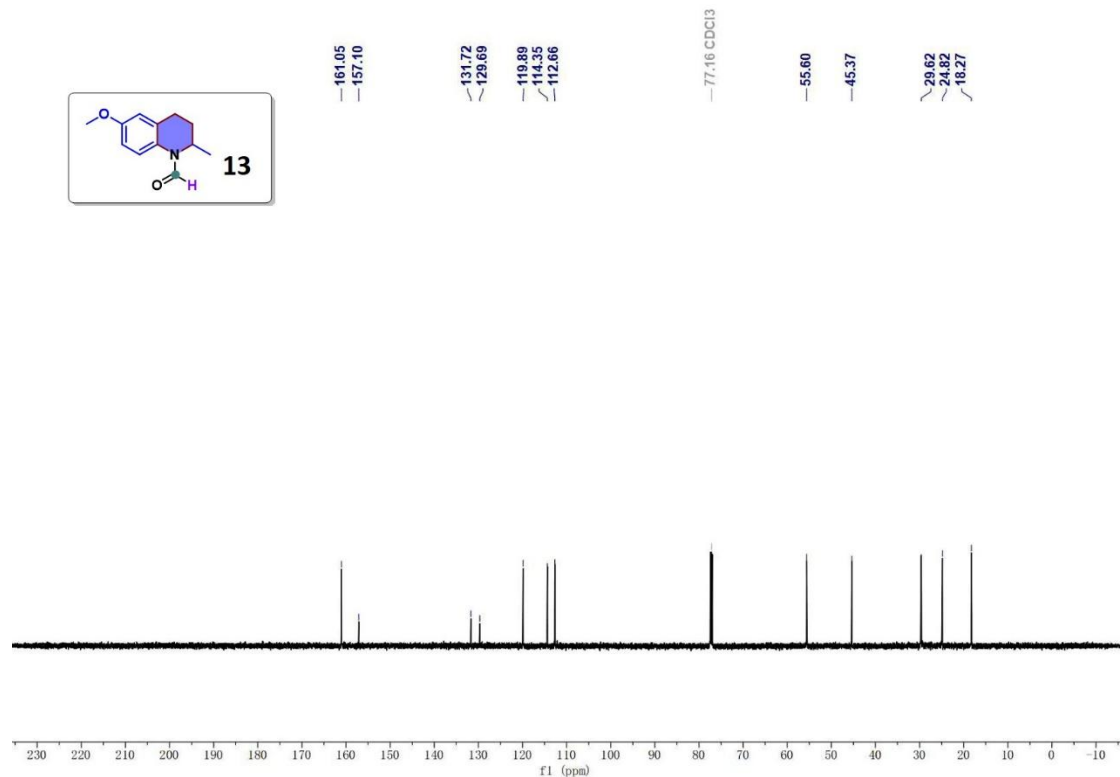


Fig. S30 ^1H NMR of **14**

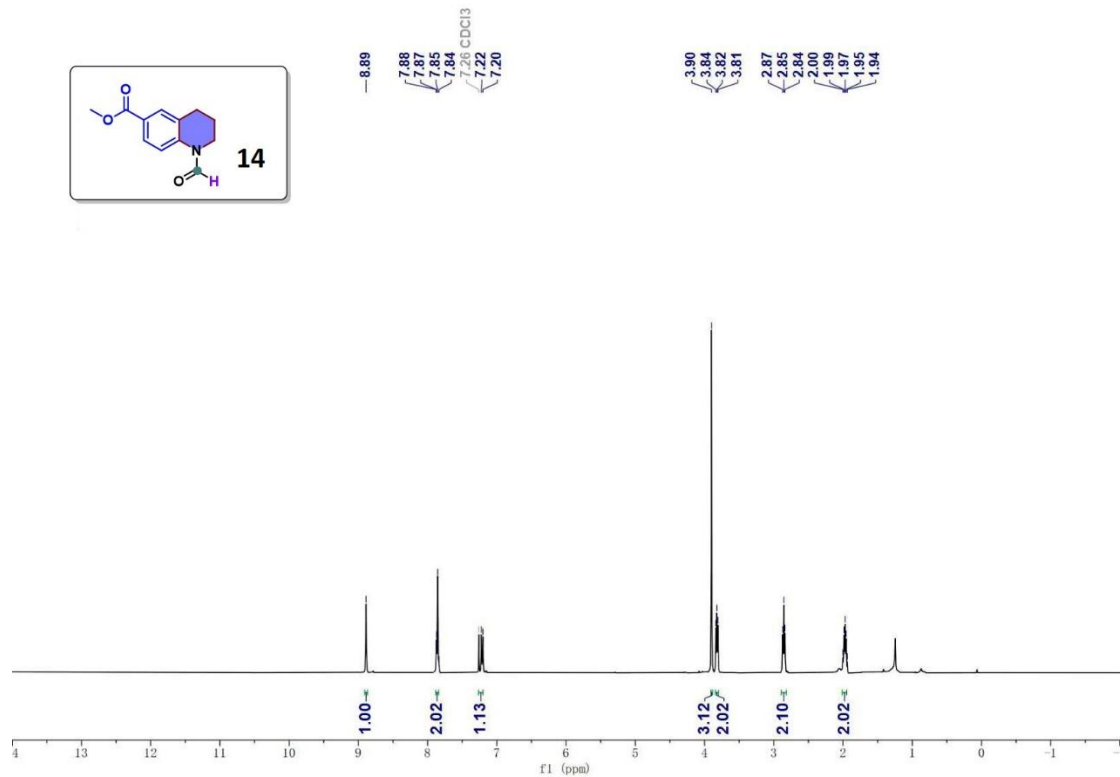


Fig. S31 ^{13}C NMR of **14**

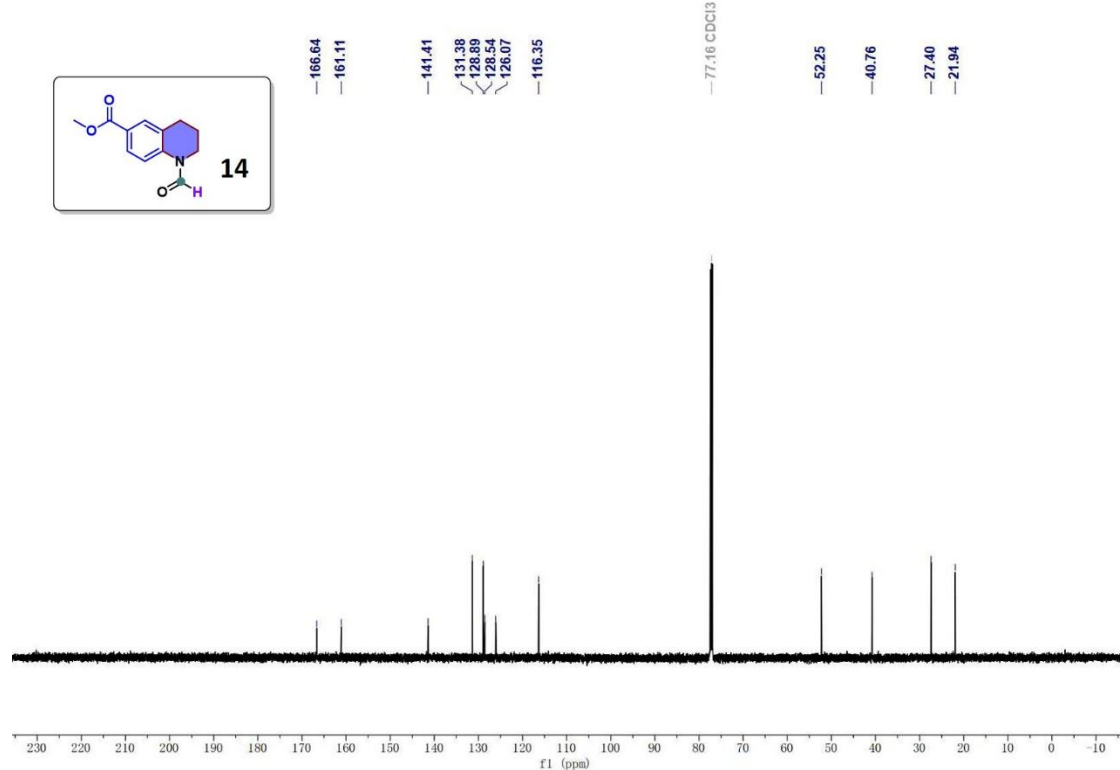


Fig. S32 ^1H NMR of **15**

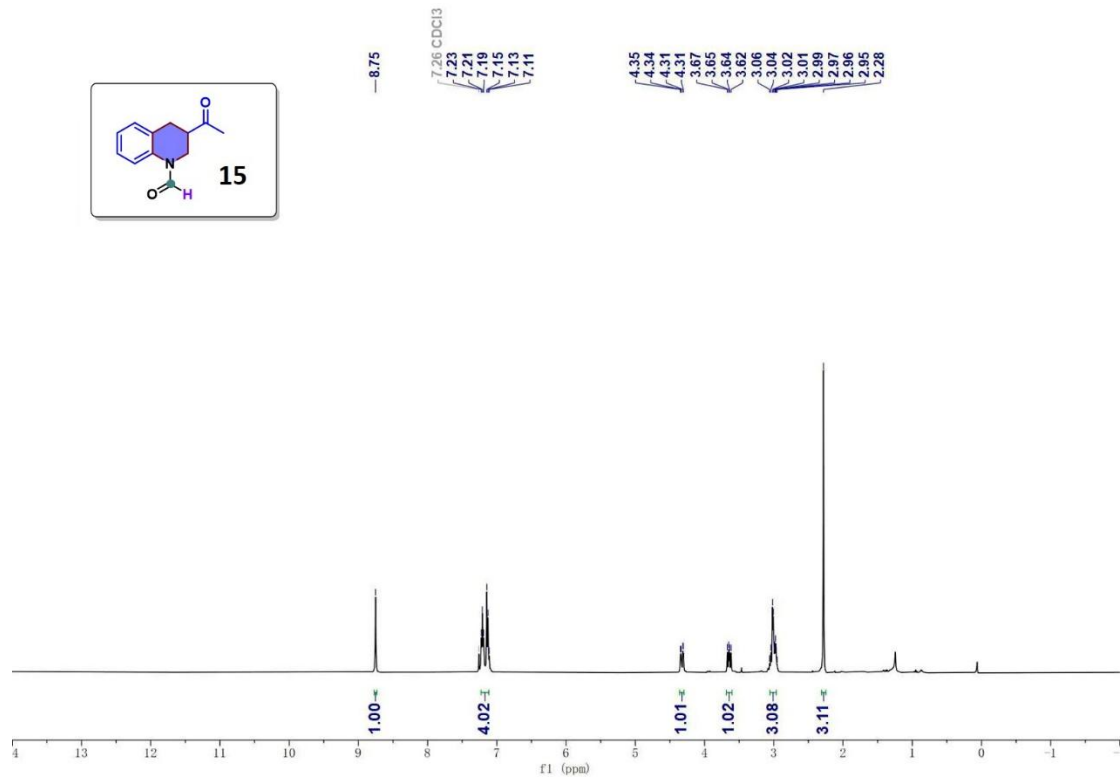


Fig. S33 ^{13}C NMR of **15**

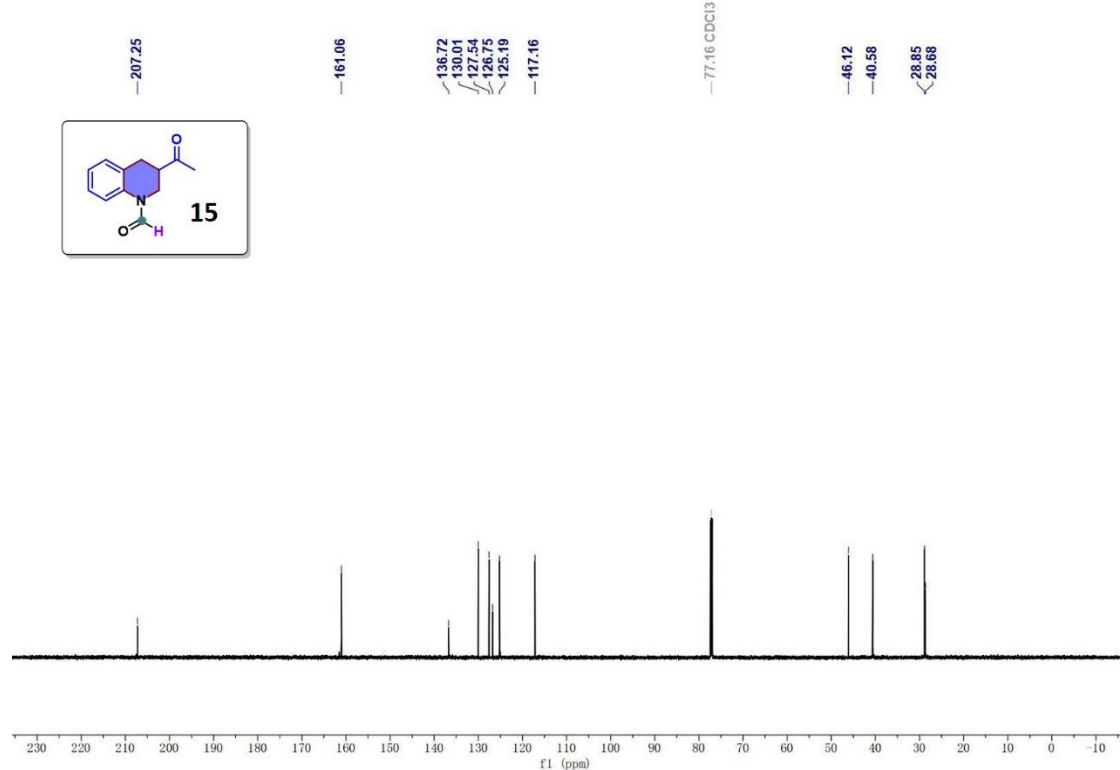


Fig. S34 ^1H NMR of **16**

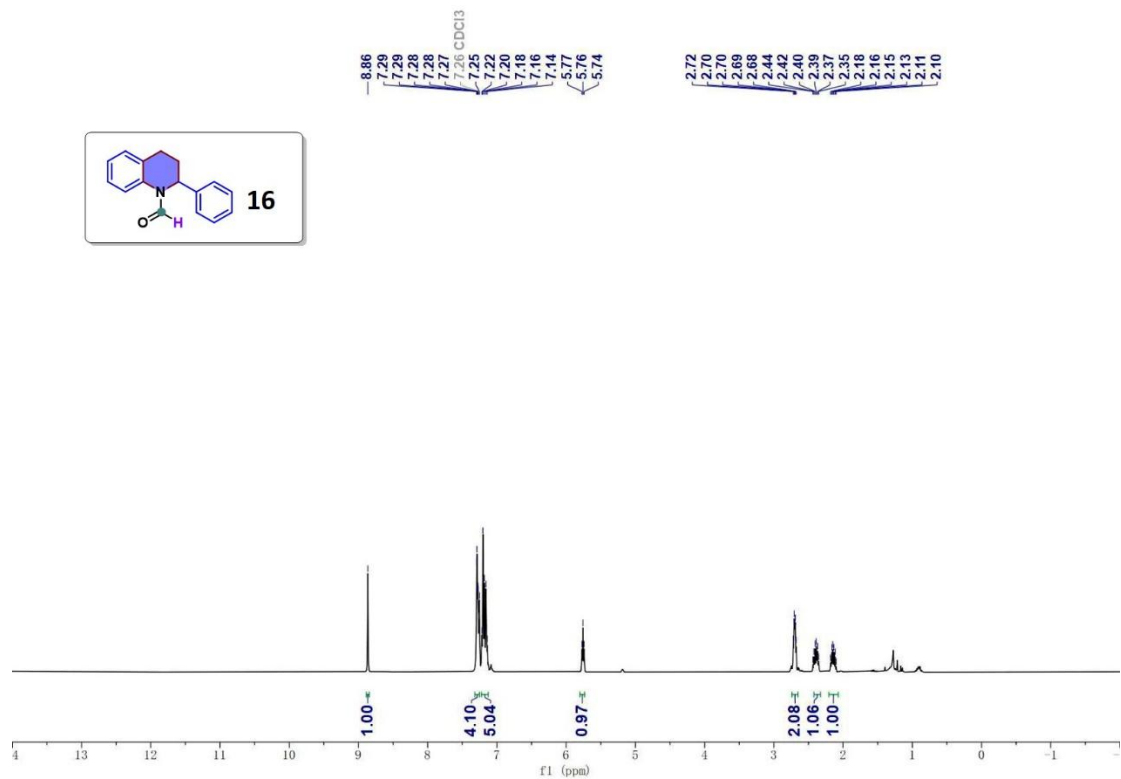


Fig. S35 ^{13}C NMR of **16**

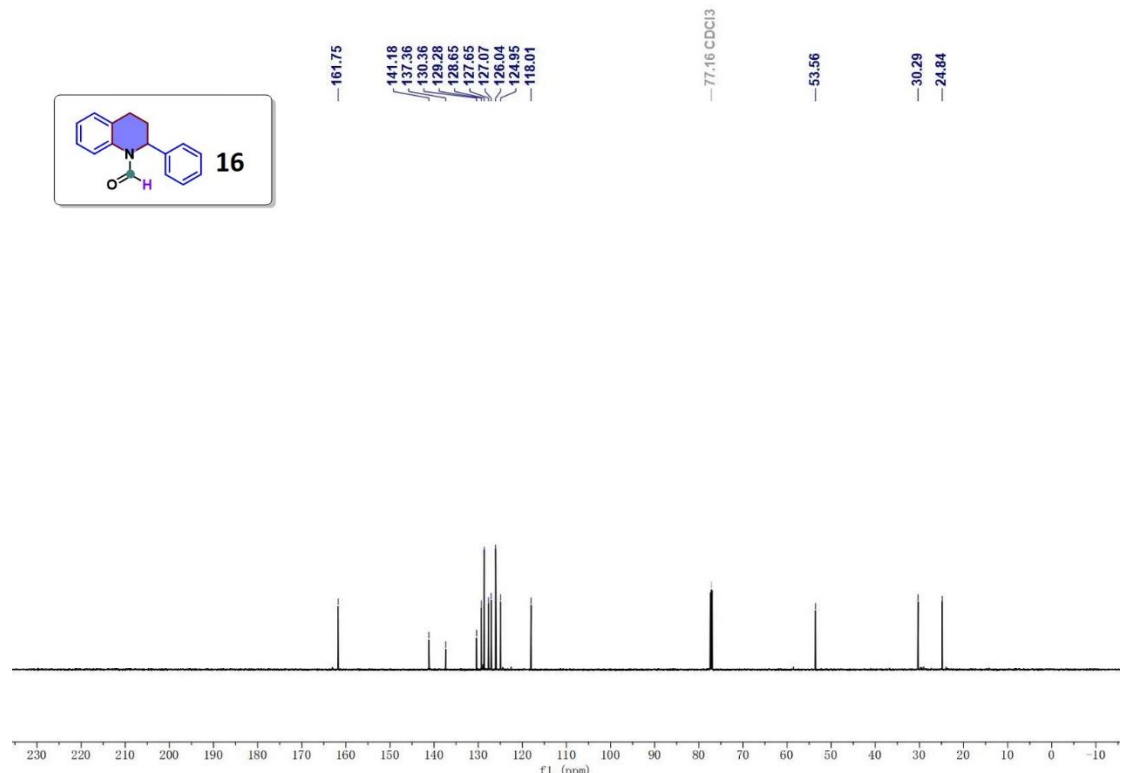


Fig. S36 ^1H NMR of **17**

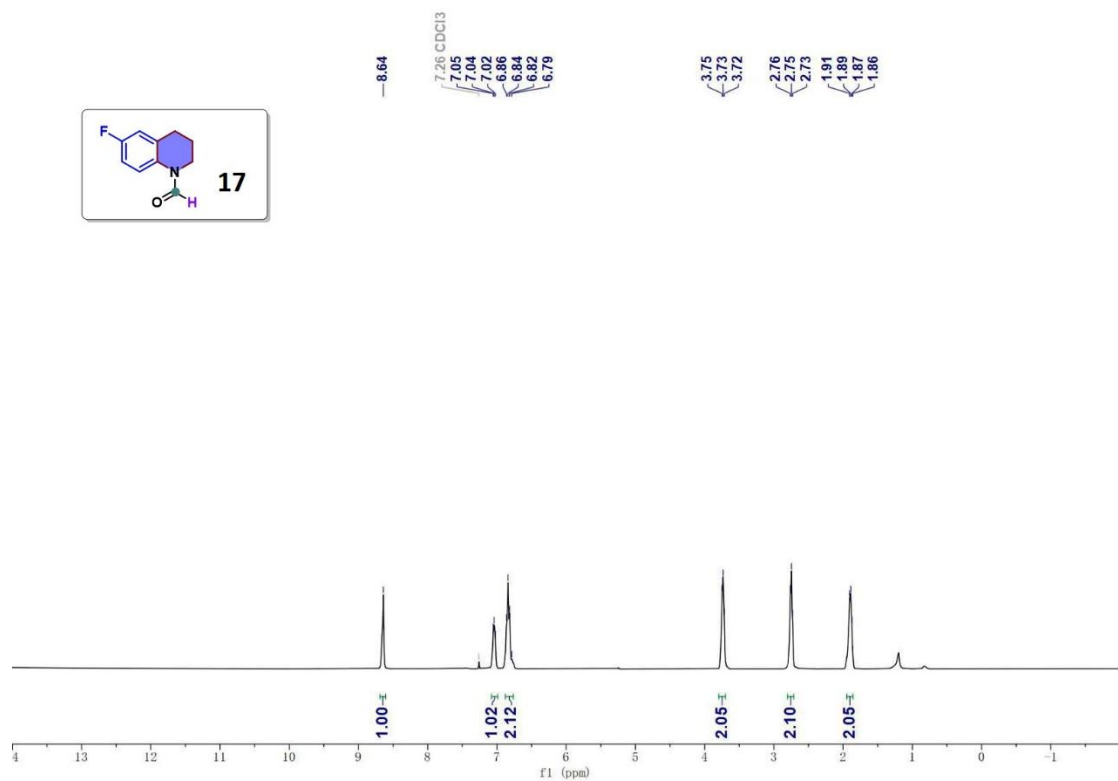


Fig. S37 ^{13}C NMR of **17**

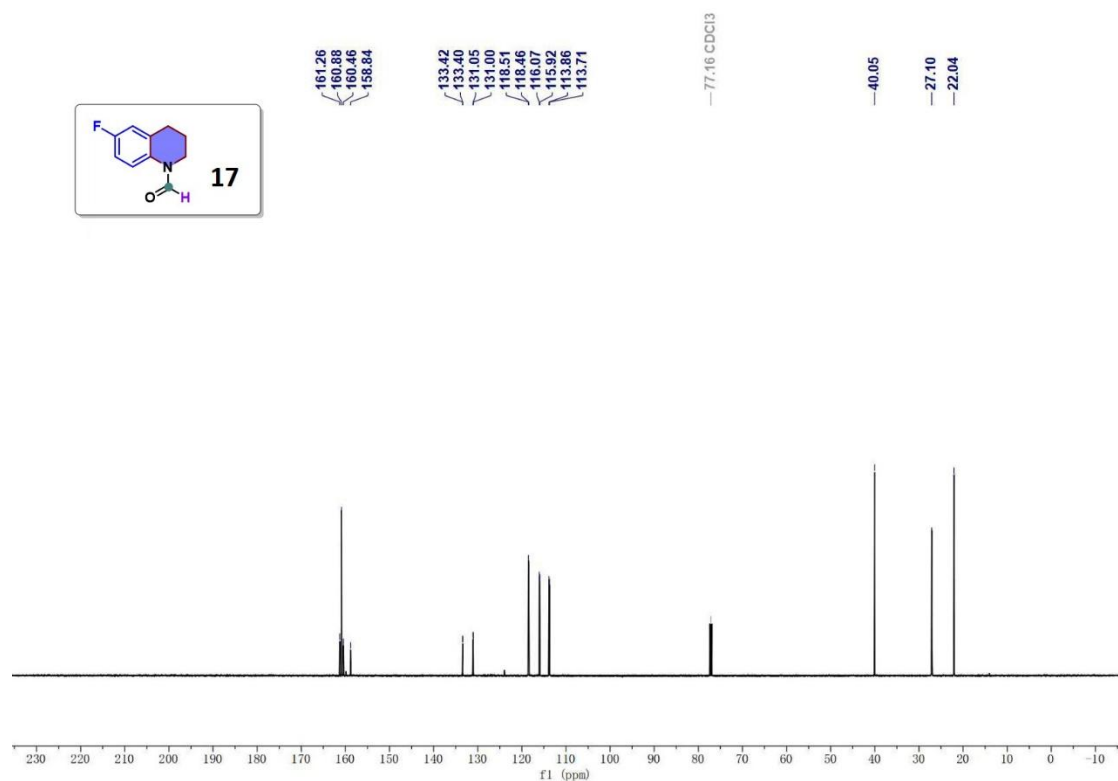


Fig. S38 ^1H NMR of **18**

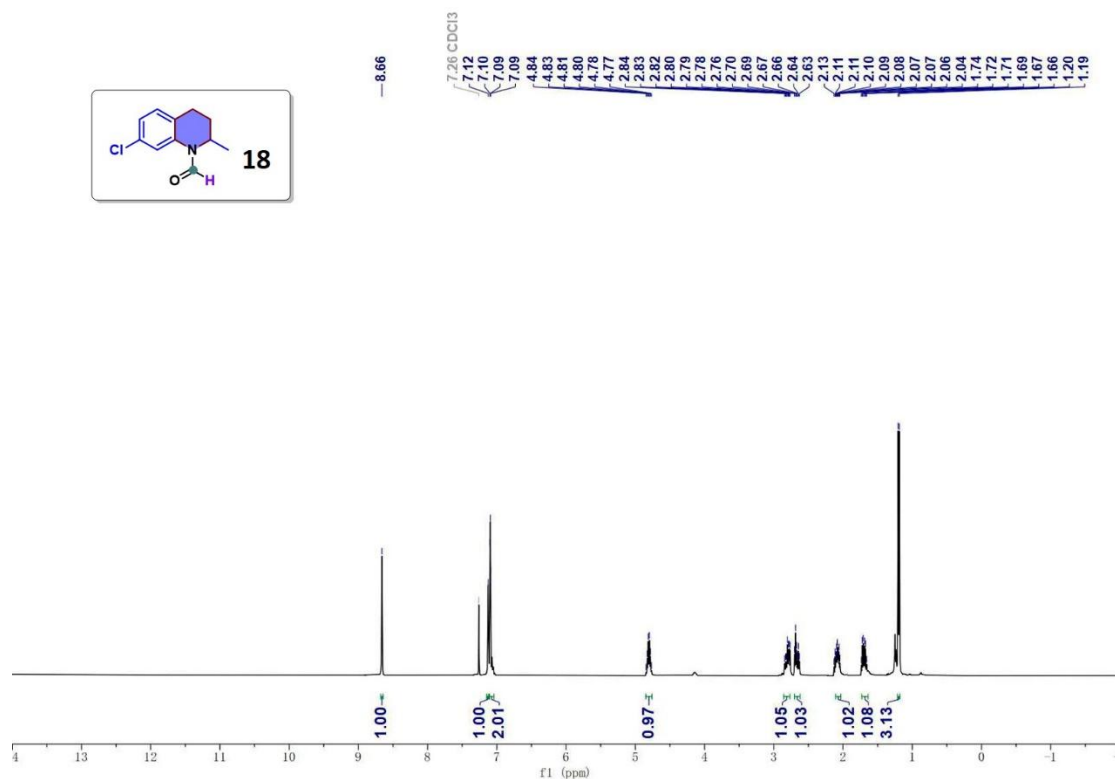


Fig. S39 ^{13}C NMR of **18**

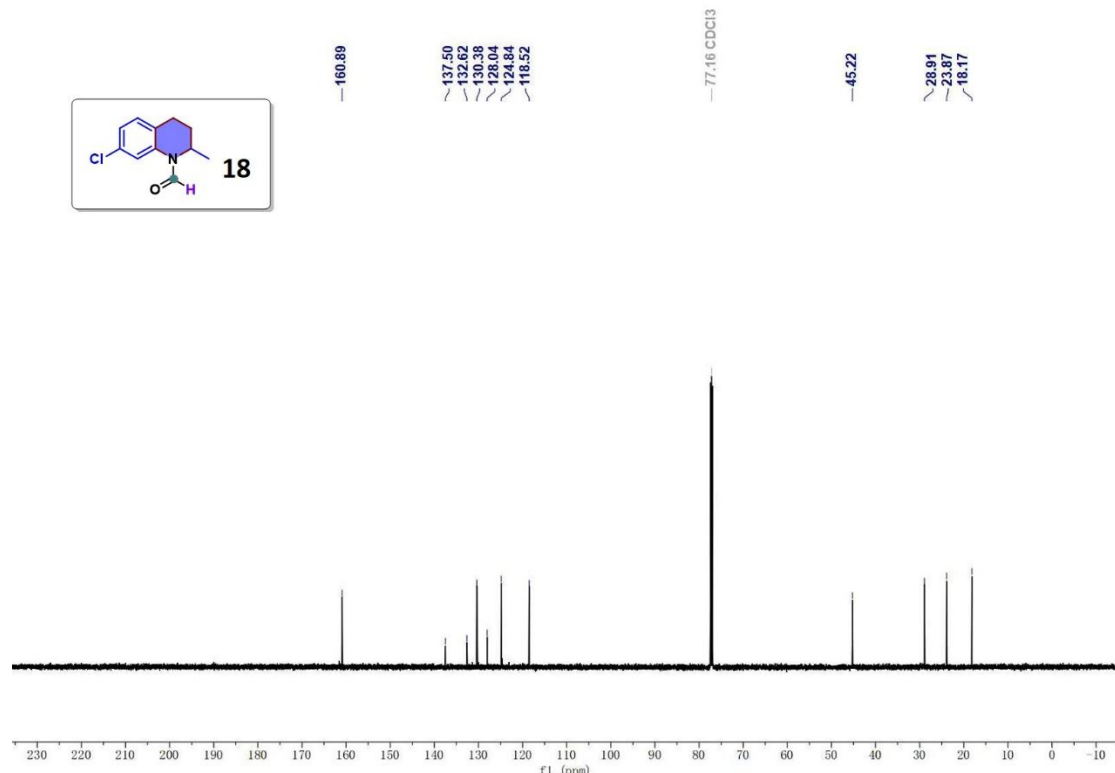


Fig. S40 ^1H NMR of **19**

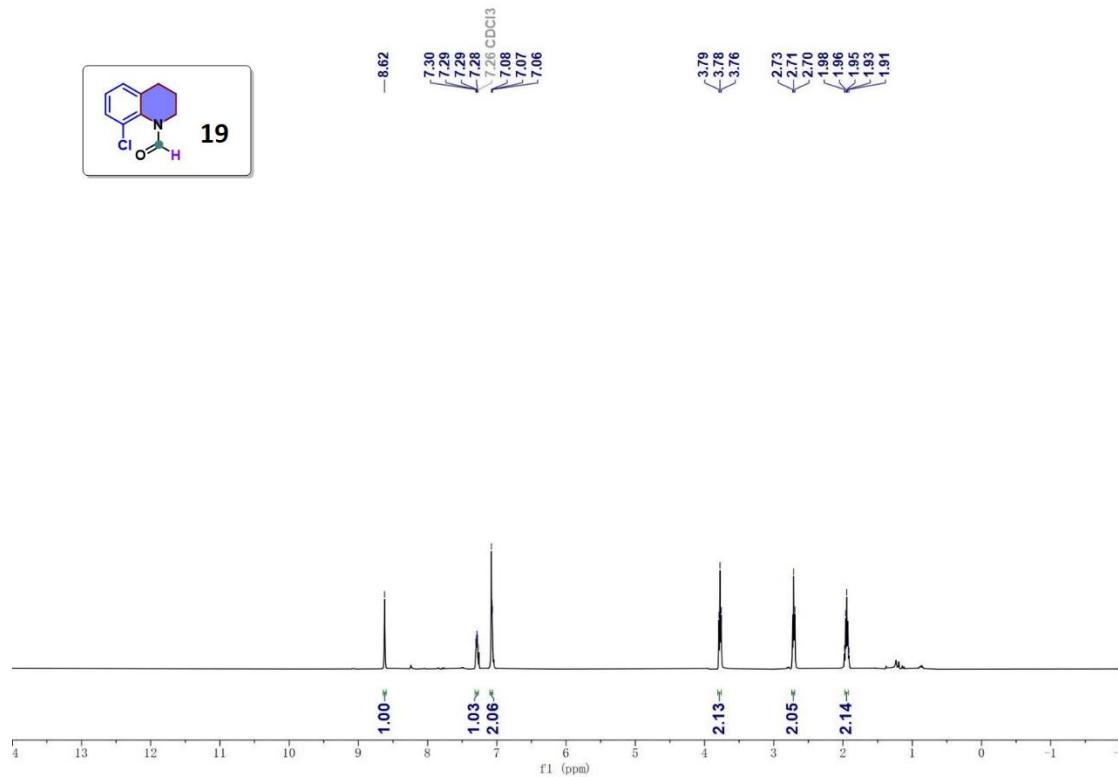


Fig. S41 ^{13}C NMR of **19**

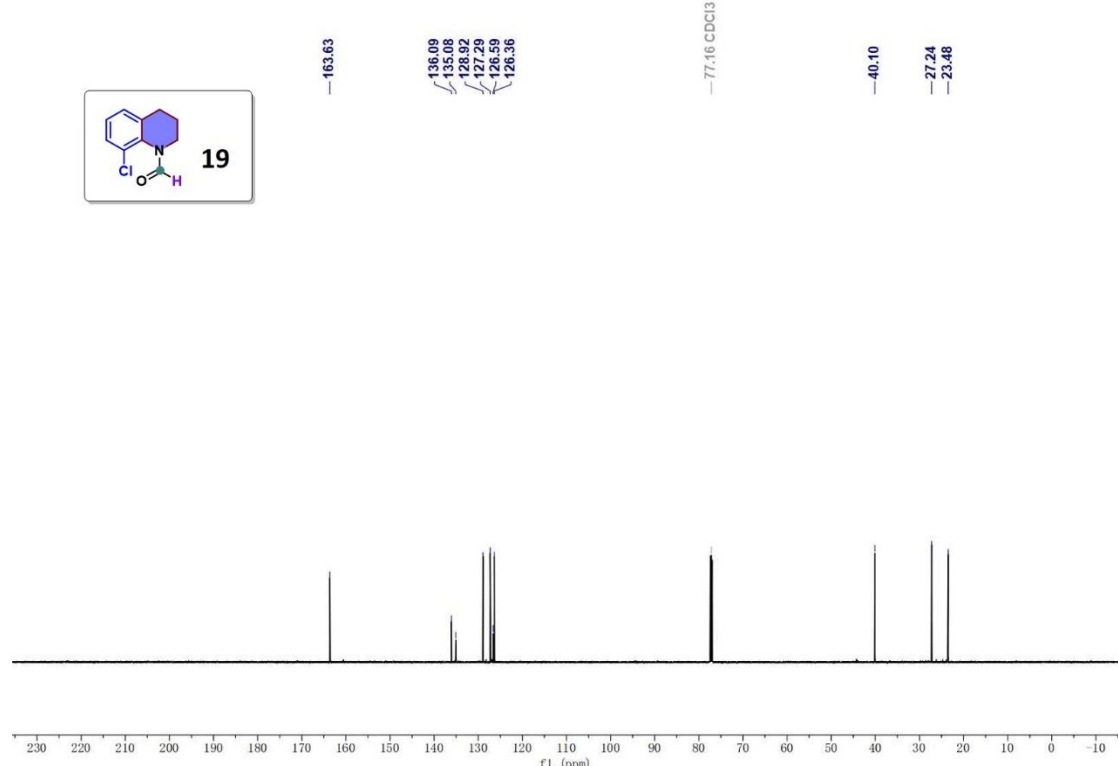


Fig. S42 ^1H NMR of **20**

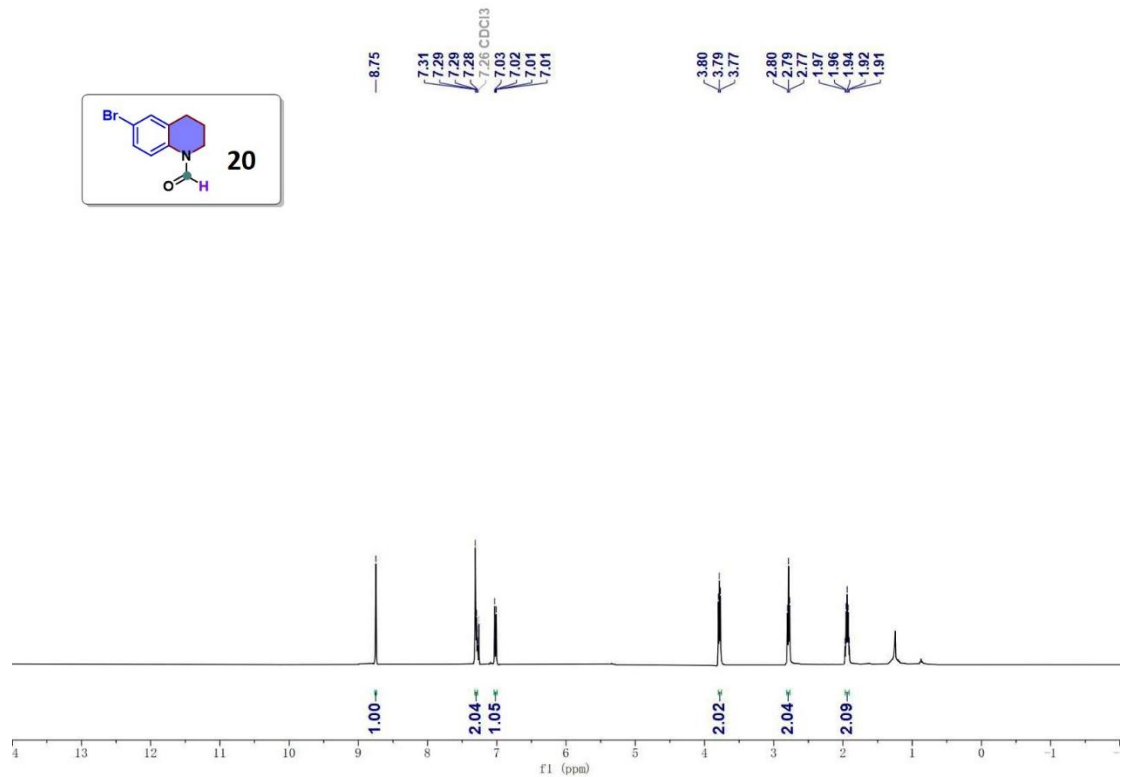


Fig. S43 ^{13}C NMR of **20**

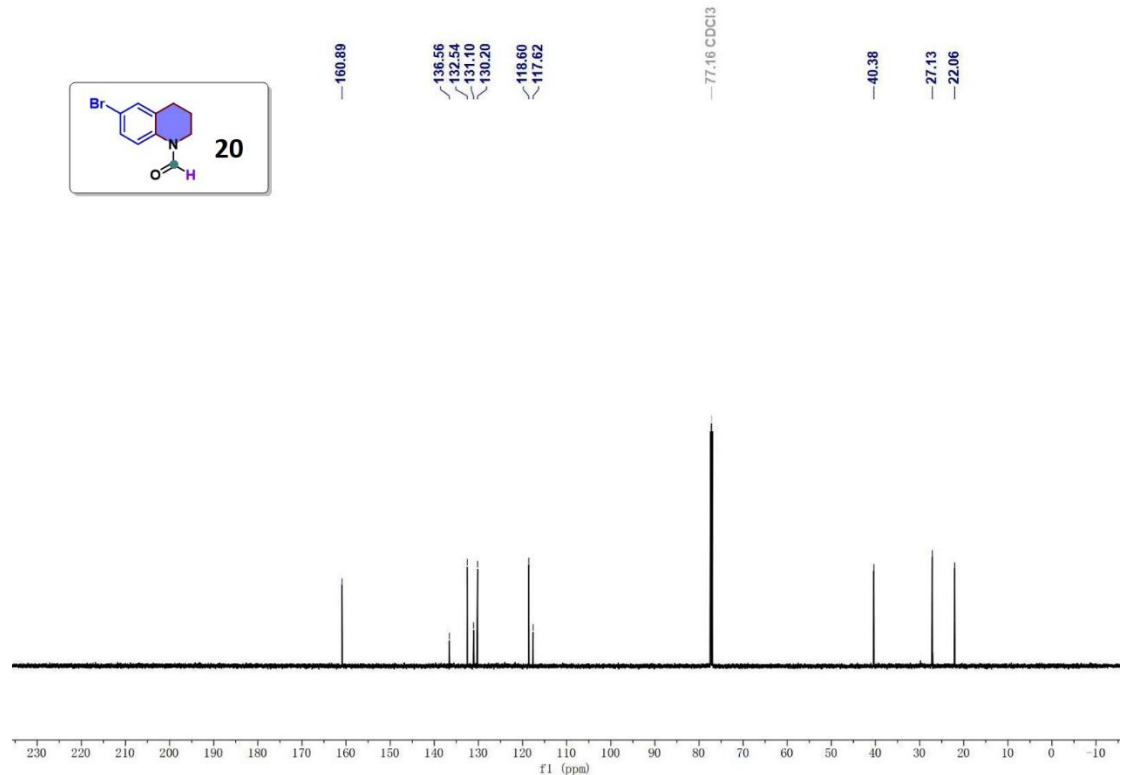


Fig. S44 ^1H NMR of **21**

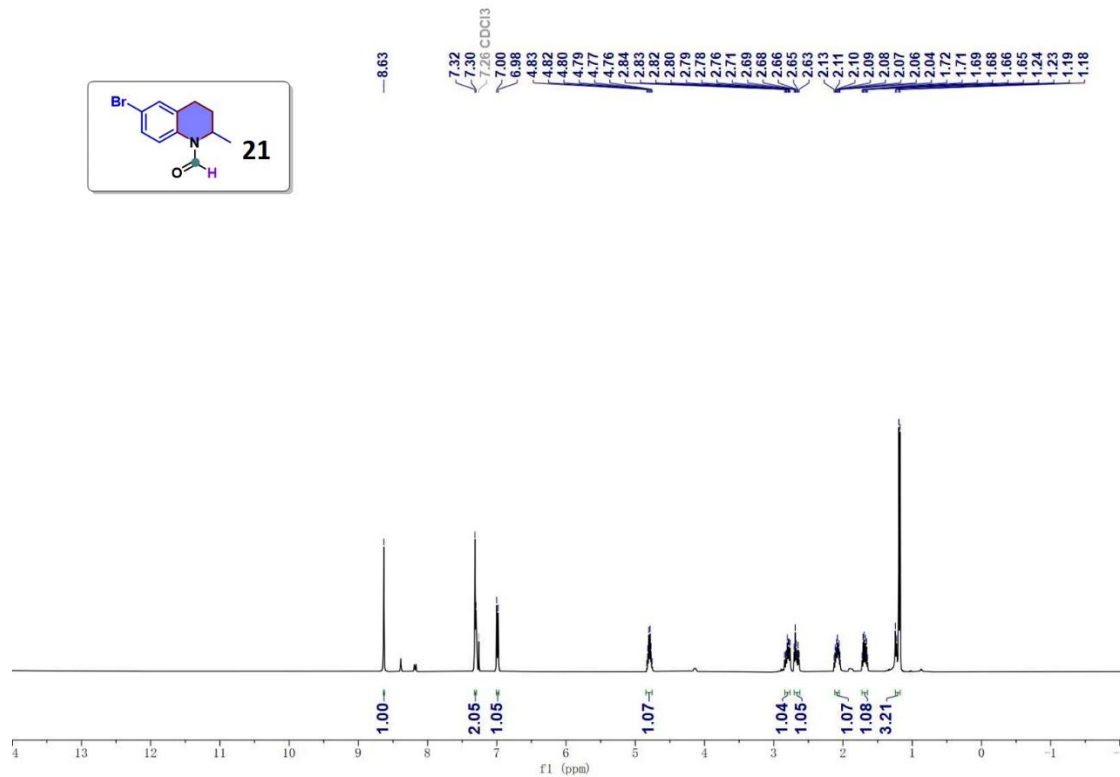


Fig. S45 ^{13}C NMR of **21**

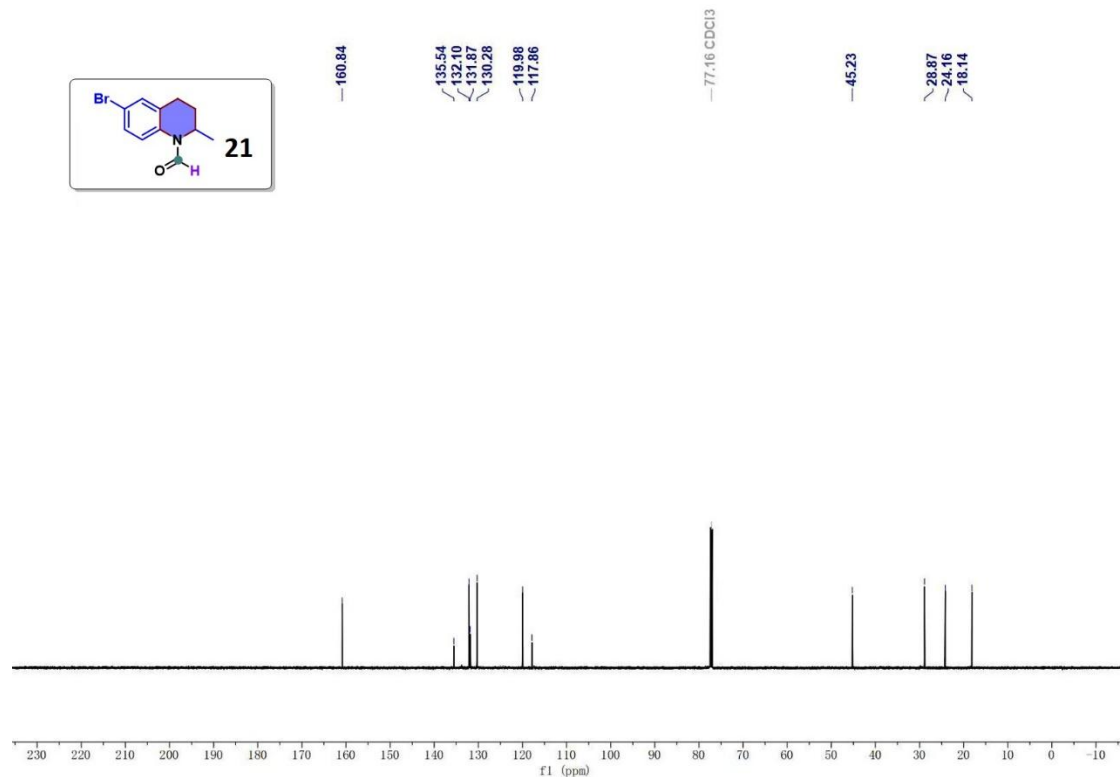


Fig. S46 ^1H NMR of **22**

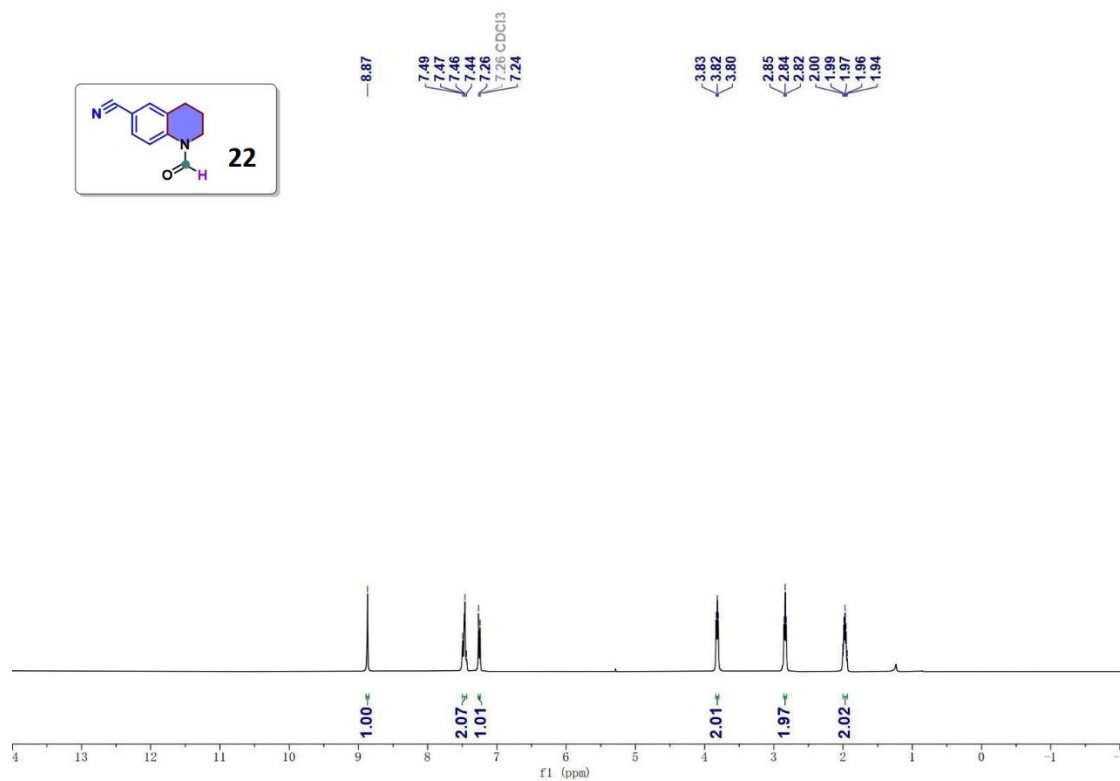


Fig. S47 ^{13}C NMR of **22**

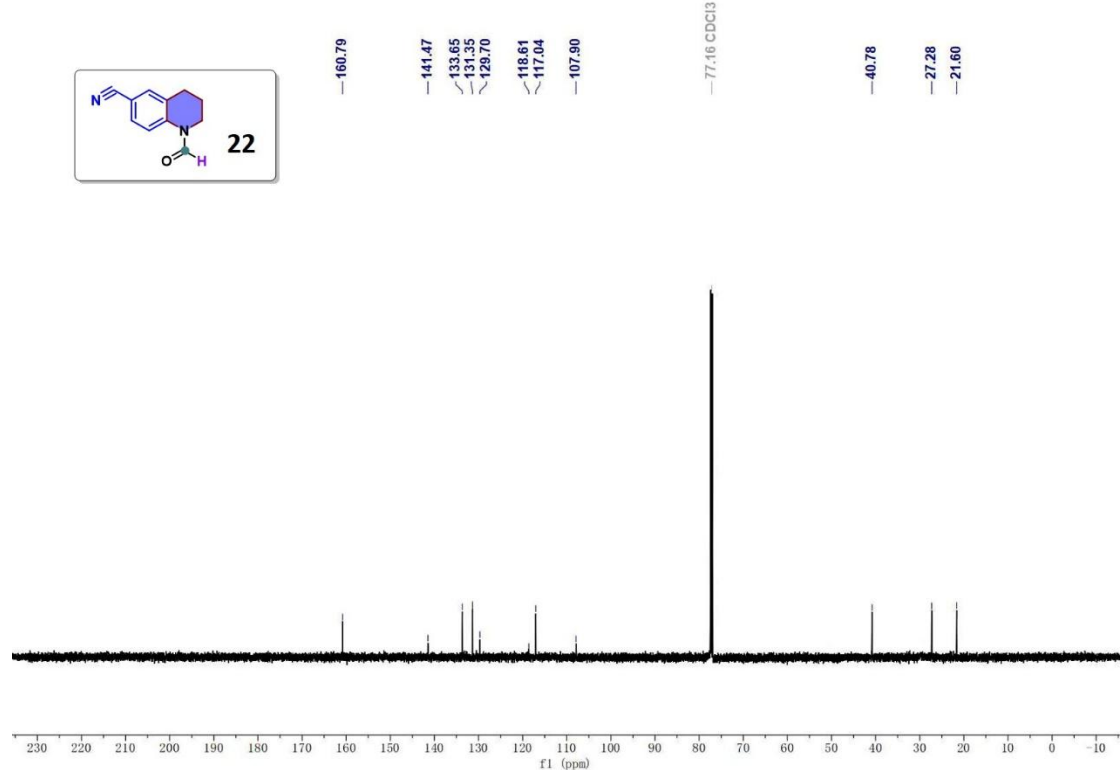


Fig. S48 ^1H NMR of **23**

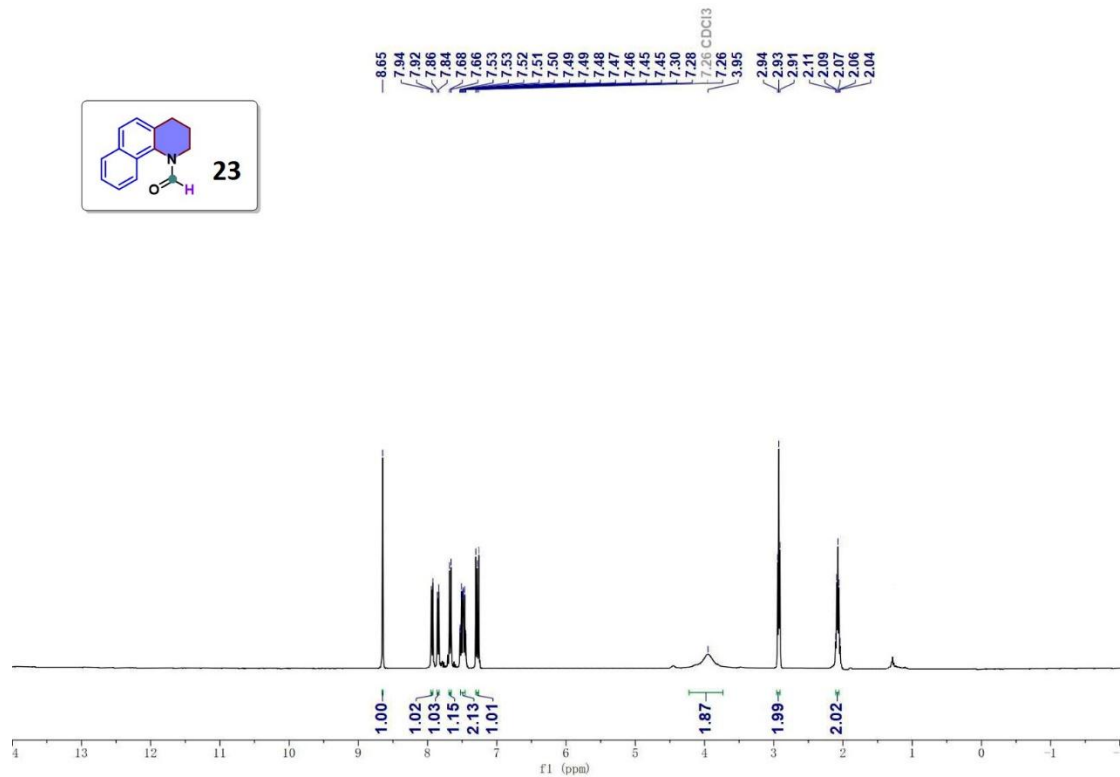


Fig. S49 ^{13}C NMR of **23**

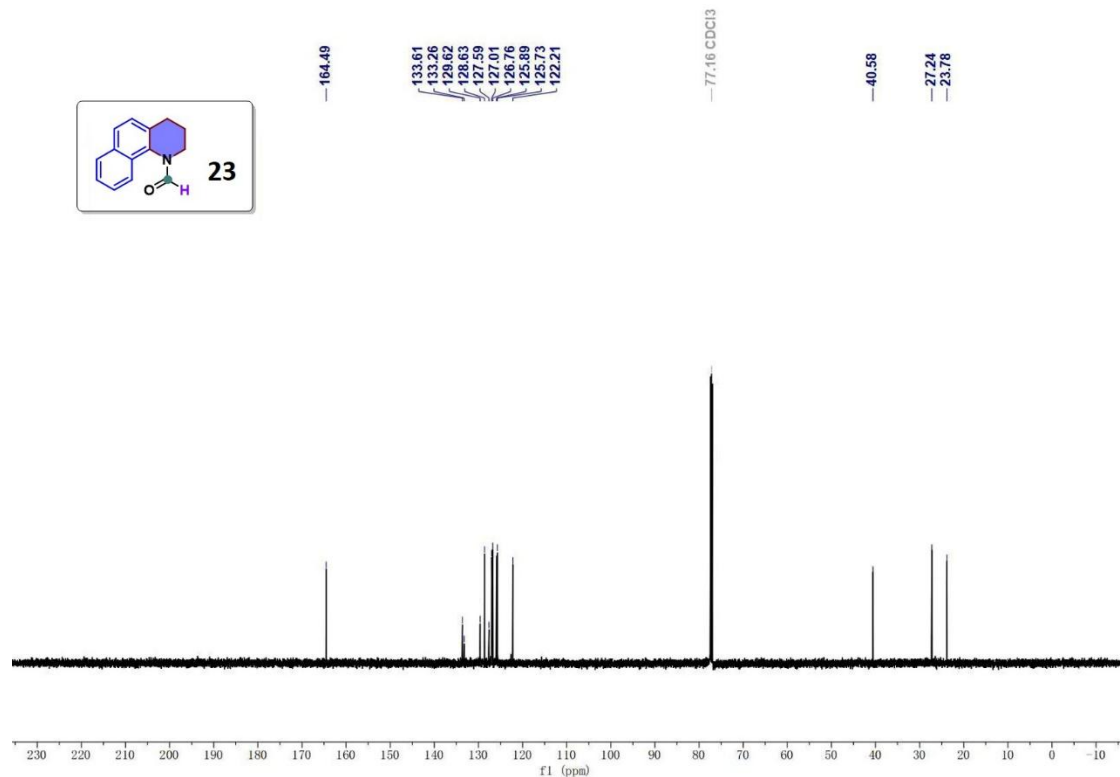


Fig. S50 ^1H NMR of **24**

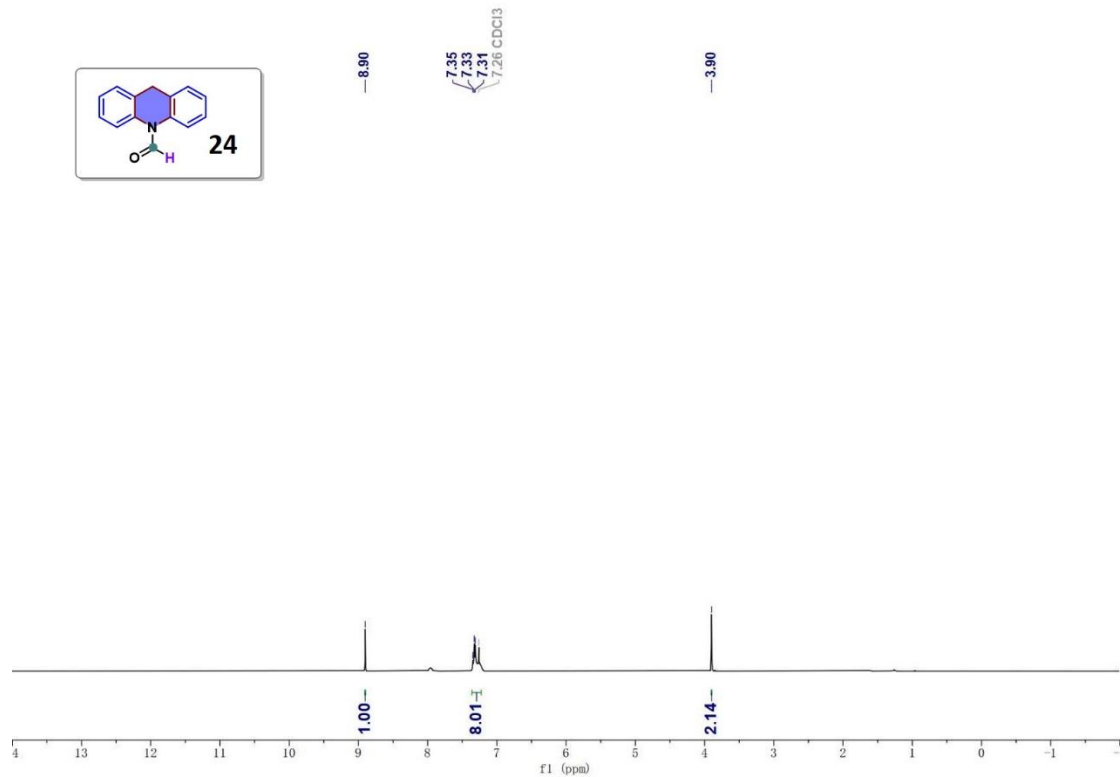


Fig. S51 ^{13}C NMR of **24**

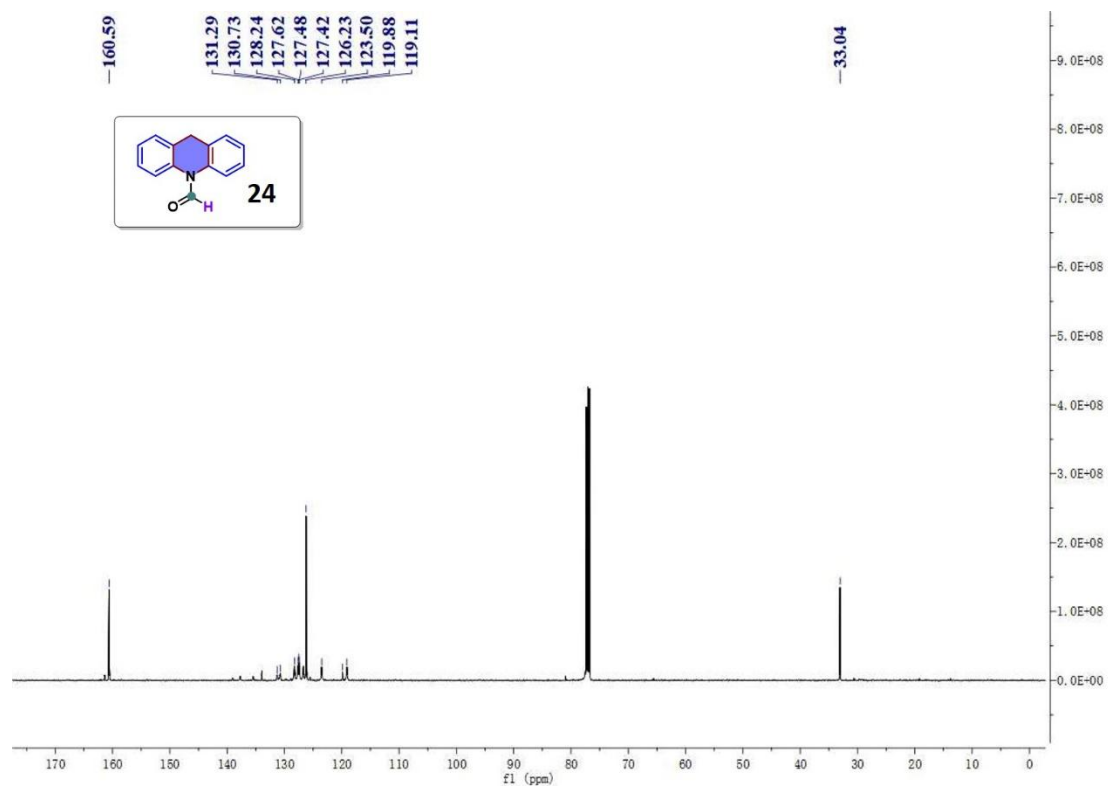


Fig. S52 ^1H NMR of **25**

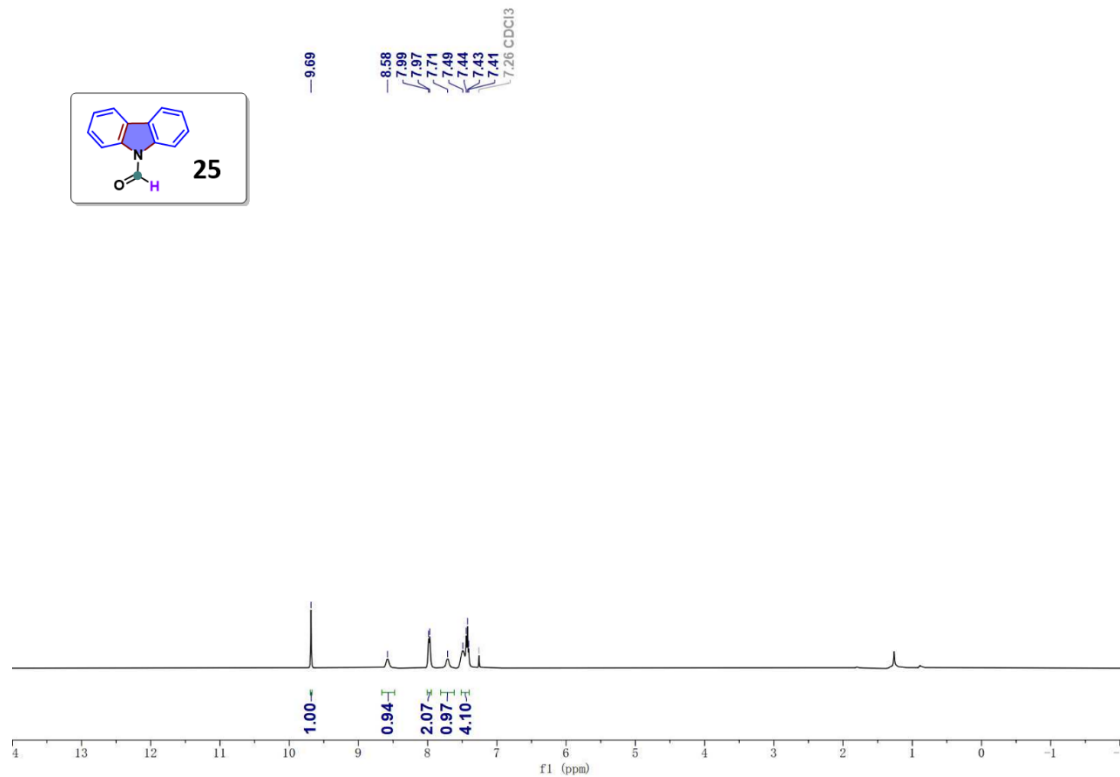


Fig. S53 ^{13}C NMR of **25**

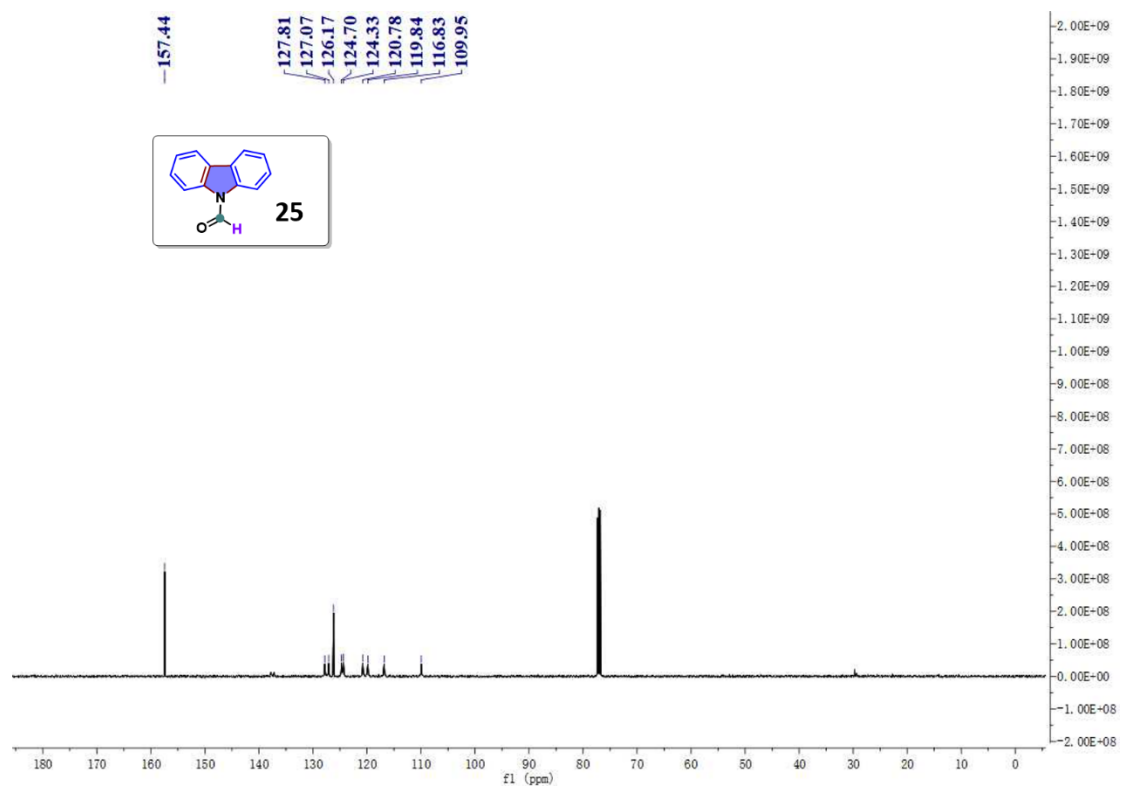


Fig. S54 ^1H NMR of **26**

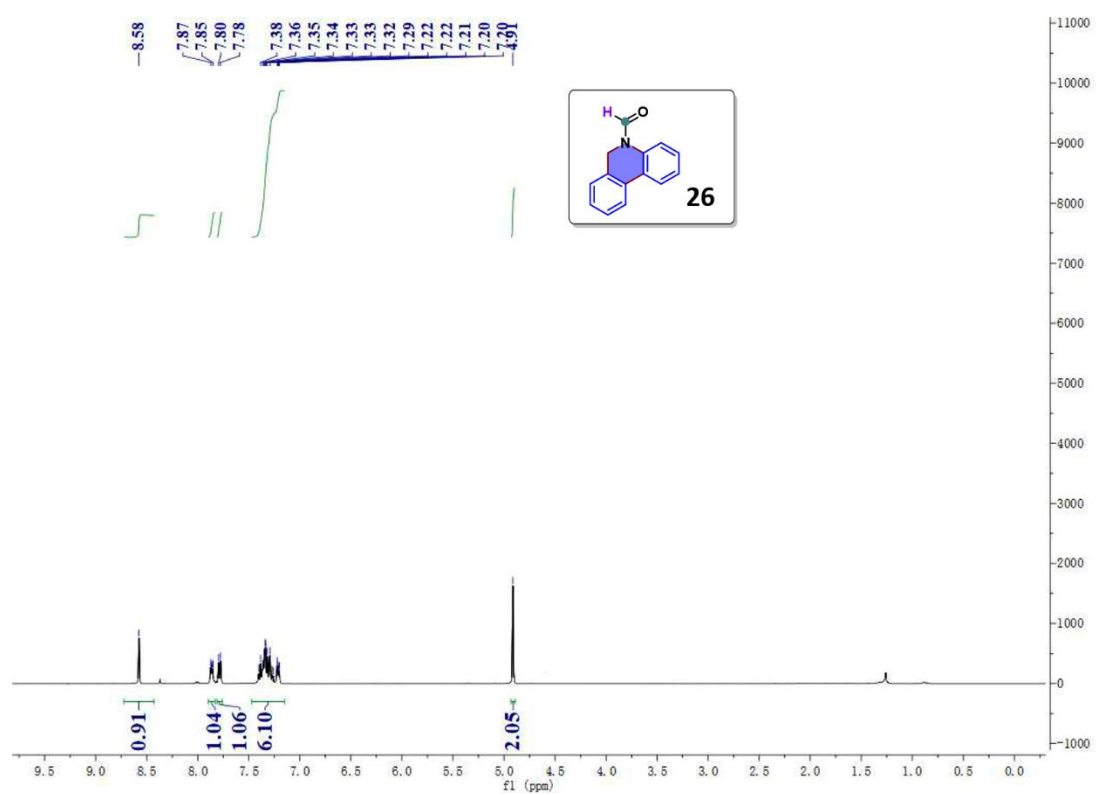


Fig. S55 ^{13}C NMR of **26**

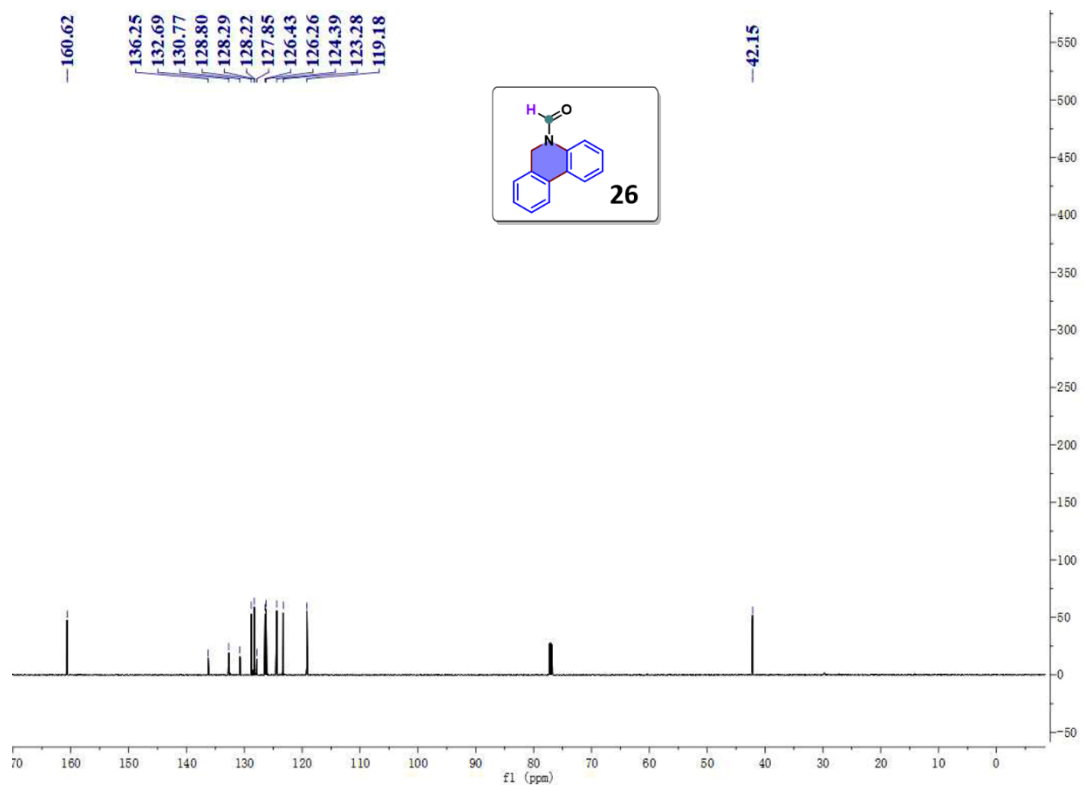


Fig. S56 ^1H NMR of **27**

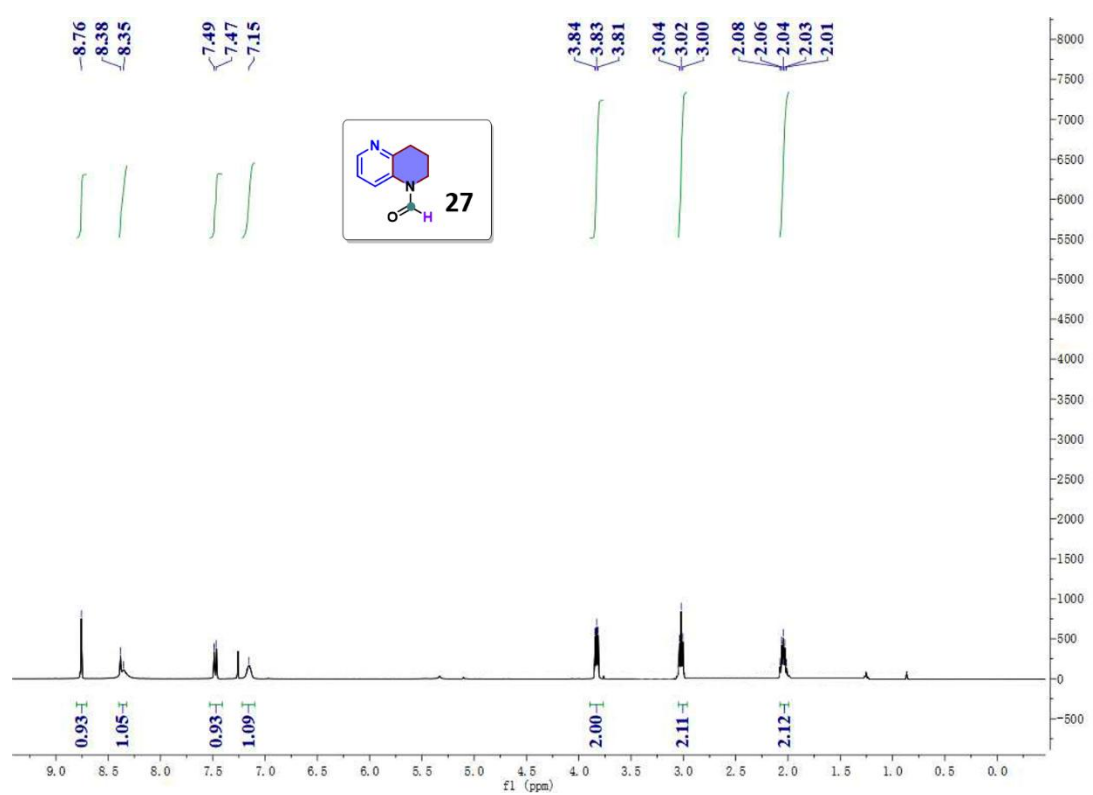


Fig. S57 ^{13}C NMR of **27**

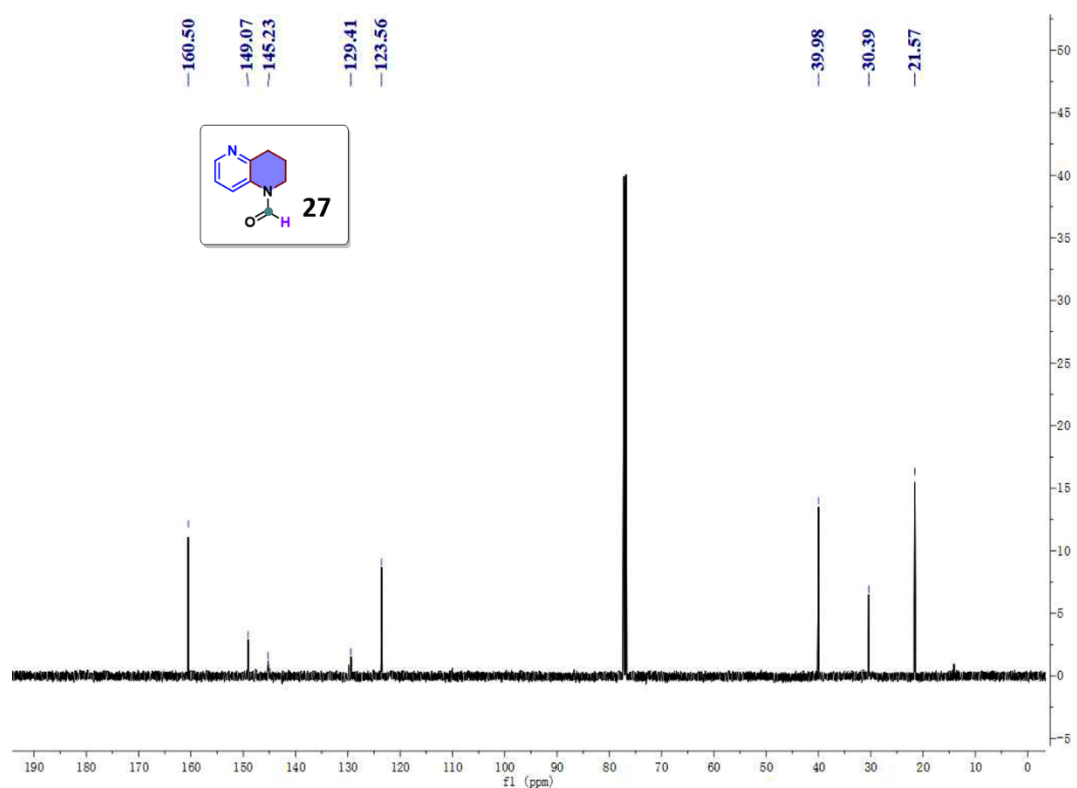


Fig. S58 ^1H NMR of **28**

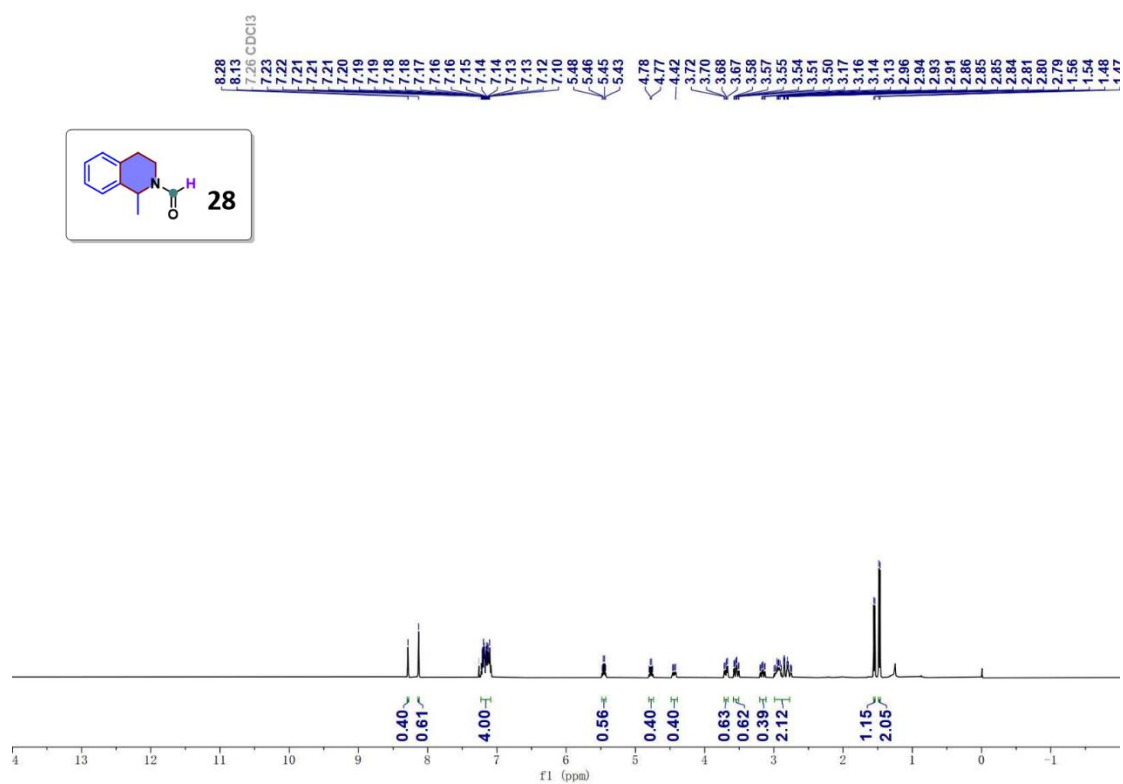


Fig. S59 ^{13}C NMR of **28**

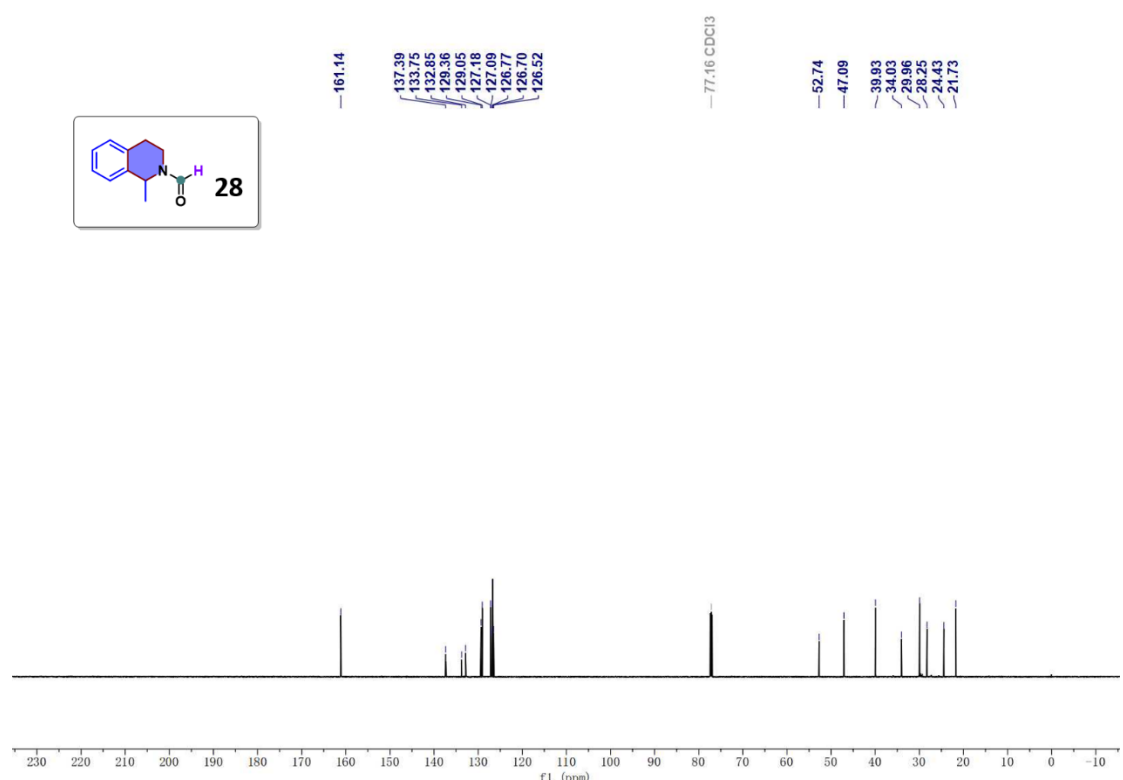


Fig. S60 ^1H NMR of **29**

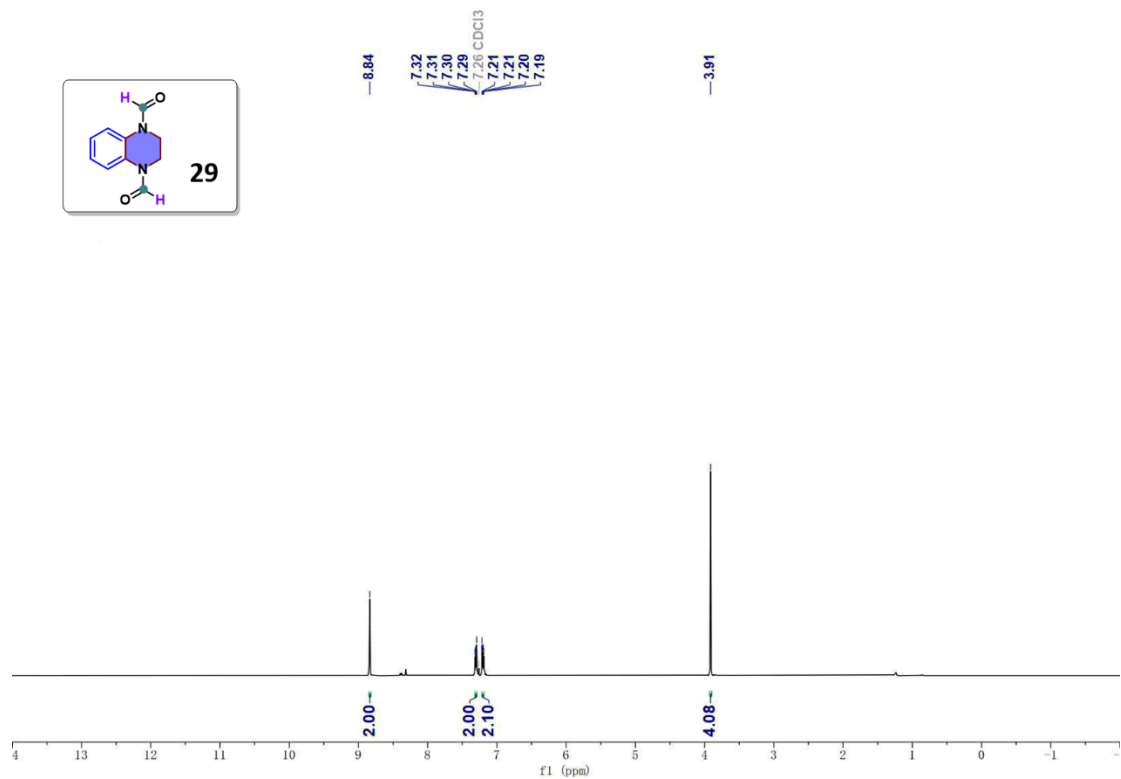


Fig. S61 ^{13}C NMR of **29**

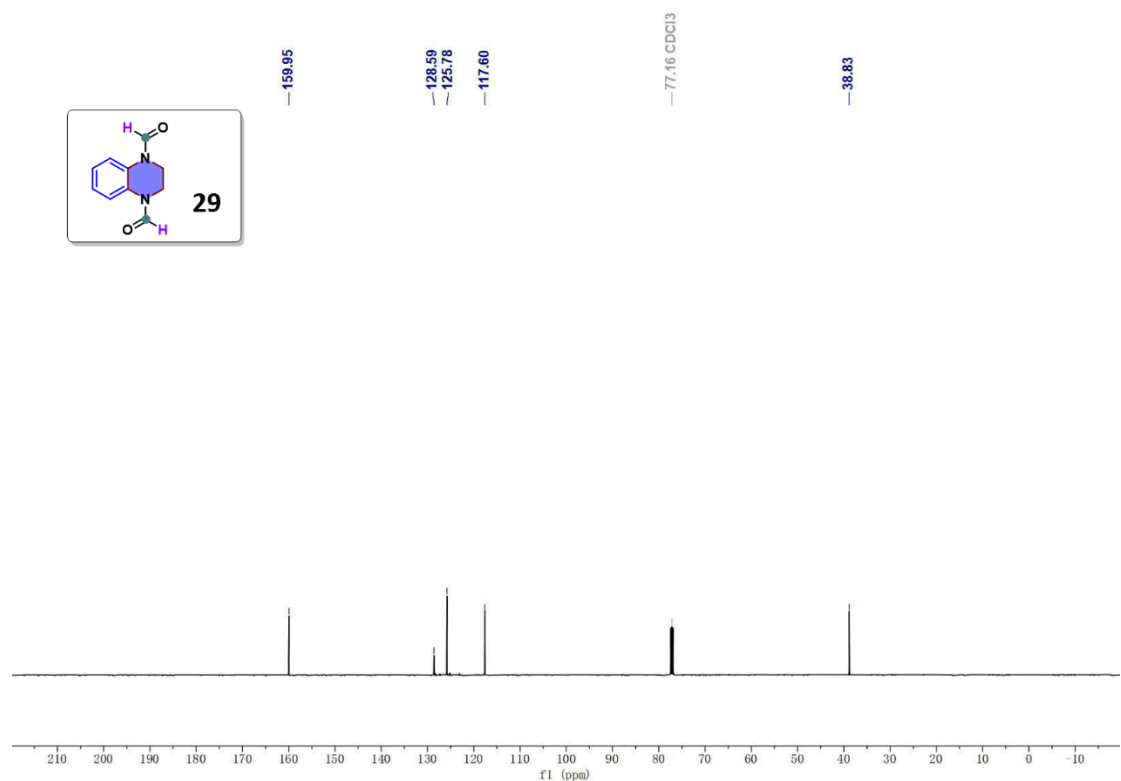


Fig. S62 ^1H NMR of **30**

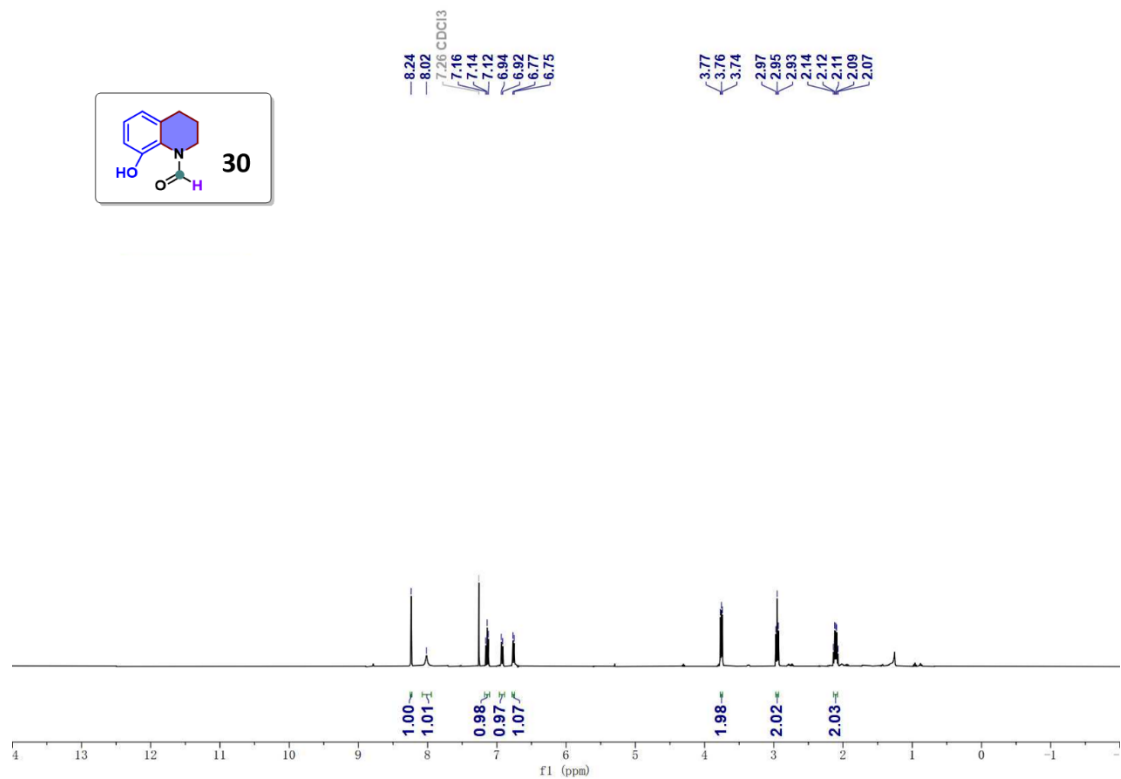


Fig. S63 ^{13}C NMR of **30**

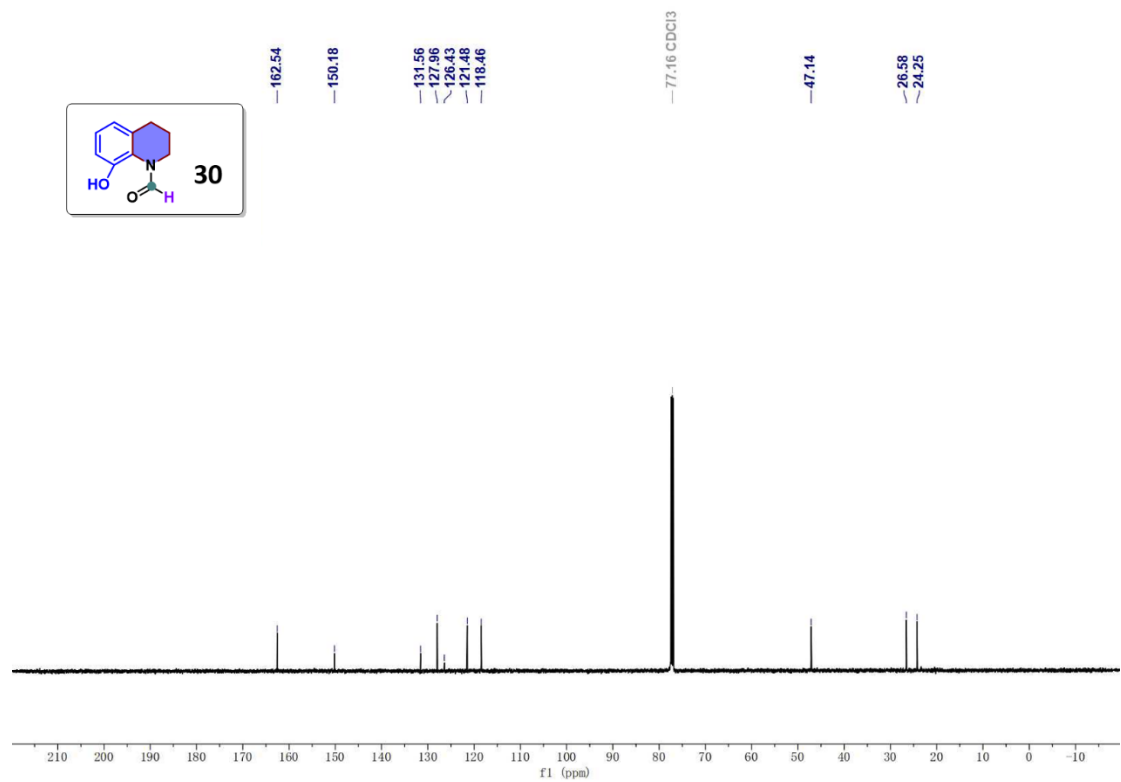


Fig. S64 ^1H NMR of **31**

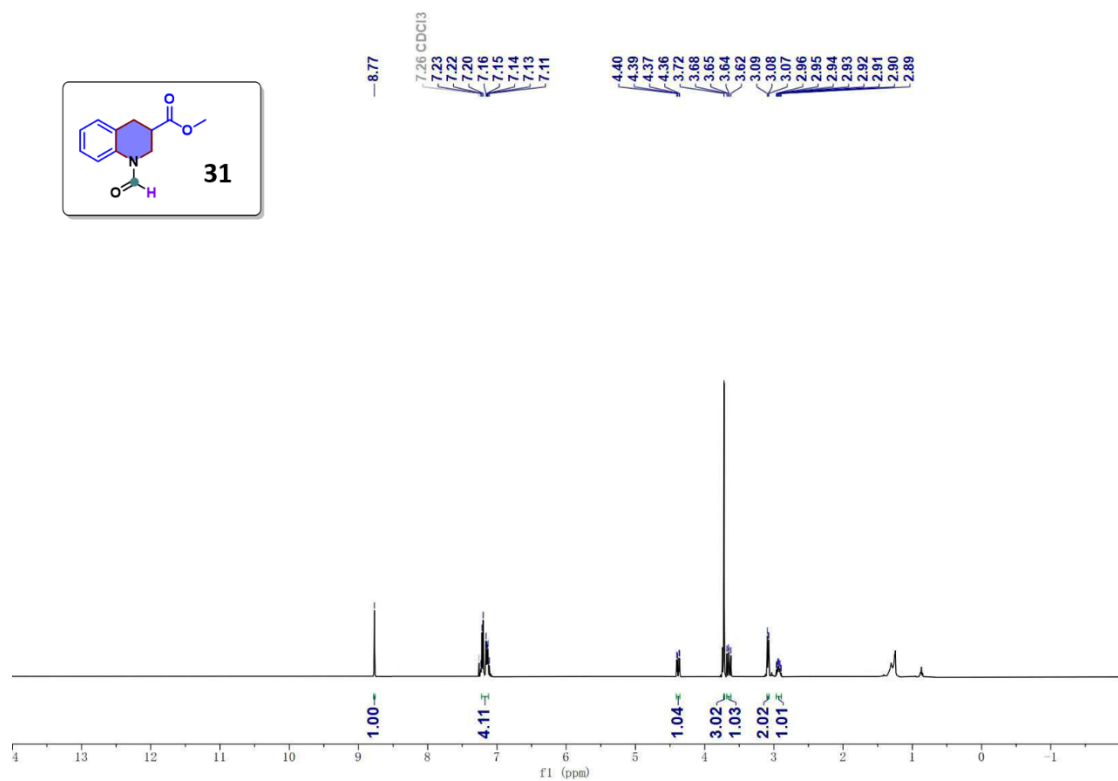


Fig. S65 ^{13}C NMR of **31**

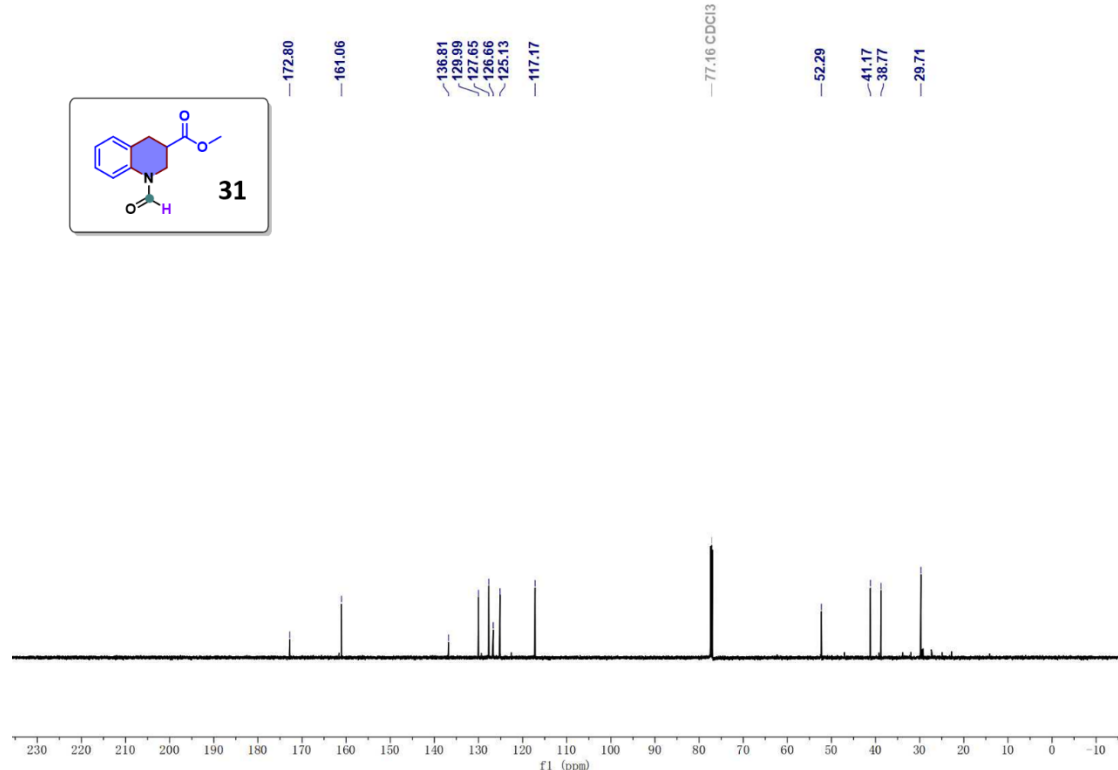


Fig. S66 HRMS of 4

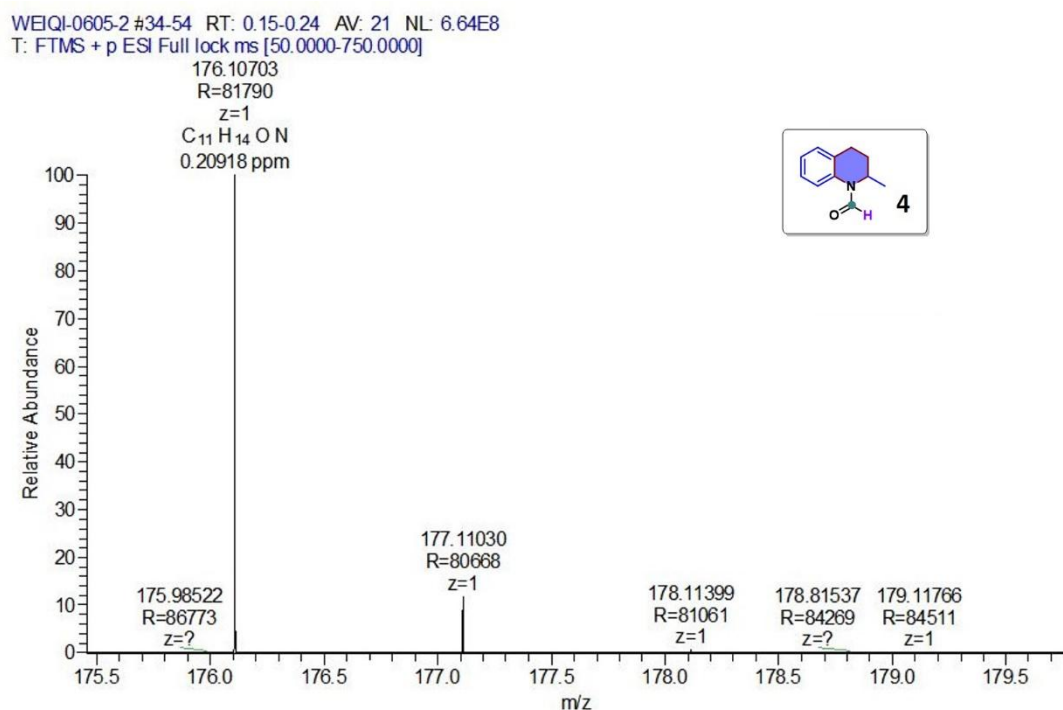


Fig. S67 HRMS of 5

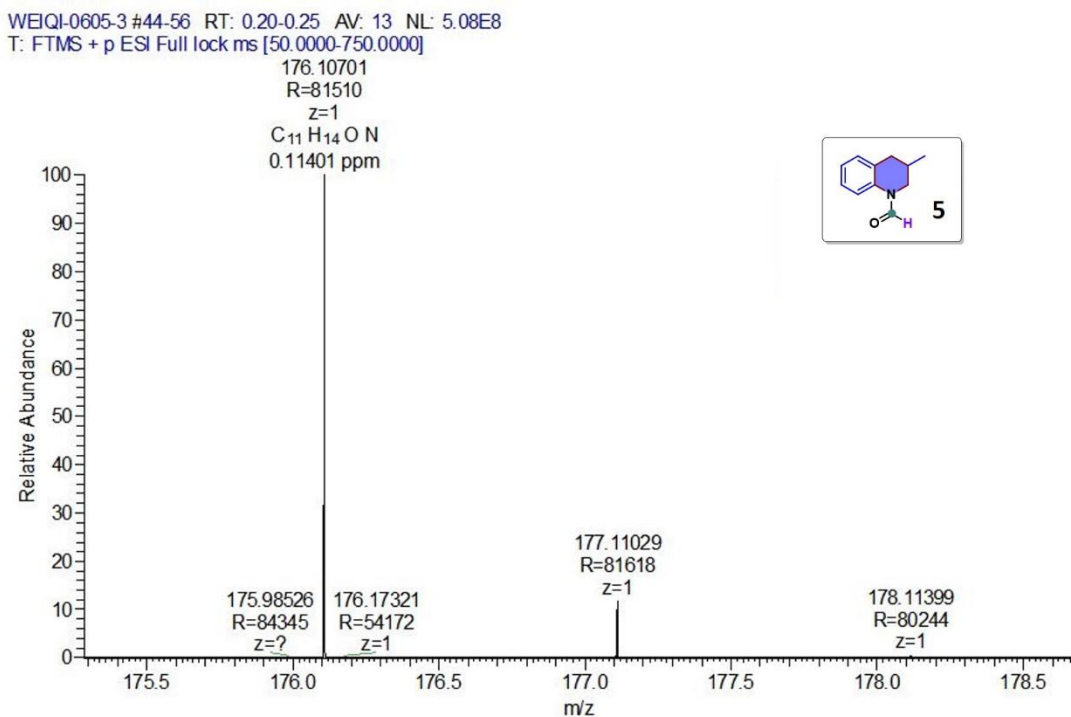


Fig. S68 HRMS of 6

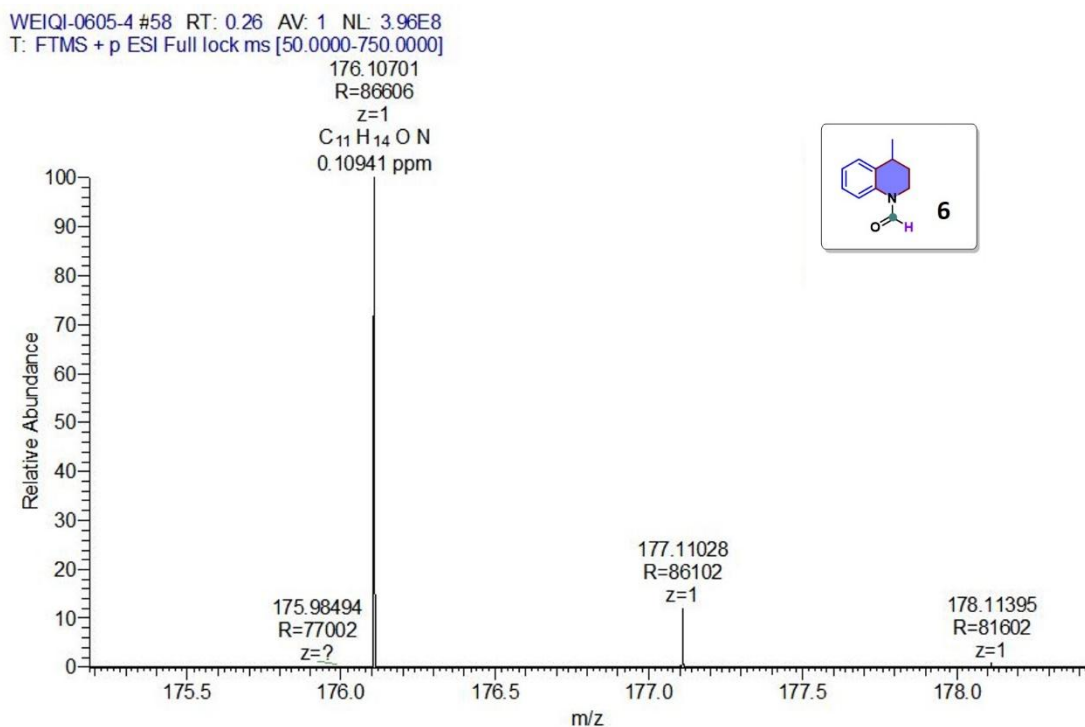


Fig. S69 HRMS of 7

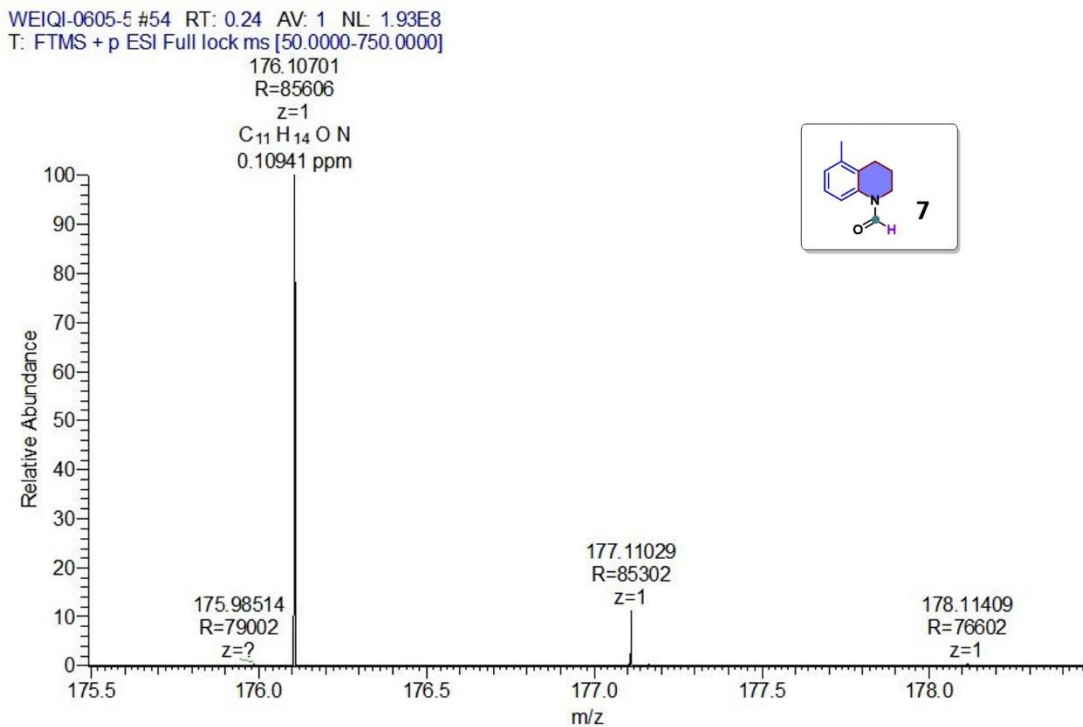


Fig. S70 HRMS of 8

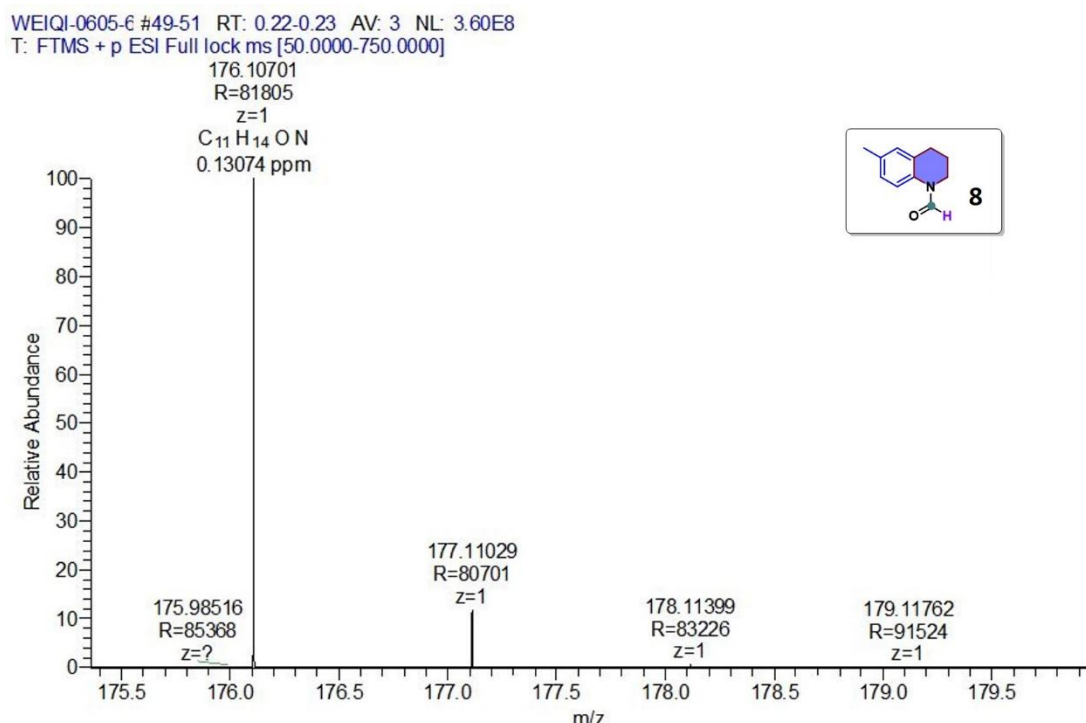


Fig. S71 HRMS of 9

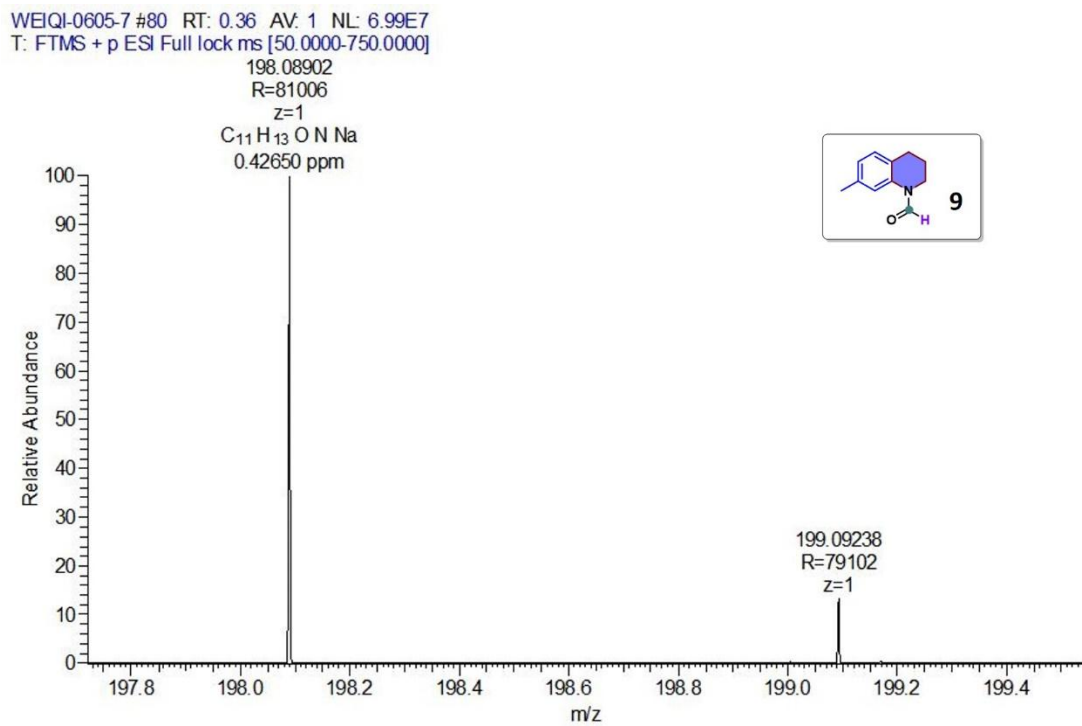


Fig. S72 HRMS of 10

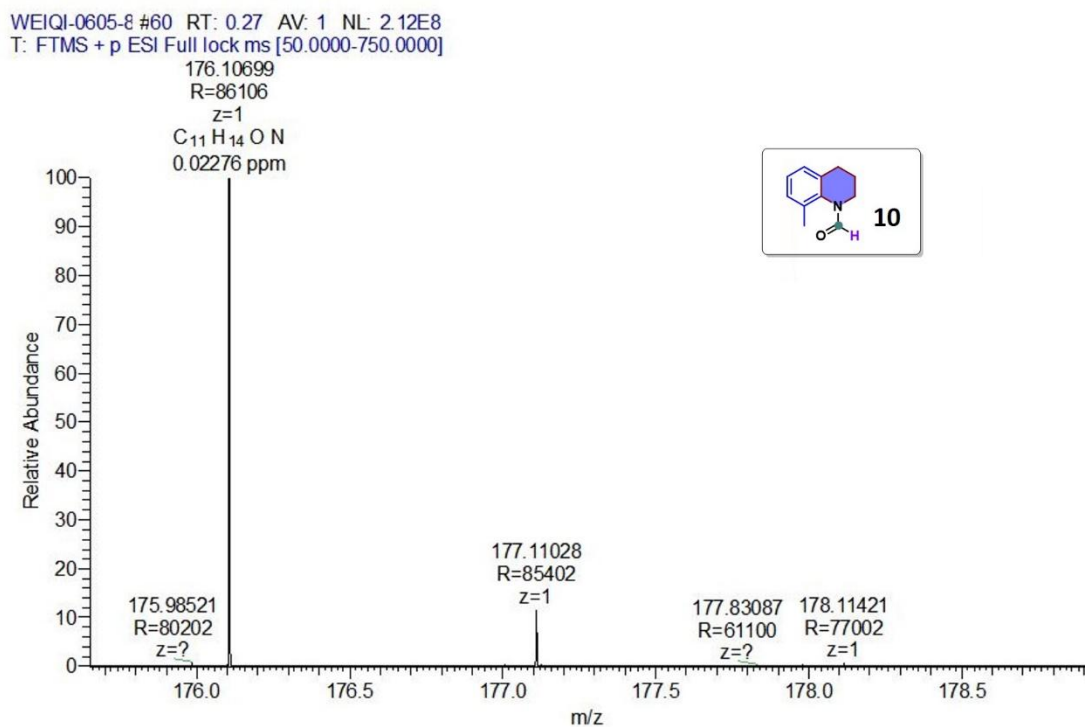


Fig. S73 HRMS of 11

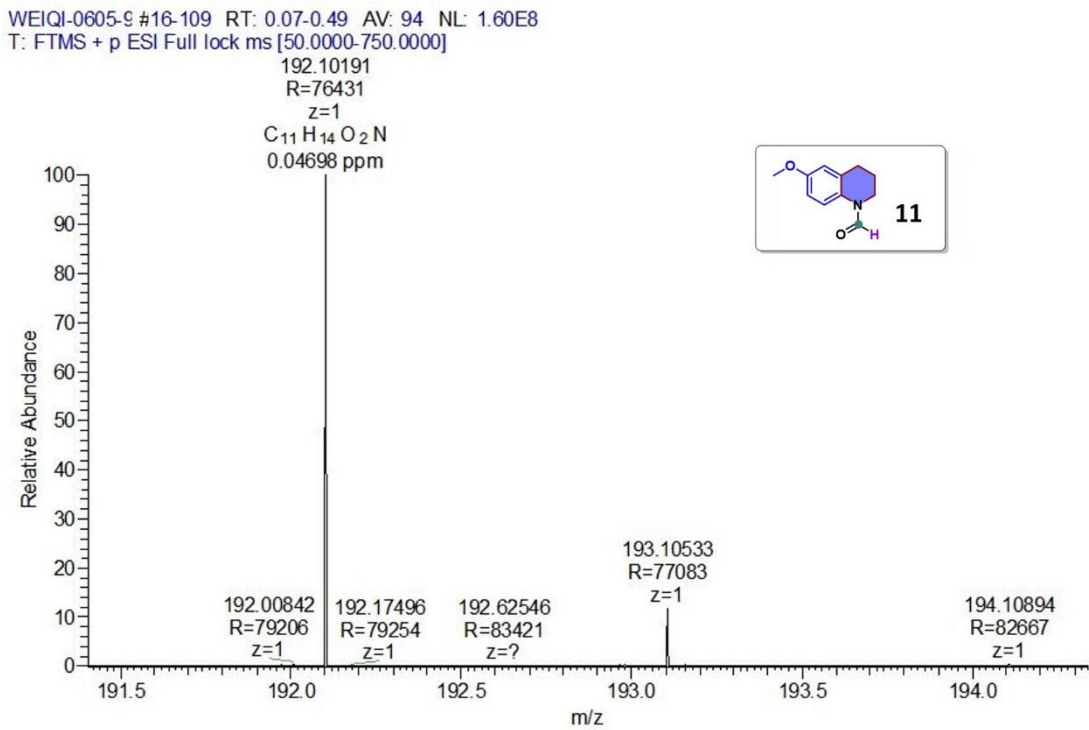


Fig. S74 HRMS of 12

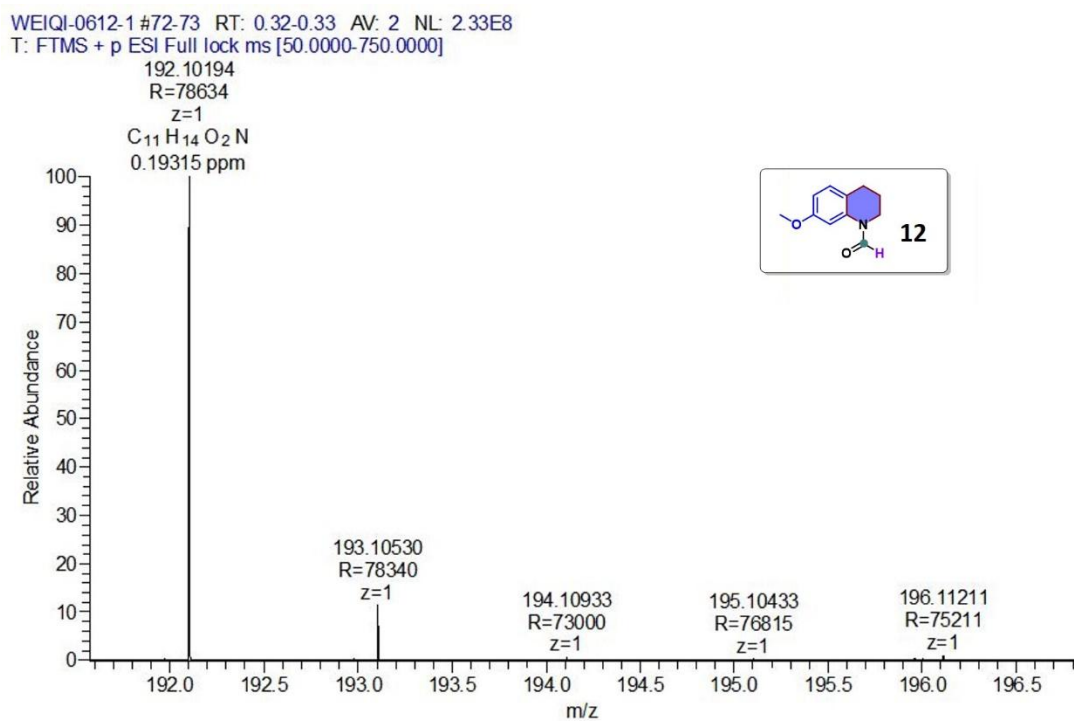


Fig. S75 HRMS of 13

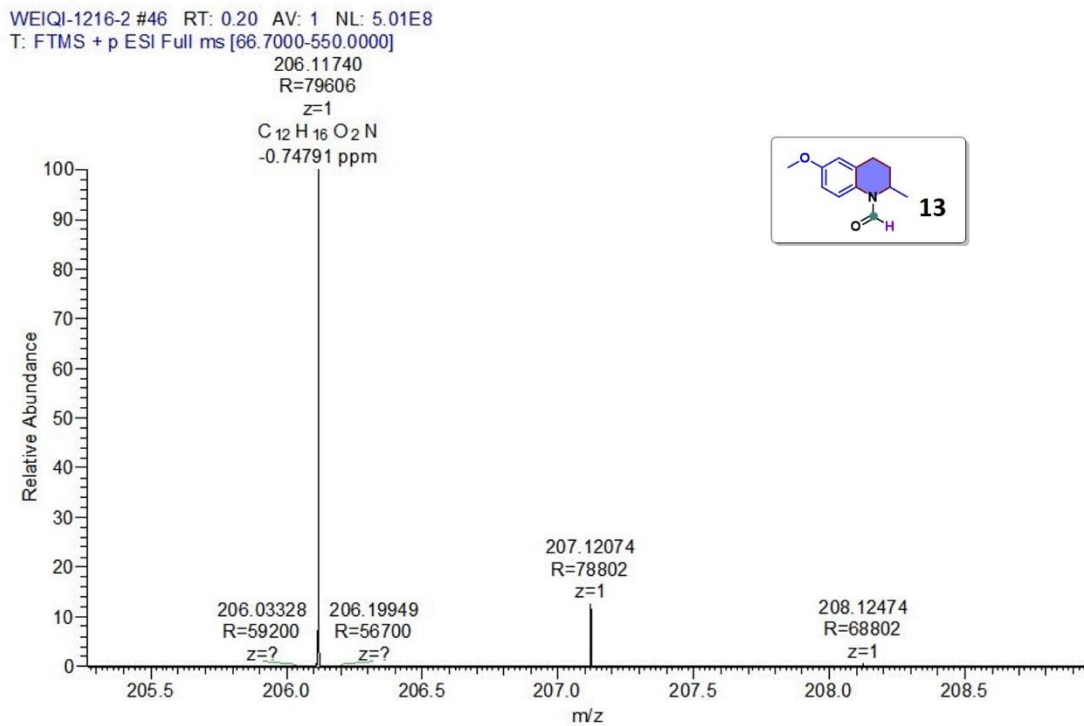


Fig. S76 HRMS of 14

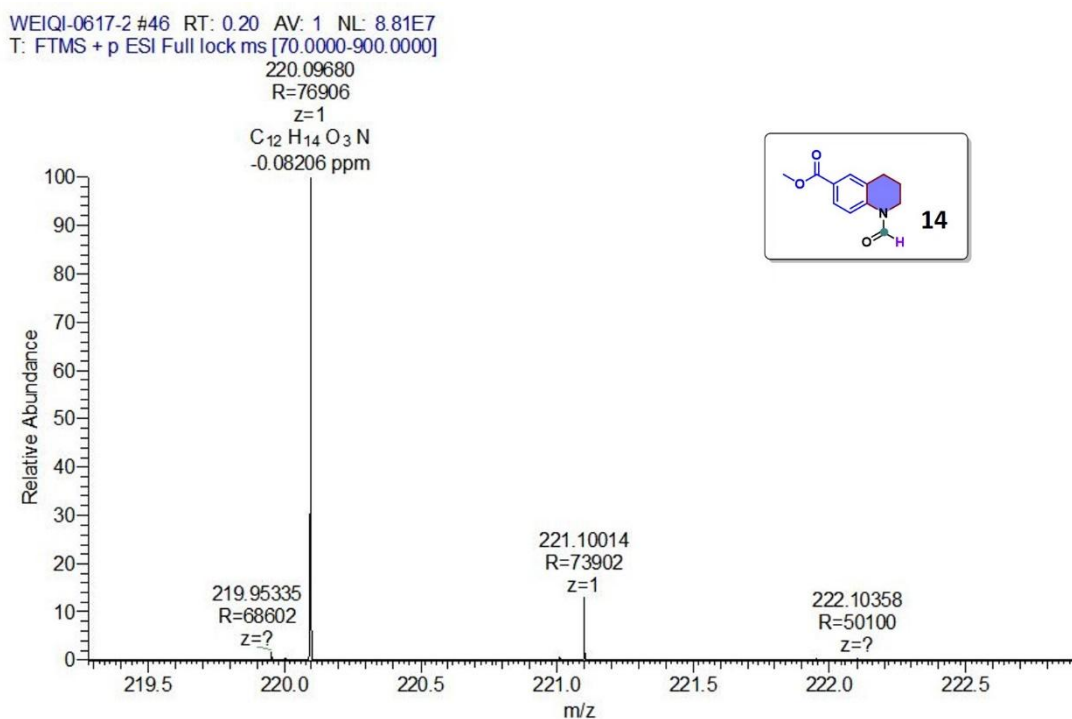


Fig. S77 HRMS of 15

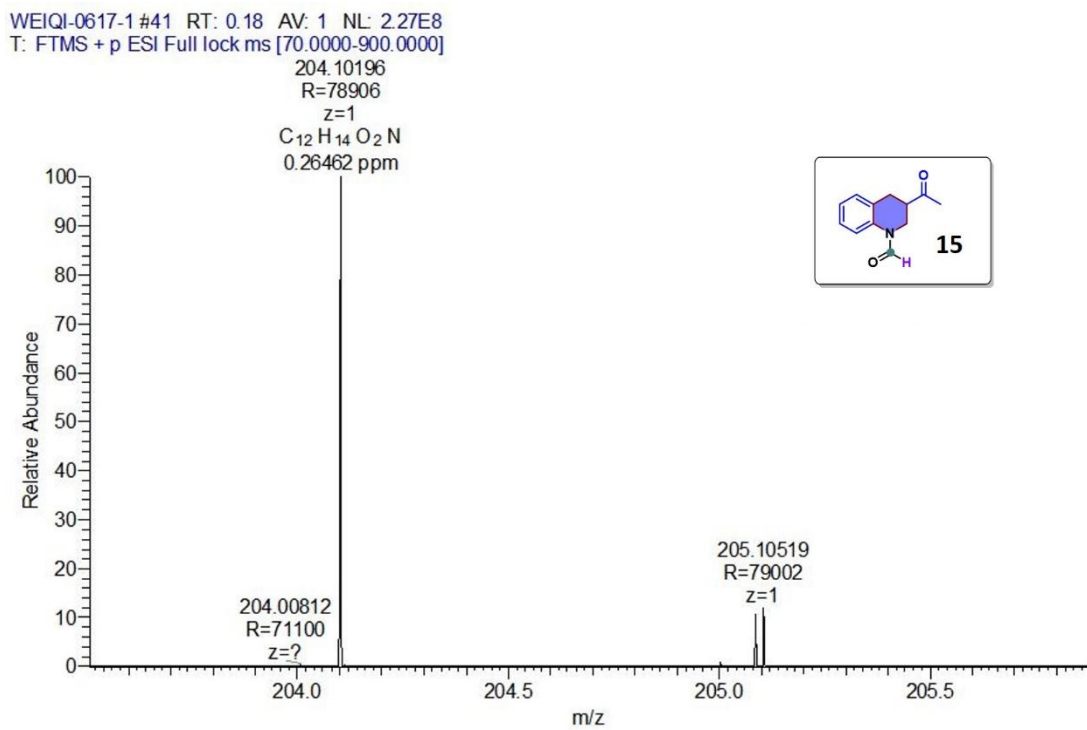


Fig. S78 HRMS of 16

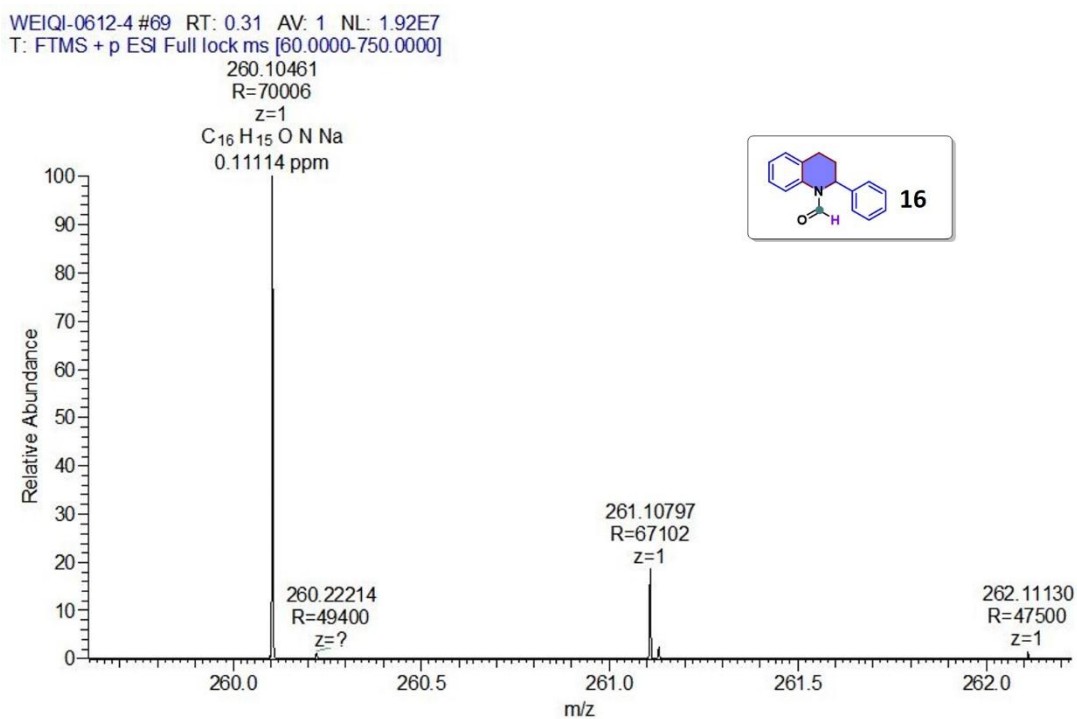


Fig. S79 HRMS of 17

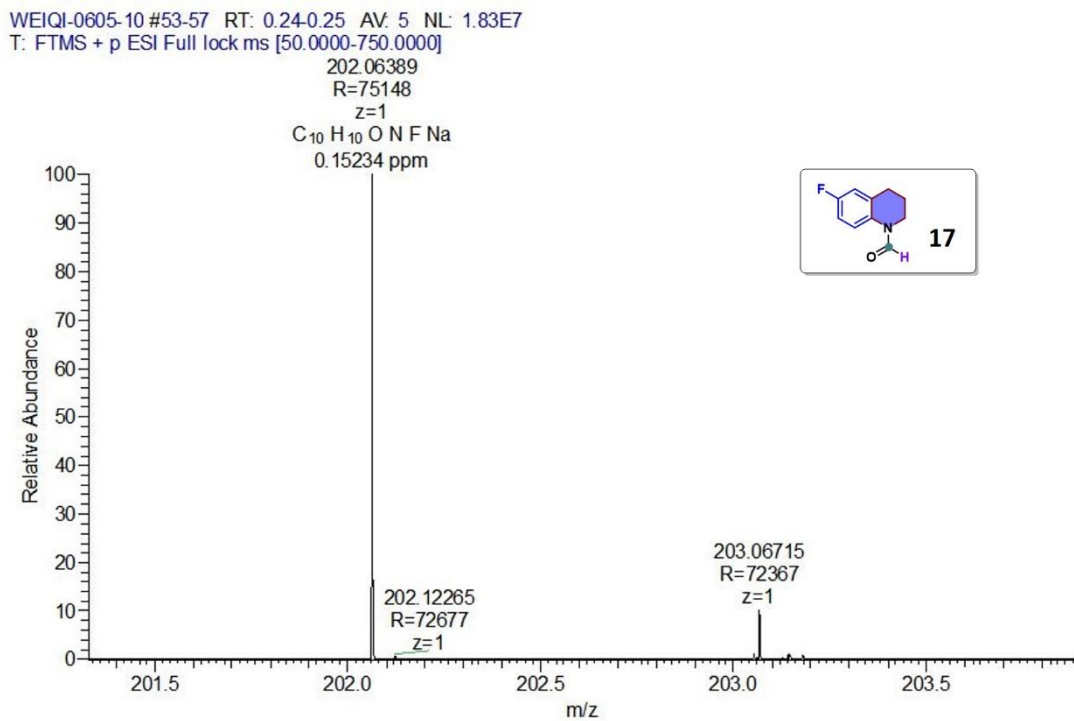


Fig. S80 HRMS of 18

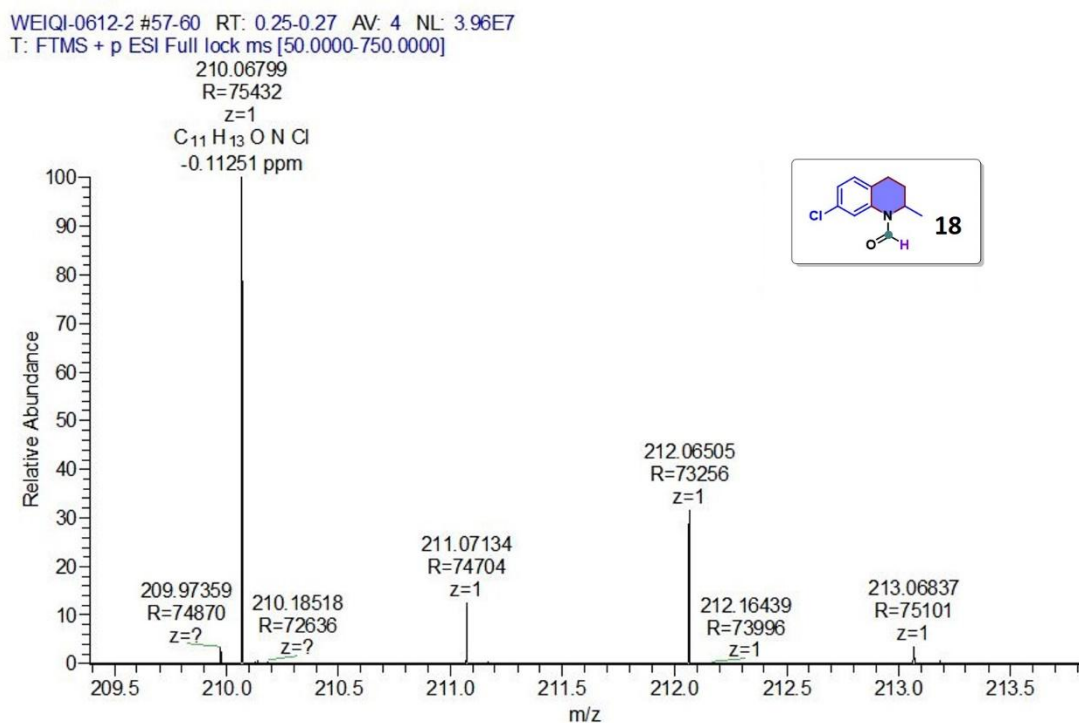


Fig. S81 HRMS of 19

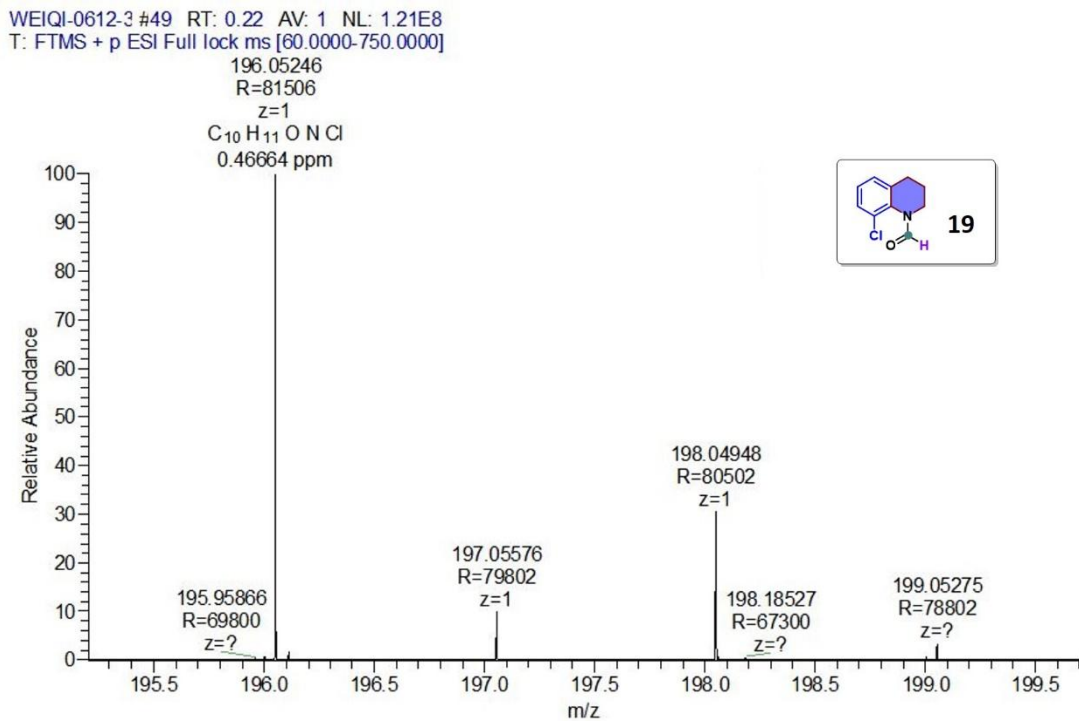


Fig. S82 HRMS of 20

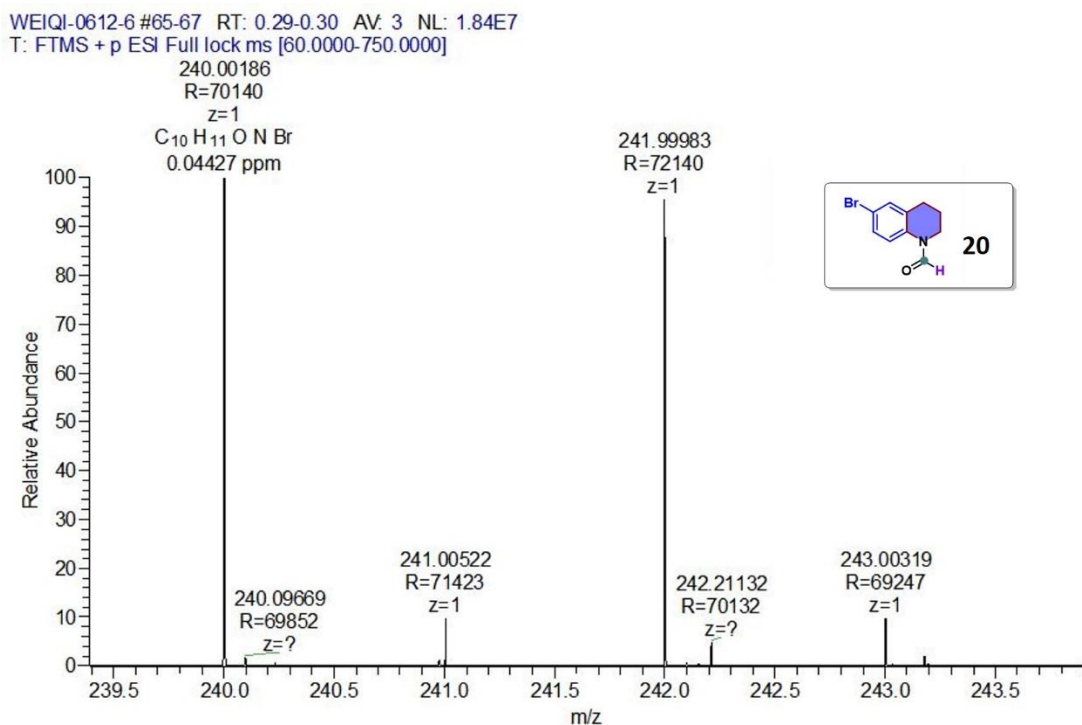


Fig. S83 HRMS of 21

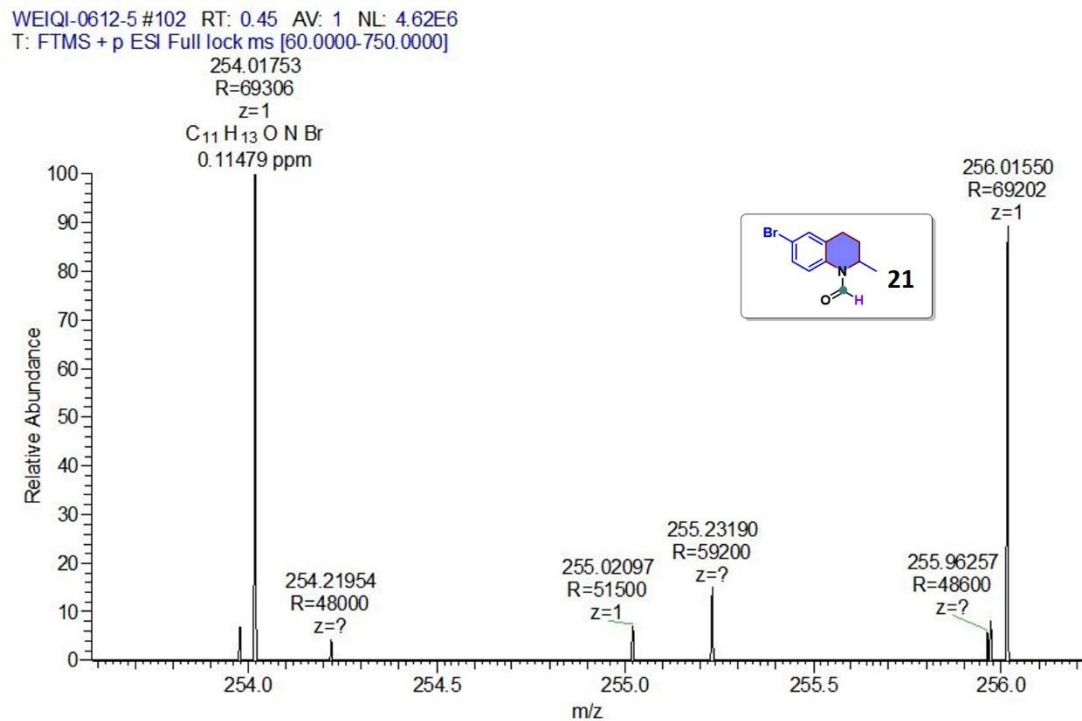


Fig. S84 HRMS of 22

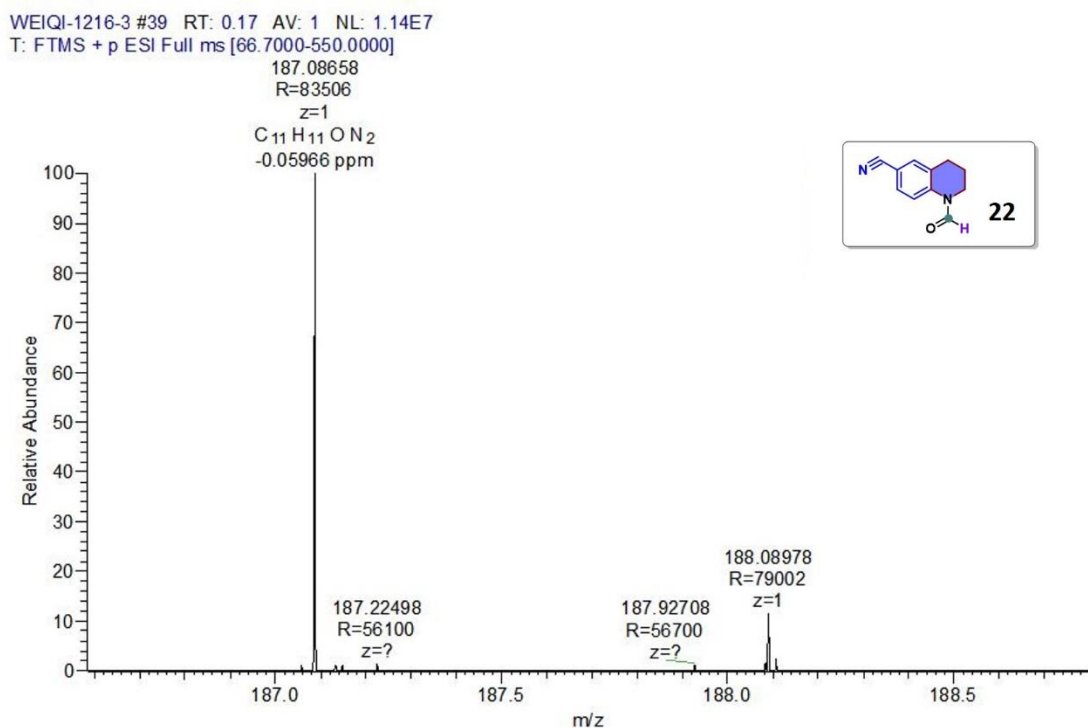


Fig. S85 HRMS of 23

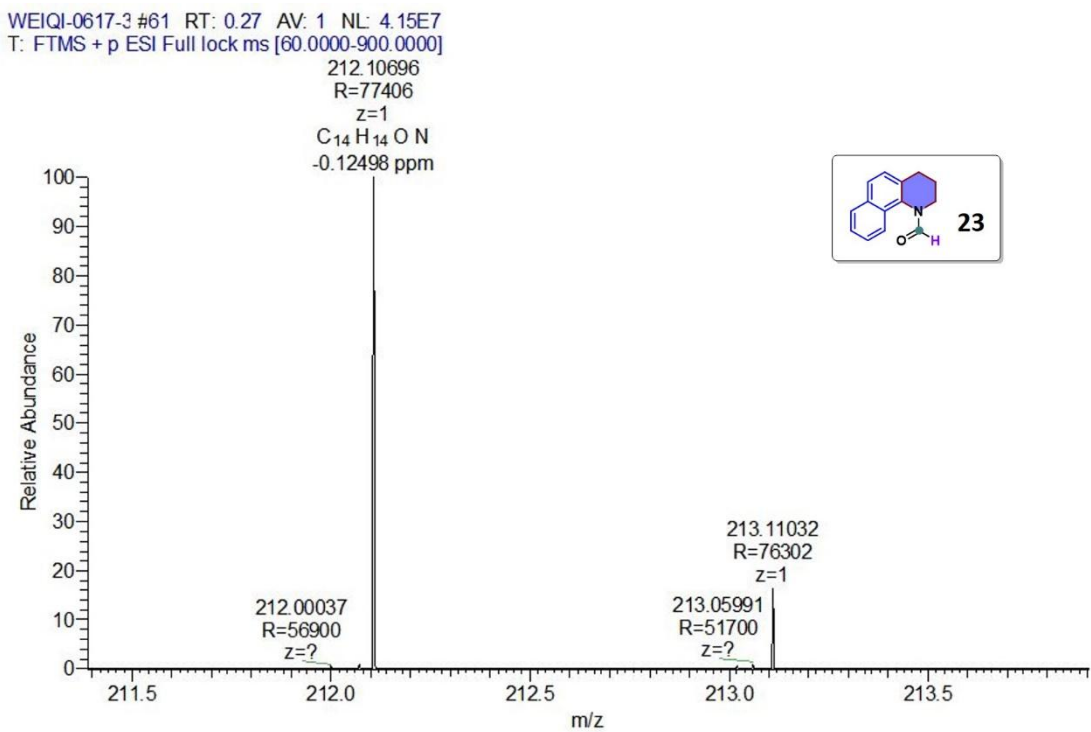


Fig. S86 HRMS of 24

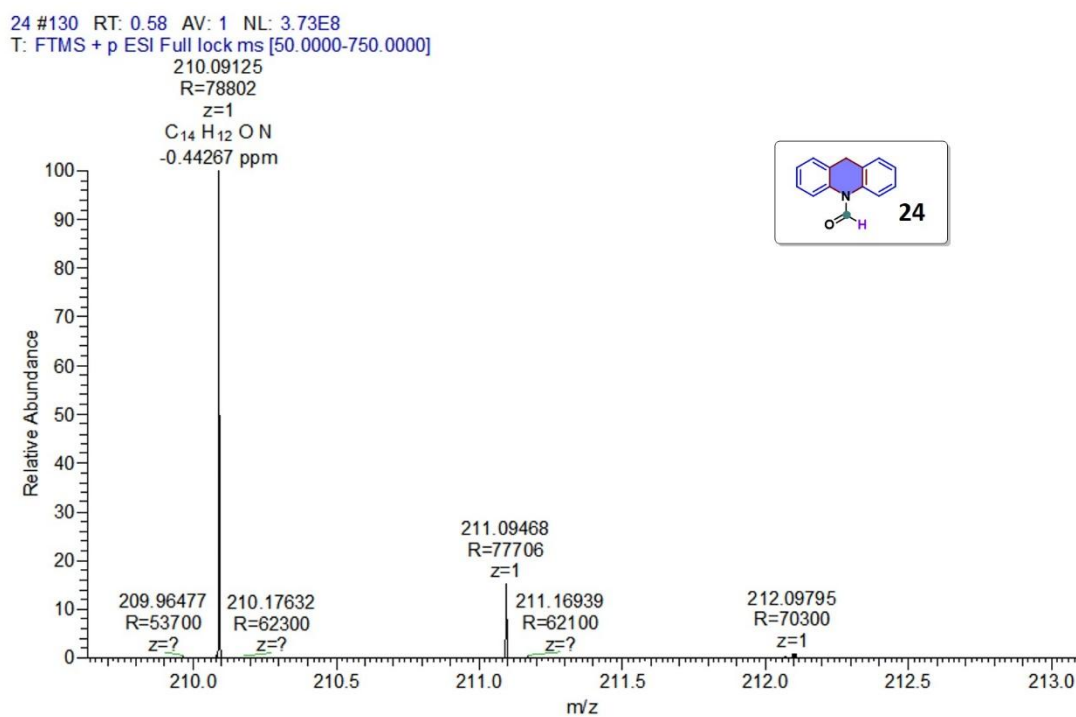


Fig. S87 HRMS of 25

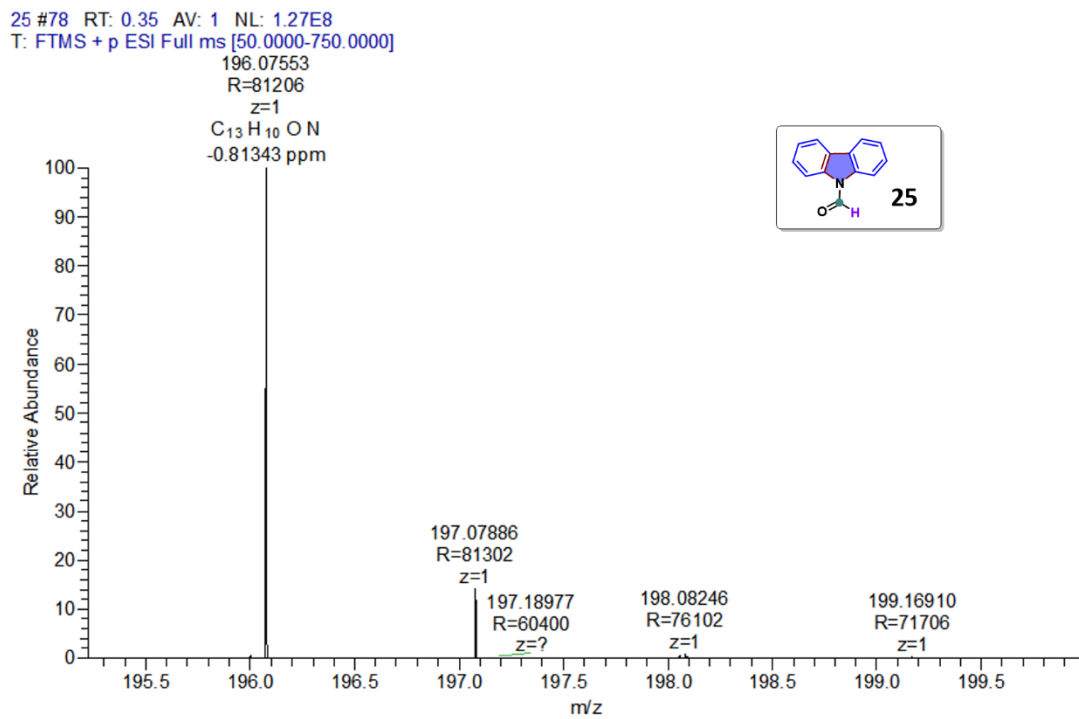


Fig. S88 HRMS of 26

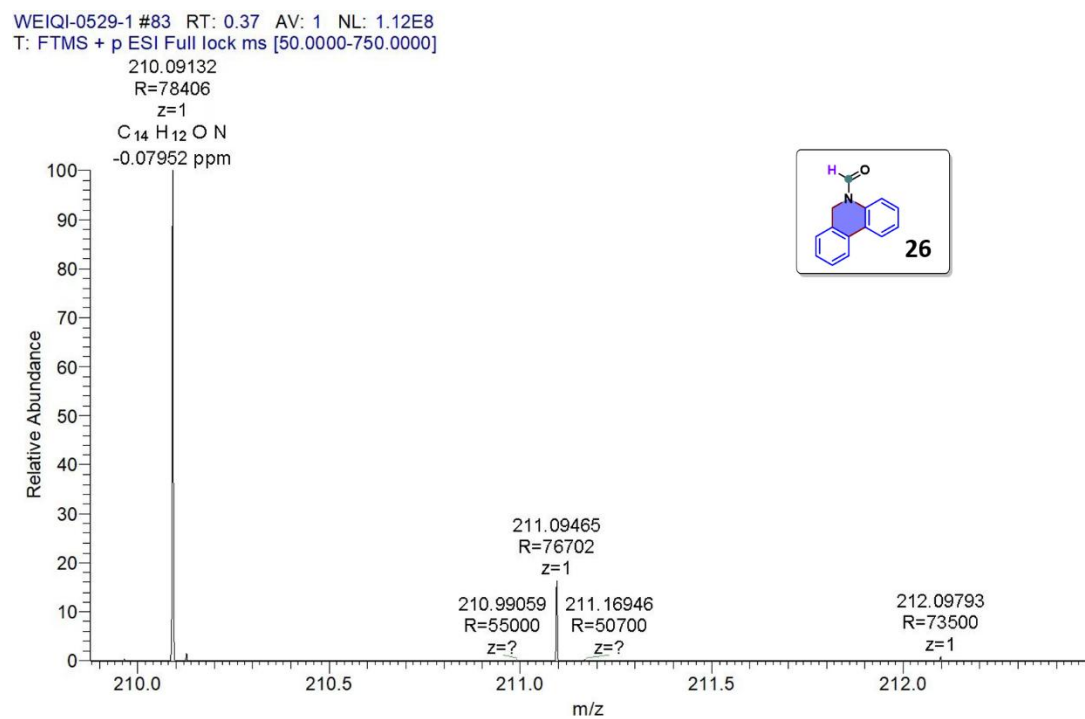


Fig. S89 HRMS of 27

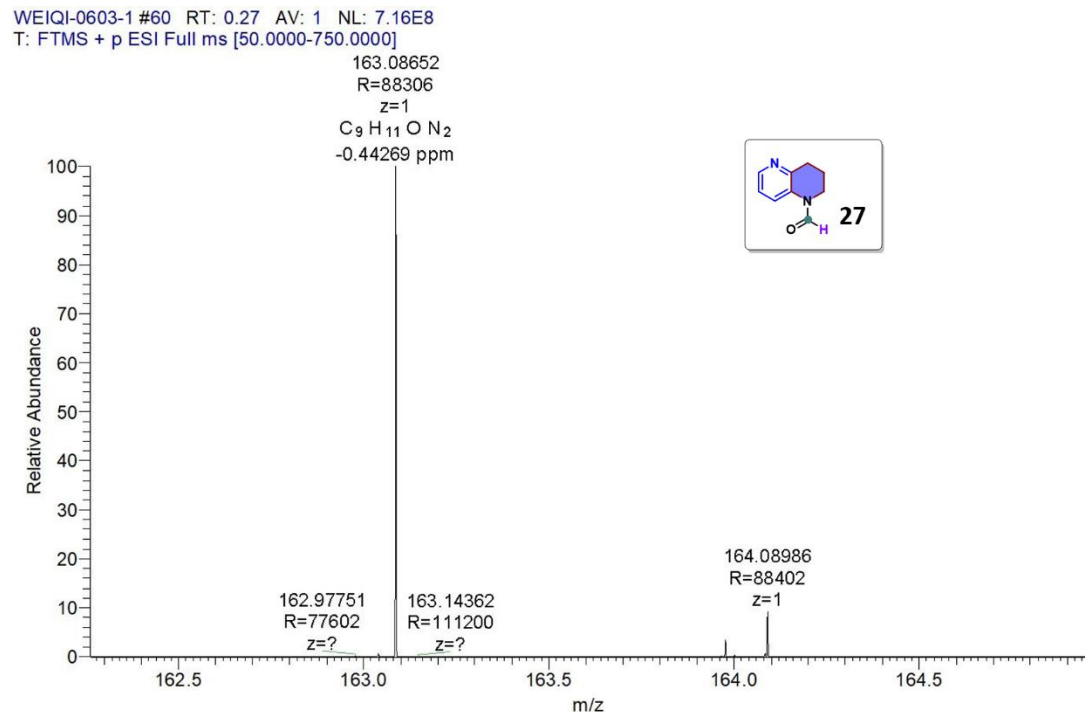


Fig. S90 HRMS of 28

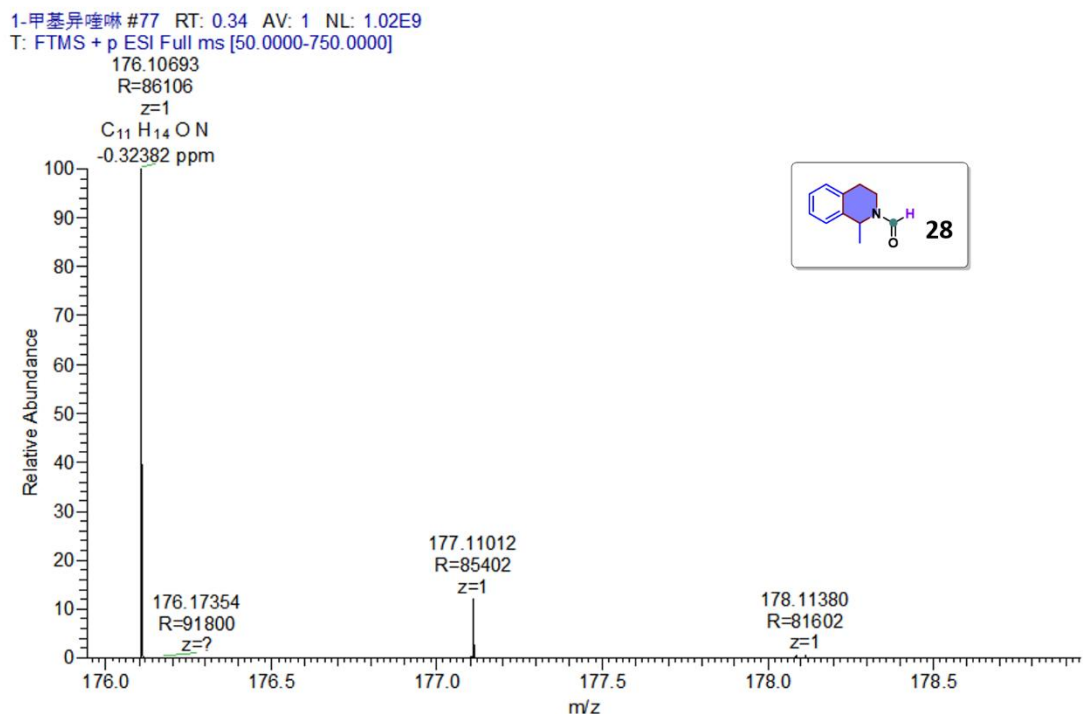


Fig. S91 HRMS of 29

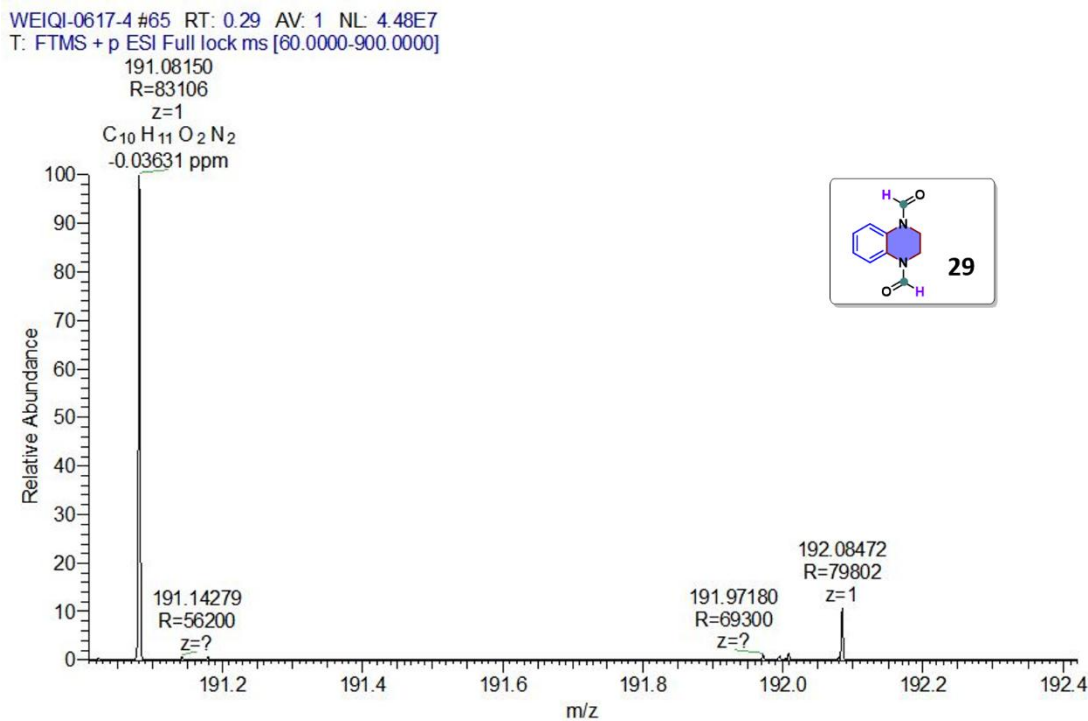


Fig. S92 HRMS of 30

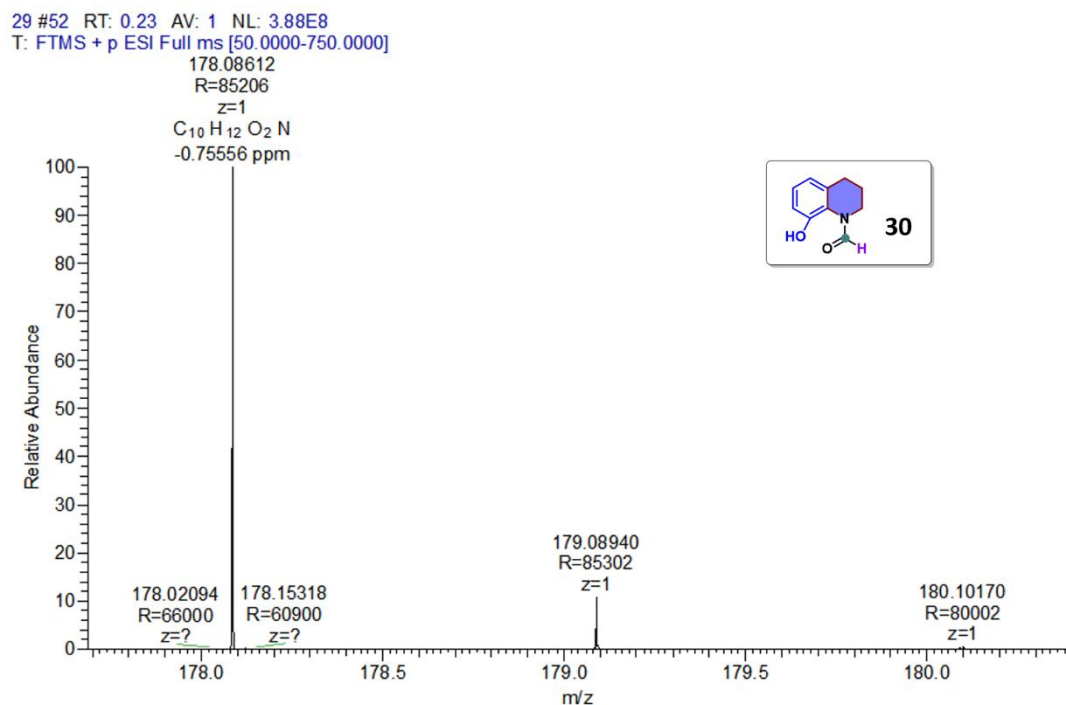
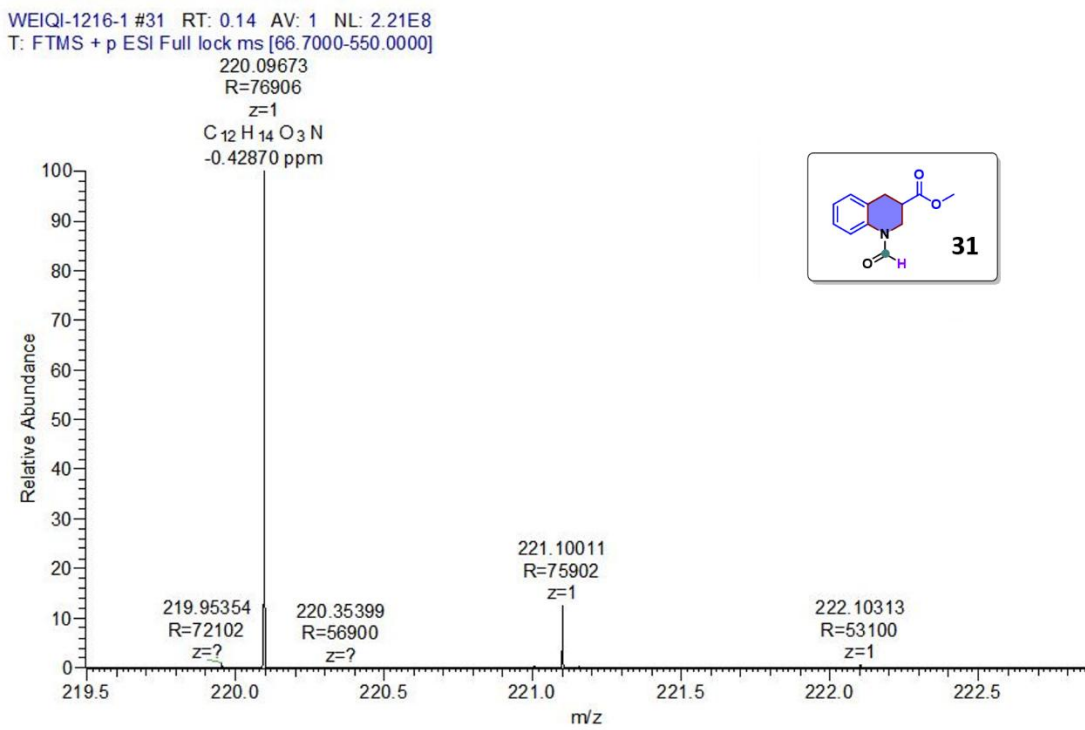


Fig. S93 HRMS of 31



VI. References

1. Levine, I. N. *Quantum Chemistry*. In *Quantum Chemistry*, 5th ed., Prentice Hall: Hoboken, NJ, **1999**.
2. Chen, F., Sahoo, B., Kreyenschulte, C., Lund, H., Zeng, M., He, L., K, Junge. K., Beller, M. *Chem. Sci.*, **2017**, 8(9), 6239-6246.
3. Han, Y., Wang, Z., Xu, R., Zhang, W., Chen, W., Zheng, L., Zhang, J., Luo, J., Wu, K., Zhu, Y., Chen, C., Peng, Q., Liu, Q., Hu, P., Wang, D., Li, Y. *Angew. Chem. Int. Ed.*, **2018**, 57(35), 11262-11266.
4. Leng, Y., Du, S., Feng, G., Sang, X., Jiang, P., Li, H., Wang, D. *ACS Appl. Mater. Interfaces*, **2019**, 12(1), 474-483.
5. Zhu, M., Tian, H., Chen, S., Xue, W., Wang, Y., Lu, H., Li, T., Chen, F., Tang, C. *J. Catal.*, **2022**, 416, 170-175.
6. Chauhan, A., Banerjee, A., Kar, A. K., Srivastava, R. *ChemSusChem*, **2022**, 15(23), e202201560.
7. Liang, H., Zhao, T., Ou, J., Liu, J., Hu, X. *ACS Sustain. Chem. Eng.*, **2023**, 11(39), 14317-14322.